NASA TMX 53829

NASA TECHNICAL
MEMORANDUM

Report No. 53829

A DISCUSSION OF ORBITAL WORKSHOP ORIENTATION AND GRAVITATIONAL EFFECTS

By Billy G. Davis
Preliminary Design Office

May 5, 1969

NASA

George C. Marshall Space Flight Center
Marshall Space Flight Center, Alabama

1. REPORT NO. TM X-53829	2. GOVERNMENT ACCESSION NO.	3. RECIPIENT'S CATALOG NO.
4. TITLE AND SUBTITLE A Discussion of Orbital Workshop Orientation and Gravitational Effects		5. REPORT DATE May 5, 1969
		6. PERFORMING ORGANIZATION CODE PD-DO-ES
7. AUTHOR(S) Billy G. Davis		8. PERFORMING ORGANIZATION REPORT #
9. PERFORMING ORGANIZATION NAME AND ADDRESS Electronics and Controls Division Preliminary Design Office Program Development Marshall Space Flight Center, Alabama 35812		10. WORK UNIT NO. 981-10-10
		11. CONTRACT OR GRANT NO.
12. SPONSORING AGENCY NAME AND ADDRESS		13. TYPE OF REPORT & PERIOD COVERED Technical Memorandum
		14. SPONSORING AGENCY CODE

15. SUPPLEMENTARY NOTES

Prepared with the cooperation and support of Astrionics Laboratory and
Advanced Systems Office of Marshall Space Flight Center.

16. ABSTRACT

As a rule, the dominant environmental force acting on a spacecraft in earth orbit is gravity gradient. Over a period of several months, the energy requirements necessary for attitude hold control against gravity gradient torques can be quite large and must be evaluated in terms of fuel weight or momentum exchange devices which impact on the preliminary spacecraft design. This report contains the equations necessary to evaluate the energy requirements due to gravitational effects for several selected orientations. First, the basic gravity gradient torque equations are derived in general form, after which various coordinate systems are defined that related the local gravity gradient vector to the spacecraft's control axes. Then the equations are evaluated for several selected attitude hold modes as solar-fixed and orbit-fixed. Finally, using fixed-time-of-year analyses and neglecting orbital regression, the energy requirements necessary for attitude hold against gravity gradient torques are summarized for the selected attitude hold modes. The material presented can be easily adapted for use in evaluating additional attitude hold orientations and utilized for "quick-look" analysis of orbital orientation and its impact on preliminary spacecraft design, especially the control system.

17. KEY WORDS Orbital Workshop Orientation Gravity Gradient Torques Attitude Hold Momentum, Fuel, CMGs Look Angles, Transformations	18. DISTRIBUTION STATEMENT STAR Announcement

19. SECURITY CLASSIF. (of this report) Unclassified	20. SECURITY CLASSIF. (of this page) Unclassified	21. NO. OF PAGES 105	22. PRICE $3.00

MSFC - Form 3292 (May 1969)

ACKNOWLEDGMENTS

TABLE OF CONTENTS

LIST OF ILLUSTRATIONS

LIST OF ILLUSTRATIONS (Continued)

LIST OF ILLUSTRATIONS (Concluded)

LIST OF TABLES

DEFINITION OF SYMBOLS

Symbol	Definition
A_{ab}	Transformational matrix between "a" and "b" coordinates
A_{mn}	Directional cosine $(m, n = 1, 2, 3)$ element of A_{ab}
C	Cosine
CG	Center of Gravity
CM	Center of Mass
E	Angle subtended by the sun line vector projected on the equatorial plane
$e = 23.5$ deg	Angle between ecliptic and equatorial planes
F_i	Gravitational force acting on the ith mass unit
H	Momentum (subscripts denote components)
$\tilde{I}$	Inertia matrix (dyadic)
I_{xy}, I_{xz}, I_{yz}	Products of inertia
I_x, I_y, I_z	Moments of inertia
i, j, k	Unit vectors (subscripts denote coordinate system)
L	Lever arm
m_i	Mass of the ith particle
P_i	Distance from CM to m_i
R_e	Radius of the earth
R_o	Distance from earth center to body CM (R_e + Altitude)

DEFINITION OF SYMBOLS (Continued)

Symbol	Definition
R_x, R_y, R_z	Vector components of $\overline{R}_o$ in body coordinates
r_i	Distance from earth center to the ith mass unit
S	Sine
T	Torque (subscripts denote components)
t	Time in seconds
t'	Time in days
W_o	Orbital angular rate
X_a, Y_a, Z_a	Body principal axes
X_b, Y_b, Z_b	Body fixed coordinates
X_e, Y_e, Z_e	Earth-equatorial coordinates
X_g, Y_g, Z_g	Geocentric inertial coordinates
X_o, Y_o, Z_o	Orbit fixed coordinates
X_1, Y_1, Z_1	Inertial coordinates
X_p, Y_p, Z_p	Local vertical (plume line) coordinates
X_r, Y_r, Z_r	Body reference coordinates
X_s, Y_s, Z_s	Solar fixed coordinates
$\overline{x}$	Vector (subscripts denote coordinate system)
$\tilde{x}$	Vector transpose of vector components
α_{mn}	Directional cosine angle, $\cos(\alpha_{mn}) = A_{mn}$

DEFINITION OF SYMBOLS (Concluded)

Symbol	Definition
α_x, α_y, α_z	Euler angles for body-principal axes misalignment
β	Solar look angle ($\beta = \gamma - 90$ deg)
γ	Angle between sun line and orbital spin vectors ($\gamma = \alpha_{13}$)
δ_x, δ_y, δ_z	Euler angles for body-reference axes misalignment
ϵ	Attitude error angle from equilibrium position
Θ	Angle between the local radius vector and the vehicle axis of minimum inertia
ι	Angle of orbital inclination (between orbital and equatorial planes)
Λ	Angle between sun-Aries and the sun-earth lines
λ	Earth's seasonal position (angle between Υ and earth-sun lines)
$\mu = GM$	Gravitational constant
Υ	Earth-sun-Aries inertial reference
φ	Angle of orbital rotation (between ascending node and spacecraft)
ψ	Angle between ecliptic and orbital planes ($\psi = \alpha_{33}$)
Ω	Angle of orbital regression (between Υ and orbital ascending node)
$\bar{\omega}$	Spacecraft angular velocity vector (body coordinates)
*	Superscript denoting matrix transpose
•	Superscript to indicate time derivative

A DISCUSSION OF ORBITAL WORKSHOP ORIENTATION AND GRAVITATIONAL EFFECTS

INTRODUCTION

Most of the material contained in this report is an extension and documentation of the work performed to support the George C. Marshall Space Flight Center (MSFC) "Early Saturn V Workshop" studies. During these preliminary design studies, this group was assigned the task of evaluating the control requirements for various attitude hold modes, especially the fuel requirements and the momentum storage capacity over an extended time interval. A quick assessment of the energy requirements necessary to attitude hold Workshop B (OWS-B) in an inertial, solar fixed mode was made using simplifying assumptions. However, earth and orbit fixed modes were also evaluated for comparative purposes. The two basic configurations studied were the side viewing and the end viewing Apollo Telescope Mount (ATM). Both have similar mass and inertial properties with the x-axis being near symmetric with minimum inertia. The material presented, herein, is in the form of "A Tutorial Discussion of Orbital Workshop Orientation and Gravitational Effects."

The "Early Saturn V Workshop" study was conducted under the following ground rules:

1. 1971-73 launch — late 1968 Phase D start

2. 28.5- to 50-degree orbital inclination

3. 270-n. mi. altitude

4. Zero-g operation

5. One to one and one-half-year lifetime

6. Dry launched workshop with integral ATM, manned Command Service Module (CSM)

7. Minimum modification to Workshop A

8. Maximum use of present equipment and subsystems

9. Three-man operation with six-man provisions as an option

The zero-g operation ground rule precludes a spin stabilization mode. "Maximum use of present equipment and subsystems" requires that the "integral ATM" be hard mounted to OWS-B which precludes a long axis perpendicular to the orbital plane (POP) mode orientation while viewing the sun. However, for completeness the POP mode orientation is evaluated, in which case both the ATM and solar panels must be gimbaled. For either a solar inertially fixed mode or a semi-solar fixed mode with one body axis constrained to lie in the orbital plane, it is not necessary to gimbal the ATM or solar panels.

Based on the ground rules, the following assumptions are made to produce worst case conditions and simplify analysis procedures:

1. Quick-look simplified analysis utilizes fixed time of year, constant circular orbit and an energy evaluation over one orbital time period.

2. Winter solstice launch at 270 n. mi. altitude

3. Solar attitude hold over one orbit

4. Energy requirements for attitude hold due primarily to gravity gradient torques

5. Hard mounted ATM for the side and end view ATM modes

6. Body axes are solar oriented for hard mounted ATM configurations.

At a 270-n. mi. altitude, gravity gradient torques will be the dominant environmental forces acting on the workshop and, for preliminary design purposes, will determine the control system energy requirements for attitude hold. Although other environmental forces such as aerodynamics and solar pressure will act on the workshop, only the gravity gradient effects are considered in this report. First, the basic gravity gradient torque equations are derived in general form, after which various coordinate systems must be defined that relate the local gravity gradient vector to the workshop's body fixed control axes. The coordinate systems are defined in physically meaningful geo-physical terms and the necessary coordinate transformations are

2

carried out. Then the gravity gradient equations are evaluated for several attitude hold modes. The end view ATM configuration is in a solar inertially fixed mode (solar mode), the side view ATM configuration is in a semisolar fixed mode with the x-axis constrained to lie in the orbital plane (XOP mode), and the gimbaled ATM configuration is in an earth fixed mode with the x-axis constrained to lie perpendicular to the orbital plane (POP Mode). The effects of principal axes misalignments on gravity gradient torques are evaluated for the POP mode and the gravity gradient mode (GG Mode) with the axis of minimum inertia aligned with the local vertical. For earth or orbital fixed modes, an experiment package designed to view the sun or stars must be mounted to the workshop on gimbals. The gimbals are articulated as needed to track the specified target, which requires definition of "look angles." Several such angles are defined and closed form solutions obtained in the section on "Solar Look Angles." Several such angles are needed to evaluate the gravity gradient equations. Finally, using simplifying assumptions, involving fixed time of year analysis which neglects orbital regression, the energy requirements necessary for attitude hold against gravity gradient are summarized for the selected attitude hold modes. A comparison of requirements indicates that the XOP mode is near optimal and is preferred over the solar inertia mode. For earth fixed modes, the POP mode has several advantages over the GG mode, in particular the effect of principal axes misalignments or attitude errors requires less fuel for control action.

It is felt that the presented material can be easily utilized for "quick look" analysis of orbital orientation and gravity gradient effects, and should be useful for preliminary design purposes. It is also felt that the material is somewhat elementary, but should give an "engineering feel" for the problems involved in selecting a preferred attitude hold orientation for an earth orbiting vehicle. The data presented can be easily adapted for use in evaluating other attitude hold orientations. For completeness the standard Euler equations are listed in the appendix.

GRAVITY GRADIENT TORQUE

The easiest means of describing the basic gravity gradient torque is in terms of two equal mass units connected by a rigid massless rod in a circular earth orbit as shown in Figure 1. The forces F_1 and F_2 represent forces from the gravitational field in a geocentric rotating reference system (local vertical coordinates) that act on the mass units m_1 and m_2, respectively.

Since the gravitational force acting on a given object varies inversely with the square of the distance between the earth's center and the object's center of mass, the force F_1 is greater than the force F_2. Each force produces a torque about the center of mass; however, since each force acts on the same lever arm, L, a torque in the counterclockwise direction exists. This torque acts to reduce the attitude error ϵ and to align the rod with the local vertical. When the attitude error angle is zero the two forces act through the center of mass of the dumbbell, and no net torque exists since the lever arms are zero. This position is referred to as a "stable equilibrium point" of an orbiting satellite under the influence of gravity.

FIGURE 1. STABLE EQUILIBRIUM

Another equilibrium point exists as indicated in Figure 2. If the dumbbell lies in a horizontal plane, the two tip masses are at the same distance from the geocenter so that the forces F_1 and F_2 are equal. Since the lever arm on which each force acts is also equal, no net torque exists. If an attitude error angle ϵ_* is introduced, the force F_1 exceeds the force F_2 and a torque is generated which tends to increase the attitude error angle. In this case the gravity gradient torque
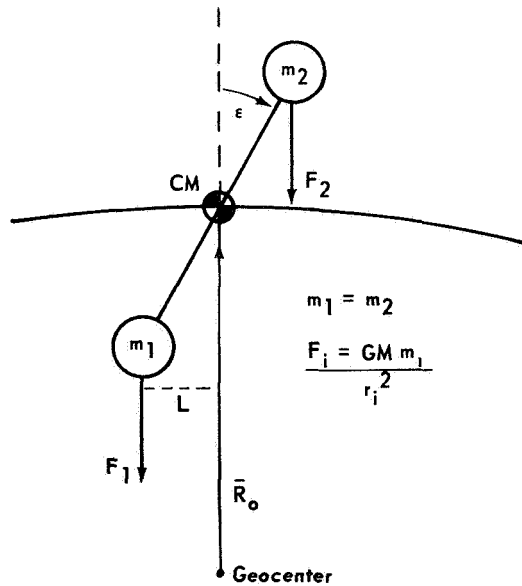
is destabilizing. Hence, the horizontal plane alignment is referred to as an "unstable equilibrium point."

For a satellite in orbit several stable or unstable equilibrium points may exist, depending upon the vehicle's mass distribution properties. In general, a rigid, non-spinning satellite with sufficient differences
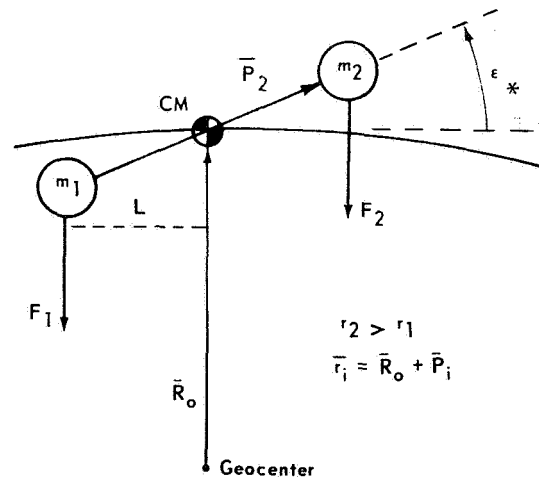
FIGURE 2. UNSTABLE EQUILIBRIUM

4

in the principal moments of inertia tends to align its axis of minimum inertia with the local vertical and its axis of maximum inertia with the orbital spin vector. In actual practice, finding equilibrium points is usually achieved through the use of elaborate digital computer programs and facilities. However, the vector components of gravity gradient torque are derived in general form using the inverse square law for the force between the earth and an orbiting body composed of mass elements.

Figure 3 represents a body composed of mass elements, m_i, in a circular orbit of radius $\overline{R}_o$, about the earth. The vector $\overline{R}_o$ is directed from the geocenter to the center of mass of the body; the vector $\overline{r}_i$ is directed from the geocenter to the ith mass element, and the vector $\overline{P}_i$ is directed from the center of mass (CM) to the ith mass element. The vectors are defined relative to two coordinate systems: an inertial frame, denoted by the subscripts 1, with its origin at the geocenter and a body-fixed moving frame, denoted by the subscript b, with its origin at the body's CM. The gravitational force vector, $\overline{F}_i$, acting on the ith mass particle is directed opposite $\overline{r}_i$ and is given by

$$\overline{F}_i = \frac{-\mu\, m_i \overline{r}_i}{(r_i)^3} \qquad (1)$$

where $\mu = GM$. G is the universal gravitational constant and M is the mass of the earth.

The moment (torque) due to $\overline{F}_i$ is given by the vector cross product,

$$\overline{T}_i = \overline{P}_i \times \overline{F}_i \qquad (2)$$

The summation of all such moments gives the gravity gradient torque, $\overline{T}_g$, which acts on the body.
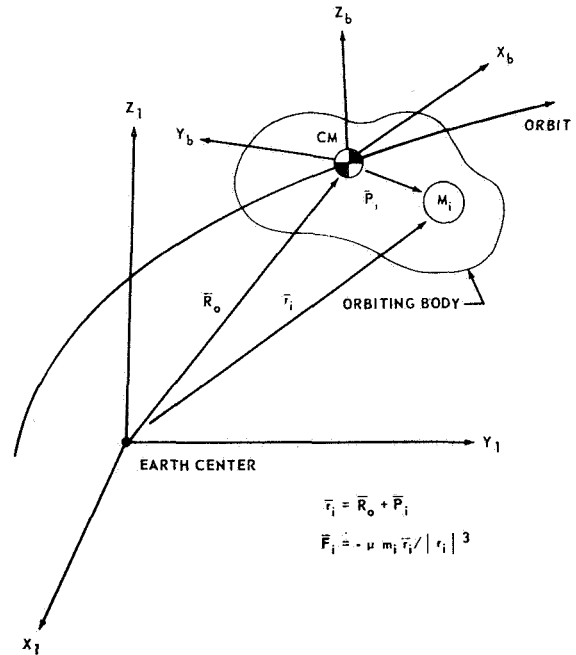
$$\overline{r}_i = \overline{R}_o + \overline{P}_i$$
$$\overline{F}_i = -\mu\, m_i \overline{r}_i / |r_i|^3$$

FIGURE 3. COORDINATES FOR GRAVITY GRADIENT TORQUES

$$\overline{T}_g = \sum \overline{P}_i \times \overline{F}_i = T_x i_b + T_y j_b + T_z k_b \tag{3a}$$

$$\overline{T}_g = -\sum \overline{P}_i \times \frac{\left(\mu m_i \overline{r}_i\right)}{\left(r_i\right)^3} \tag{3b}$$

Assume that in body coordinates

$$\overline{P}_i = X_i i_b + Y_i j_b + Z_i k_b$$

$$\overline{R}_o = R_x i_b + R_y j_b + R_z k_b \tag{4}$$

and from Figure 3, $\overline{r}_i = \overline{R}_o + \overline{P}_i$. Expanding $1/(r_i)^3 = 1/|\overline{r}_i|^3$ in a power series gives

$$\frac{1}{|\overline{r}_i|^3} = \frac{1}{|\overline{R}_o + \overline{P}_i|^3} = \frac{1}{\left\{\left[\left(X_i + R_x\right)^2 + \left(Y_i + R_y\right)^2 + \left(Z_i + R_z\right)^2\right]^{1/2}\right\}^3}$$

$$= \left\{X_i^2 + Y_i^2 + Z_i^2 + R_x^2 + R_y^2 + R_z^2 + 2\left(X_i R_x + Y_i R_y + Z_i R_z\right)\right\}^{-3/2}$$

$$= \left(\overline{P}_i \cdot \overline{P}_i + \overline{R}_o \cdot \overline{R}_o + 2\overline{R}_o \cdot \overline{P}_i\right)^{-3/2} = \left(P_i^2 + R_o^2 + 2\overline{R}_o \cdot \overline{P}_i\right)^{-3/2}$$

$$= \left(\frac{1}{R_o^3}\right)\left(1 + \frac{P_i^2 + 2\overline{R}_o \cdot \overline{P}_i}{R_o^2}\right)^{-3/2}$$

$$= \left(\frac{1}{R_o^3}\right)\left[1 - \left(\frac{3}{2}\right)\left(\frac{P_i}{R_o}\right)^2 - \frac{3\,\overline{R}_o \cdot \overline{P}_i}{R_o^2} + \text{----------}\right]$$

$$= \left(\frac{1}{R_o^3}\right)\left(1 - \frac{3\,\overline{R}_o \cdot \overline{P}_i}{R_o^2}\right) \quad , \tag{5}$$

where the second and higher order terms in P_i may be neglected since $P_i \ll R_o$. Substituting equation (5) into the torque equation (3b) gives

$$T_g = -\sum P_i \times \frac{\mu m_i}{R_o^3}\left(\overline{R}_o + \overline{P}_i\right)\left(1 - \frac{3\overline{R}_o \cdot \overline{P}_i}{R_o^2}\right)$$

$$= -\sum\left(\overline{P}_i \times \overline{R}_o + \overline{P}_i \times \overline{P}_i\right)\left(\frac{\mu m_i}{R_o^3}\right)\left(1 - \frac{3\overline{R}_o \cdot \overline{P}_i}{R_o^2}\right)$$

$$= -\sum\left(\overline{P}_i \times \overline{R}_o\right)\left(\frac{\mu m_i}{R_o^3}\right)\left(1 - \frac{3\overline{R}_o \cdot \overline{P}_i}{R_o^2}\right)$$

$$= \frac{-\mu}{R_o^3}\left[\sum m_i\left(\overline{P}_i \times \overline{R}_o\right) - 3\sum m_i\left(\overline{P}_i \times \overline{R}_o\right)\left(\frac{\overline{R}_o \cdot \overline{P}_i}{R_o^2}\right)\right] \qquad (6)$$

By definition of the CM in body coordinates, $\sum_i m_i \overline{P}_i = 0$, the first term of equation (6) is zero leaving[1]

$$T_g = \frac{3\mu}{R_o^5}\left\{\sum m_i\left(\overline{P}_i \times \overline{R}_o\right)\left(\overline{R}_o \cdot \overline{P}_i\right)\right\}$$

$$= \frac{3\mu}{R_o^5}\left\{\sum m_i\left[\left(Y_i R_z - Z_i R_y\right)i_b + \left(Z_i R_x - X_i R_z\right)j_b\right.\right.$$

$$\left.\left. + \left(X_i R_y - Y_i R_x\right)k_b\right]\left(X_i R_x + Y_i R_y + Z_i R_z\right)\right\} \qquad . \qquad (7)$$

By carrying out the indicated scalar multiplication and using the following definitions for products and moments of inertia

$$I_x = \sum m_i\left(Y_i^2 + Z_i^2\right) \qquad , \qquad (8)$$

$$I_y = \sum m_i\left(Z_i^2 + X_i^2\right) \qquad ,$$

---

1. If the origin of the body coordinates is not assumed to be located at the CM then the first term of equation (6) is not zero and the ensuing equations are not valid.

$$I_z = \sum m_i \left(X_i^2 + Y_i^2 \right) \quad ,$$

$$I_{xy} = I_{yx} = \sum m_i X_i Y_i \quad ,$$

$$I_{xz} = I_{zx} = \sum m_i X_i Z_i \quad ,$$

$$I_{yz} = I_{zy} = \sum m_i Y_i Z_i$$

with the relations

$$\sum m_i \left(Y_i^2 - Z_i^2 \right) = \sum m_i \left(Y_i^2 + X_i^2 - X_i^2 - Z_i^2 \right) = I_z - I_y \quad , \qquad (9)$$

$$\sum m_i \left(Z_i^2 - X_i^2 \right) = \sum m_i \left(Z_i + Y_i^2 - Y_i^2 - X_i^2 \right) = I_x - I_z \quad ,$$

$$\sum m_i \left(X_i^2 - Y_i^2 \right) = \sum m_i \left(X_i^2 + Z_i^2 - Z_i^2 - Y_i^2 \right) = I_y - I_x \quad .$$

the gravity gradient torque equation becomes

$$\overline{T}_g = \frac{3\mu}{R_o^5} \left[\left(I_z - I_y \right) R_y R_z + I_{zy} \left(R_z^2 - R_y^2 \right) + I_{xy} R_x R_z - I_{xz} R_x R_y \right] i_b$$

$$+ \frac{3\mu}{R_o^5} \left[\left(I_x - I_z \right) R_z R_x + I_{xz} \left(R_x^2 - R_z^2 \right) + I_{yz} R_y R_x - I_{yx} R_y R_z \right] j_b$$

$$+ \frac{3\mu}{R_o^5} \left[\left(I_y - I_x \right) R_x R_y + I_{yx} \left(R_y^2 - R_x^2 \right) + I_{zx} R_z R_y - I_{zy} R_z R_x \right] k_b \quad .$$

$$(10)$$

The gravity gradient torque components in body fixed coordinates, denoted by T_x, T_y, and T_z, are obtained by equating to the vector coefficients in the torque equation above.

8

Since the torque and momentum components will be derived for several selected vehicle orientations, the equations can be simplified by using the following definitions for the multiplicative coefficients containing vehicle and orbital parameters:

$$C_x = (3GM/2R_o^3)(I_z - I_y) \ , \tag{11}$$

$$C_y = (3GM/2R_o^3)(I_x - I_z) \ , \ \text{and}$$

$$C_z = (3GM/2R_o^3)(I_y - I_x) \ , \quad \text{with the relation}$$

$$C_x + C_y + C_z = 0 \ .$$

At this point, it is assumed that the moments and products of inertia are known or will be given. It is further assumed that the parameters which define the orbit will be specified, as the orbital inclination, orbital altitude, time or year, and position of orbital injection. Hence, $\overline{R}_o$ will be known or can be calculated in terms of a local vertical coordinate system. But for use in the torque equation, the components of $\overline{R}_o$ must be derived in terms of the body fixed frame. Such a derivation will require the definition and use of several coordinate systems and transformations between systems. The actual number of coordinate systems depends upon the specific mission of the orbiting vehicle and its desirable attitude orientation, and upon the accuracy in evaluating the torque components and the time interval over which the evaluation is to be made. Also, the transformations between coordinates should be related to parameters that have physical significance. Once the components R_x, R_y, and R_z have been obtained they are substituted into the gravity gradient torque equation (10), which is valid for any spacecraft in a circular orbit about the earth with body coordinates centered at the CM.

COORDINATE SYSTEMS

In computing gravity gradient torques on the Solar oriented orbital workshop (OWS) several coordinate transformations are necessary to relate the orbital plane, the earth's equatorial plane, and the sun line in the ecliptic

plane, as slowly changing functions of time, to the OWS body coordinates. These three planes relative to the celestial sphere provide the basic references for development of the coordinate systems. In this development, standard reference systems as given in "Project Apollo Coordinate System Standards," June 1965, OMSF report number SE 008-001-1, will be utilized. All the coordinate systems which are defined in the following paragraphs are right-hand systems and the rotational angles are measured in a positive sense using the right-hand rule. First, the concept of an inertial reference must be established.

A belt of sky extending about 9 degrees to each side of the ecliptic plane is called the "Zodiac." Since ancient times, the Zodiac has been sectioned at intervals of 30 degrees along the ecliptic. Each 30-degree section is designated by a "sign of the Zodiac" and bears the name of the constellation which occupied it in the second century B.C. At that time the sun entered the Zodiac Aries, Υ, at the vernal equinox. The sun-Aries line is used as an inertial reference in the ecliptic plane, and the earth's perihelion is specified by the angle, Λ, subtended by the sun-Aries and sun-earth lines in the ecliptic plane. The earth at winter solstice is near perihelion, the actual deviation as well as the angle Λ are obtained from ephemeris tables using sidereal time.

For practical design purposes it can be assumed that the earth's orbit is circular instead of elliptical and that the earth's position at winter solstice is identical with perihelion with $\Lambda = 90$ degrees. Furthermore, the earth-moon barycenter is assumed to be identical with earth center. These assumptions result in considerable simplifications in heliocentric sun-earth inertial reference coordinates and orbital dynamics. The earth moves about the sun at a constant angular rate, the earth's solstices and equinoxes occur at even 90-degree intervals measured from Aries, the moon's gravitational effects are ignored, and ephemeris tables and calculations are not necessary to specify the earth's seasonal position.

Some of the simplified earth-sun relations are shown in Figure 4. The heliocentric inertial coordinates are denoted by (X_1, Y_1, Z_1) with Λ specifying the earth's seasonal position. Note that when the inertial coordinates are moved to earth center the position of the sun is specified by the angle, λ, between the earth-Aries and earth-sun lines. It is apparent from Figure 4 that $\lambda = \Lambda + 180$ degrees and that both λ and Λ have the same angular rate which is about 0.9565 degree per solar day. At the vernal equinox the sun is between the earth and Aries with $\lambda = 0$ degree, while at the winter solstice the earth-sun line is perpendicular to the earth-Aries line with $\lambda = 270$ degrees. The earth's equatorial plane makes a constant angle, $e = 23.45$ degrees with the ecliptic plane. The ascending line of modes is identical with the Aries inertial reference.

10

FIGURE 4. EARTH-SUN INERTIALLY REFERENCED TO ARIES

Additional properties of the ecliptic, equatorial and orbital planes which are utilized to specify the inertial position of an earth orbiting spacecraft are shown in Figure 5. The top part of Figure 5 represents planar look at the earth and sun as viewed from Aries. Note that the sun's vertical rays relative to the earth's surface obtain their maximum deviation from the equator at either the winter or summer solstice. A spacecraft launched at winter solstice with the ascending line of nodes on the morning terminator could achieve a maximum angle, ψ , between the ecliptic and orbital plane. The angle of orbital inclination is denoted by ι , and Max ψ = e + ι degrees. However, due to orbital regression, ψ takes on all its possible values over a time interval determined by the orbital altitude and inclination. The top part of Figure 5 depicts the equatorial/orbital line of nodes aligned with the Aries inertial reference, but due to orbital regression the two lines of nodes are soon misaligned by the angle Ω shown in the lower part of Figure 5.

The lower part of Figure 5 indicates the angular relations necessary to relate a spacecraft's orbital position to either inertial or solar coordinates. The subscript numbers on angles indicate the sequence in which the rotations must occur. The count may be either forward or backward, but the arrows indicate a forward count rotation that brings the solar into the spacecraft orbital coordinate system. The subscript letters on letters indicate specific reference frames which are defined in the following paragraphs. The coordinates used in this report are earth centered unless specified otherwise. The relation between the solar, inertial and geocentric coordinates are illustrated in Figure 6.

(X_s, Y_s, Z_s) are solar fixed coordinates with the X_s-axis directed from the earth to the sun, the Z_s-axis points north and perpendicular to the ecliptic plane, and the Y_s-axis completes the right-hand triad.

(X_1, Y_1, Z_1) are inertial coordinates with the X_1-axis inertially fixed, pointing toward Aries, and the Z_1-axis perpendicular to the ecliptic plane pointing north. The third axis, Y_1 , completes the right-hand triad. The solar coordinates are transformed into the inertial system by rotating negatively about Z_s by the angle λ . This rotation represents the apparent rotation of the earth in the ecliptic plane relative to the sun as measured from the vernal equinox.

(X_g, Y_g, Z_g) are geocentric inertial coordinates with the X_g-axis in the equatorial plane pointing toward Aries (aligned with X_1), the Z_g-axis
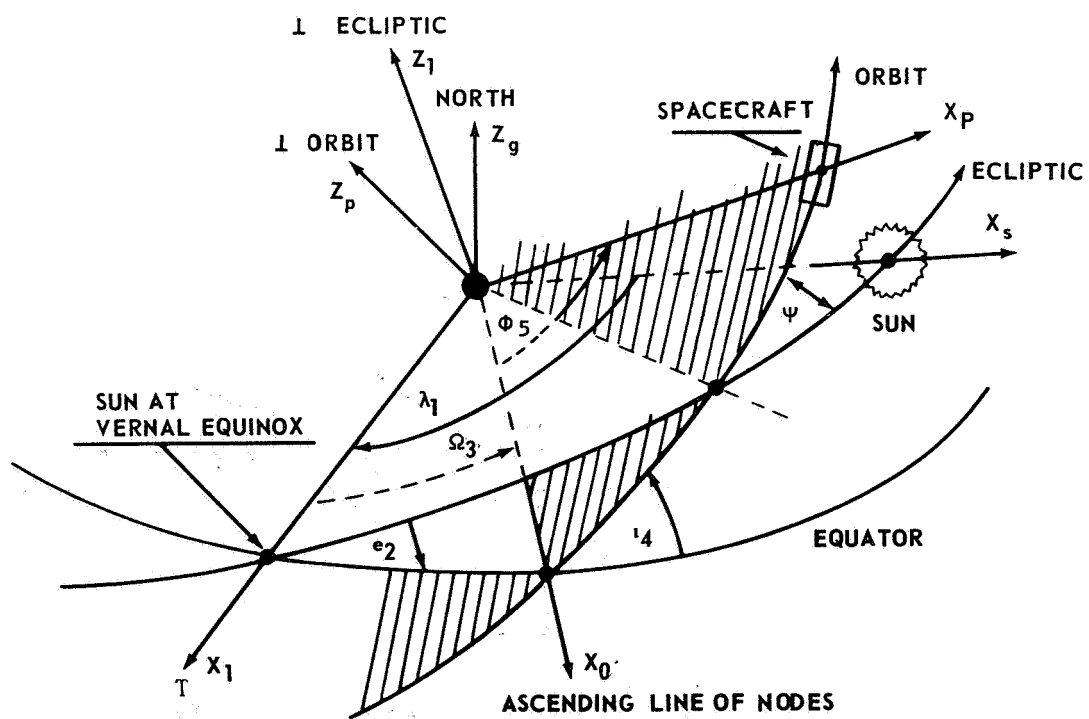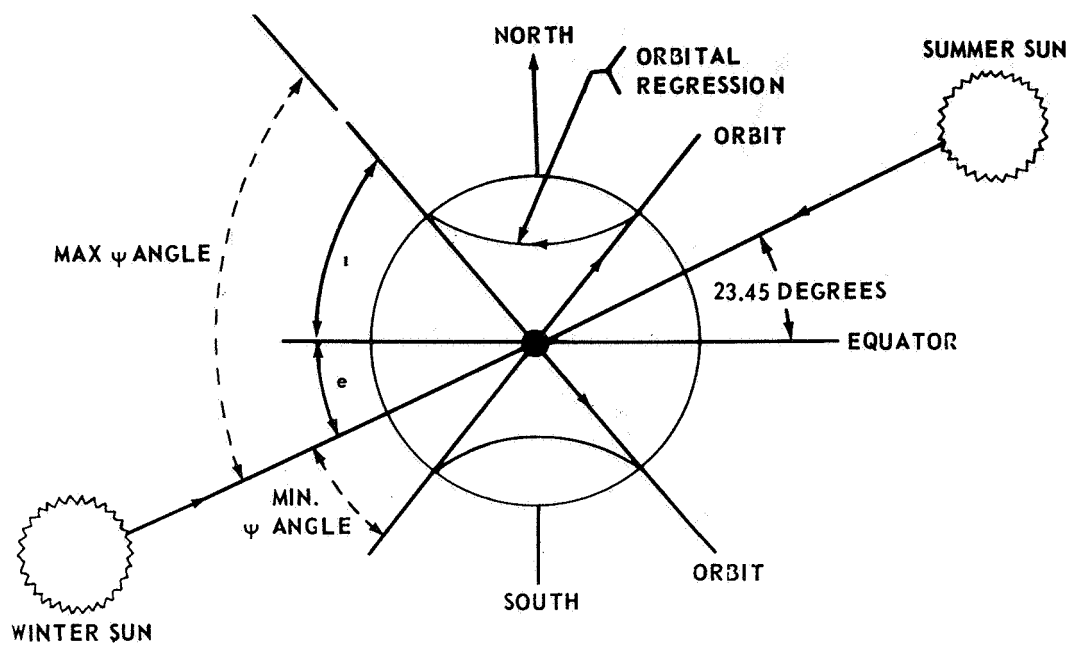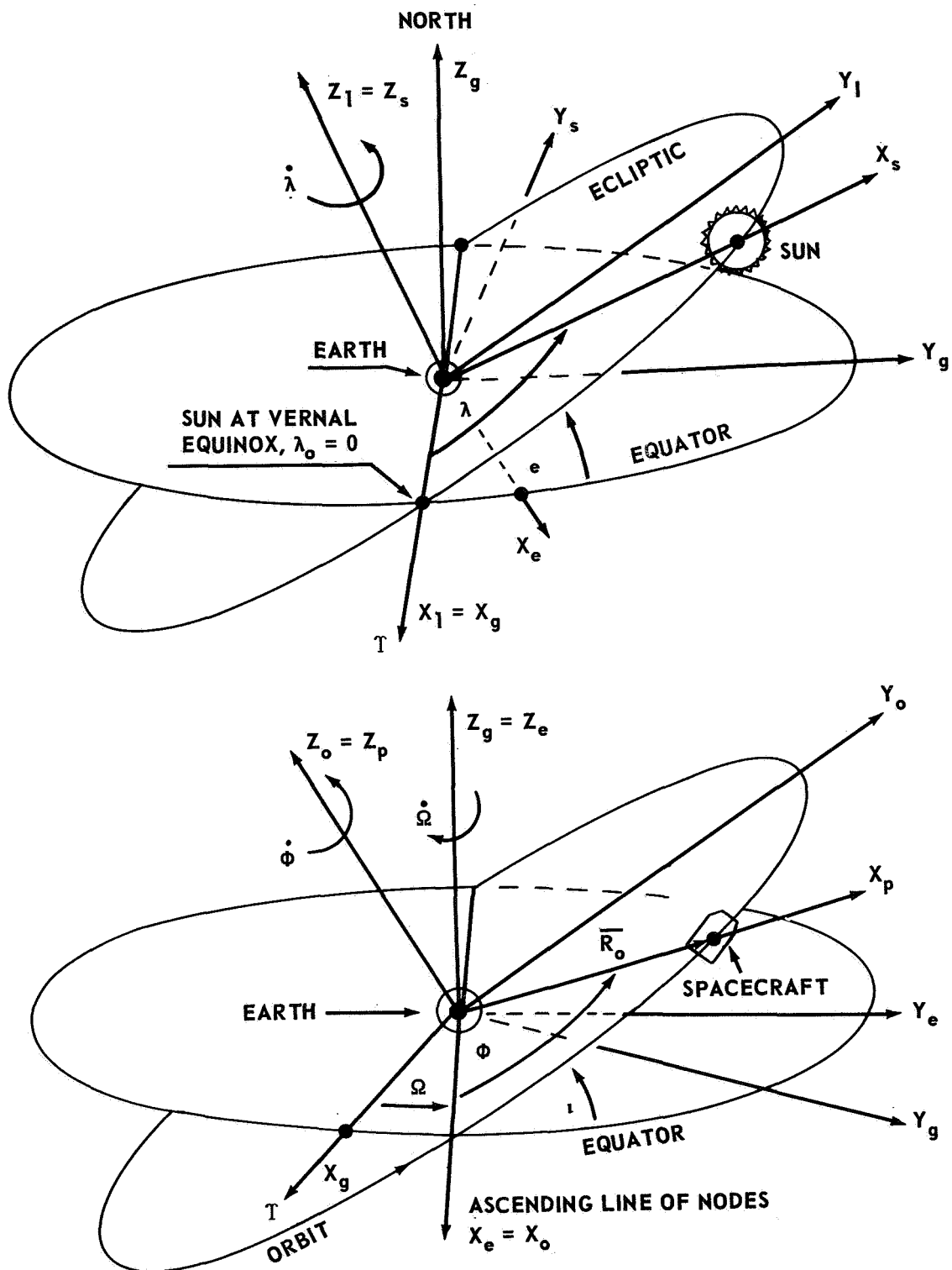
12

FIGURE 5.   EARTH-ORBIT-ECLIPTIC GEOMETRY

13

FIGURE 6. GEOCENTRIC COORDINATE SYSTEMS

directed along the earth's mean rotational axis, positive northward, the Y_g-axis completing a right-hand system in the equatorial plane. The inertial coordinates are transformed into the geocentric inertial system by a negative rotation about X_1 by the angle $e = 23.5$ degrees . The angle e , between the ecliptic and equatorial planes, is always constant and $X_1 = X_g$ is always on the ascending line of nodes between the two planes.

The relation between the local vertical relative to the spacecraft and the orbital and equatorial planes is also illustrated in Figure 6. The time varying angles are the orbital angle, φ , which specifies the spacecraft position relative to the ascending line of nodes between the orbital and equatorial planes, and the orbital regression angle, Ω , which specifies the ascending line of node position relative to inertial direction of Aries (the line of nodes between the equatorial and ecliptic planes) .

(X_e, Y_e, Z_e) is an earth-equatorial system with X_e on the ascending line of nodes between the equatorial and orbit planes, $Z_e = Z_g$ is perpendicular to the equatorial pointing northward and Y_e completes the triad in a positive sense. The geocentric coordinates are transformed into the earth equatorial system by a rotation about Z_g by the angle Ω , between the ecliptic-equatorial and equatorial-orbit lines of nodes. The angle Ω is denoted as the orbital regression angle, and its time derivative as the orbital regression rate. The regression rate is always negative for orbital inclinations less than 90 degrees, hence Ω will usually be a negative angular rotation.

(X_o, Y_o, Z_o) is an orbit-fixed coordinate system with $X_o = X_e$ on the ascending line of nodes between the equatorial and orbit planes, Z_o is perpendicular to the orbit plane pointing northward (aligned with the orbital spin vector) , and Y_o completes the triad. The earth-equatorial system is transformed into the orbital system by a rotation about X_e by the orbital inclination angle, denoted by ι . The angle of inclination can be either positive or negative, but it always remains constant once its initial value is given. The angle of inclination is usually measured positively from the ascending line of nodes, when the spacecraft crosses the equator going from southern to northern hemisphere. When negative values of inclination are used, the reverse type crossing is used as a reference node (retrograde orbits) .

(X_p, Y_p, Z_p) is a rotating local vertical system with X_p directed along the local gravity vector from the earth's center to the spacecraft in orbit. The triad is completed by Y_p . The third axis, Z_p , is perpendicular to the orbital plane directed northward and aligned with the spacecraft (S/C) momentum vector. The orbital fixed coordinates are transformed into the local vertical system by rotating about $Z_o = Z_p$ by the orbital angle φ , which is defined by the orbital angular rate, W_o , times orbital time, t .

The transformation from solar to local vertical coordinates is symbolically expressed by the following sequence of rotations.

$$X_s \longrightarrow X_1 \xrightarrow{\ -e\ } X_g \longrightarrow X_e \xrightarrow{\ \iota\ } X_o \longrightarrow X_p$$

$$Y_s \longrightarrow Y_1 \longrightarrow Y_g \longrightarrow Y_e \longrightarrow Y_o \longrightarrow Y_p$$

$$Z_s \xrightarrow{\ -\lambda\ } Z_1 \longrightarrow Z_g \xrightarrow{\ \Omega\ } Z_e \longrightarrow Z_o \xrightarrow{\ \varphi\ } Z_p$$

The environmental forces acting on the spacecraft are usually given or calculated in the local vertical coordinate system, for example, gravity acts along the negative X_p axis. However, the effect of the environmental forces on the spacecraft motion are usually evaluated in terms of body fixed coordinates. The body fixed system is usually chosen such that the cross products in inertia are zero and/or the body is ideally oriented with respect to a defined reference coordinate system. Hence, definition of at least two additional coordinate systems is necessary.

(X_r, Y_r, Z_r) are mission dependent reference coordinates on which the body axes are to be oriented. If the spacecraft is unperturbed, the body axes (X_b, Y_b, Z_b) are identical to the reference axes. However, if the spacecraft is perturbed from the desired reference, then a three-angle modified Euler transformation (type 3, 2, 1) is necessary to relate the two systems. The modified Euler angles are standard airplane angles which are valid for small angle approximations.

16

(X_b, Y_b, Z_b) are body fixed coordinates which are usually chosen so that the cross products in inertia are zero. The roll axis, X_b, is aligned with the longitudinal body axis. For spacecraft, Z_b is aligned with a bench-mark perpendicular to X_b, and Y_b completes the triad. For aircraft, Z_b completes the triad and Y_b is aligned with the right wing perpendicular to X_b. In either case, Y_b is the pitch axis and Z_b is the yaw axis. For the orbital workshop X_b is along the longitudinal axis and positive in the direction of thrust application; Y_b is along a solar panel (right wing), and Z_b is aligned with benchmark position III. The side view ATM points in the negative Z_b direction (aligned with Position I) and the end view ATM points in the negative X_b direction.

In ATM mode operation it is desirable to have the workshop solar oriented. Hence the solar coordinates are chosen as the reference coordinates and the unperturbed body axes are related to the reference coordinates. The perturbed body axes are then related to the reference coordinates by a modified Euler angle transformation.

The environmental forces in local vertical coordinates are related to the reference coordinates through the previously defined transformations in the orbital, equatorial, and ecliptic planes.
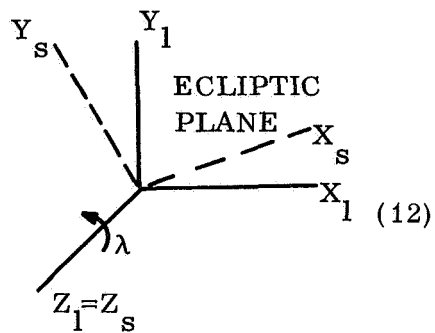
TRANSFORMATIONS

Because the ATM must be solar oriented, solar coordinates must, in some manner, be related to the reference coordinates. This relation depends, of course, on the particular OWS configuration as the side or end view ATM. But in any case, the transformation between the various coordinate systems, as defined in the preceding section, must be developed to find the components of the orbital radius vector, which are known in local vertical coordinates, in solar coordinates. First, the individual transformation matrices are obtained, and are then combined to give the transformation matrix between local vertical and solar coordinates. The resultant matrix is composed of nine directional cosines which are a function of the rotational angles. The matrices are denoted by capital letters with subscripts that indicate the coordinate systems being

related. For example, A_{sl} means that the matrix operates on a vector in inertial coordinates to produce its components in terms of solar coordinates. Vectors are denoted by letters with superscript bars and with one subscript letter to indicate the coordinate system. A superscript tilde indicates the vector transpose of a conventional vector, $\tilde{X}$, as used in forming vector-matrix equations. Unit vectors are denoted by i, j, and k in the respective x, y, and z directions with one subscript to indicate the coordinate system.

The previously defined sequence of transformations is carried out in a rotation-by-rotation manner starting with solar and ending with local vertical coordinates:
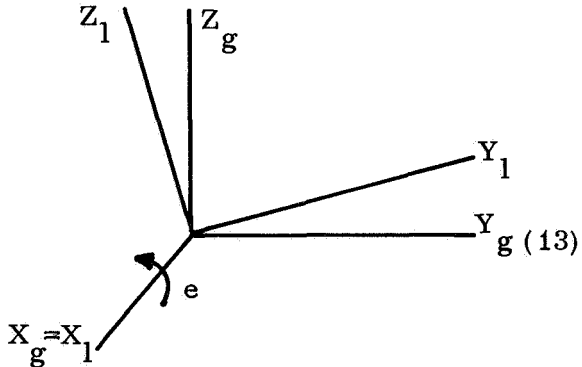
1. The solar-inertial transformation is obtained by a rotation about Z_1 by the angle λ :

$$\tilde{X}_s = A_{sl} \tilde{X}_l \quad ;$$

$$A_{sl} = \begin{bmatrix} C\lambda & S\lambda & 0 \\ -S\lambda & C\lambda & 0 \\ 0 & 0 & 1 \end{bmatrix}$$

(12)

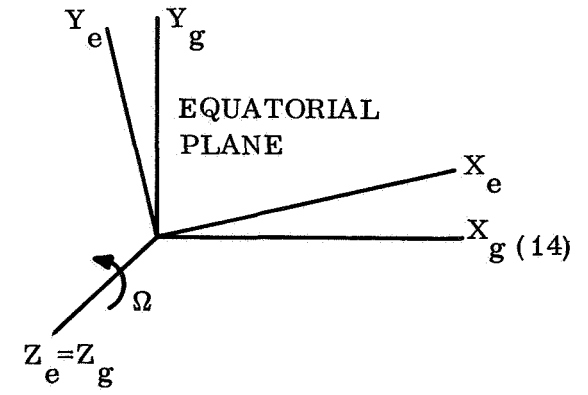2. The inertial-geocentric inertial transformation is obtained by a rotation about X_g by the angle of earth's inclination, e:

$$\tilde{X}_l = A_{lg} \tilde{X}_g \quad ;$$

$$A_{lg} = \begin{bmatrix} 1 & 0 & 0 \\ 0 & Ce & Se \\ 0 & -Se & Ce \end{bmatrix} .$$

(13)

3. The geocentric inertial-equatorial transformation is obtained by a rotation about Z_g by the angle of nodal regression, Ω :
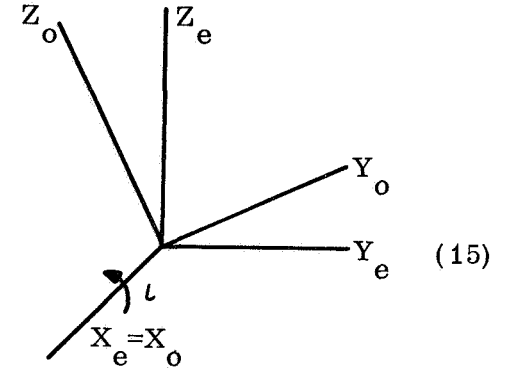
18

$$\tilde{X}_g = A_{ge} \tilde{X}_e \quad ;$$

$$A_{ge} = \begin{bmatrix} C\Omega & -S\Omega & 0 \\ S\Omega & C\Omega & 0 \\ 0 & 0 & 1 \end{bmatrix} . \qquad (14)$$

4. The equatorial-orbital transformation is obtained by a rotation about X_e by the angle of orbital inclination, ι :
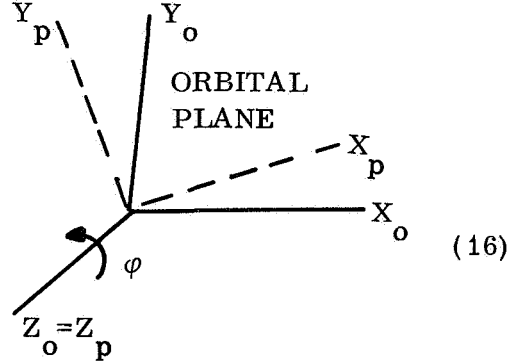
$$\tilde{X}_e = A_{eo} \tilde{X}_o \quad ;$$

$$A_{eo} = \begin{bmatrix} 1 & 0 & 0 \\ 0 & C\iota & -S\iota \\ 0 & S\iota & C\iota \end{bmatrix} . \qquad (15)$$

5. The orbital-local vertical transformation is obtained by a rotation about Z_o by the orbit position angle, φ :

$$\tilde{X}_o = A_{op} \tilde{X}_p \quad ;$$

$$A_{op} = \begin{bmatrix} C\varphi & -S\varphi & 0 \\ S\varphi & C\varphi & 0 \\ 0 & 0 & 1 \end{bmatrix} . \qquad (16)$$

The individual transformations are combined to produce the transformation from local vertical to solar coordinates:

$$\tilde{X}_s = A_{sp} \tilde{X}_p \quad ; \qquad \tilde{X}_p = A_{sp}^{*} \tilde{X}_s \qquad (17)$$

where

$$A_{sp} = A_{sl} A_{lg} A_{ge} A_{eo} A_{op}$$

and the superscript $*$ represents the transposition of the matrix.

The elements of A_{sp} are obtained by substituting for the individual transformations and performing the indicated matrical multiplications in the order indicated. The result is

$$A_{sp} = \begin{bmatrix} A_{11} & A_{12} & A_{13} \\ A_{21} & A_{22} & A_{23} \\ A_{31} & A_{32} & A_{33} \end{bmatrix} \qquad (18)$$

where the directional cosines are

$$A_{11} = C\varphi\,(C\lambda C\Omega + S\lambda S\Omega\,Ce) + S\varphi\,C\iota(-C\lambda S\Omega + S\lambda C\Omega\,Ce)$$
$$+ S\varphi\,S\iota(S\lambda Se) \qquad ,$$

$$A_{12} = -S\varphi(C\lambda C\Omega + S\lambda S\Omega\,Ce) + C\varphi\,C\iota(-C\lambda S\Omega + S\lambda C\Omega\,Ce)$$
$$+ C\varphi\,S\iota(S\lambda Se) \qquad ,$$

$$A_{13} = -S\iota(-C\lambda S\Omega + S\lambda C\Omega\,Ce) + C\iota(S\lambda Se) \qquad (19)$$

$$A_{21} = C\varphi\,(-S\lambda C\Omega + C\lambda S\Omega\,Ce) + S\varphi\,C\iota(S\lambda S\Omega + C\lambda C\Omega\,Ce)$$
$$+ S\varphi\,S\iota(C\lambda Se) \qquad ,$$

$$A_{22} = -S\varphi\,(-S\lambda C\Omega + C\lambda S\Omega\,Ce) + C\varphi\,C\iota(S\lambda S\Omega + C\lambda C\Omega\,Ce)$$
$$+ C\varphi\,S\iota(C\lambda Se) \qquad ,$$

20

$$A_{23} = -S\iota(S\lambda S\Omega + C\lambda C\Omega Ce) + C\iota(C\lambda Se)\qquad,$$

$$A_{31} = C\varphi(-S\Omega Se) + S\varphi C\iota(-C\Omega Se) + S\varphi S\iota(Ce)\qquad,$$

<div align="right">(19)
(cont'd)</div>

$$A_{32} = S\varphi(S\Omega Se) + C\varphi C\iota(-C\Omega Se) + C\varphi S\iota(Ce)\qquad,$$

$$A_{33} = C\Omega(S\iota Se) + C\iota Ce$$

The directional cosines, as derived, are functions of five physically meaningful angles of which: (1) two are constant, the equatorial to ecliptic plane angle (e) and, once specified, the orbital inclination angle (ι) ; (2) two vary slowly with time, the seasonal position of the earth as it rotates about the sun at about one degree per day is given by the angle λ and the orbital precession (nodal regression) angle (Ω) with a rate of about five degrees per day depending on the orbital inclination and altitude; and (3) one varies rapidly with time, the orbital angle φ which specifies the position of the satellite in orbit and varies at the orbital rate, W_o . These angles and their angular rates are given in Table I.

In examination of the directional cosines, it becomes evident that they are quasi-cyclic functions of the three time varying angles λ, Ω, and φ . It is also evident that for one year or longer time periods the directional cosines will take on all their possible values; hence, the time-of-day, time-of-year, launch location and the initial values of λ_0 and Ω_0 are not significant factors in evaluating the energy requirements to overcome gravity gradient effects. The variation of the gravity gradient is primarily due to the change in the directional cosines for a fixed vehicle orientation. However, for short time periods, on the order of a few orbits, the variation in λ and Ω is small enough that for practical considerations they may be treated as constants which have been selected to produce worst case conditions. One such selection is $\lambda = \lambda_0 = 270$ degrees for the time of winter solstice and $\Omega = \Omega_0 = 180$ degrees for the maximum angle condition between the orbital and ecliptic planes at the winter solstice.

Substitution of $\lambda = 270$ degrees **and** $\Omega = 180$ degrees into the directional cosines produces the following simplified directional cosines which are only valid for short time periods near the time of winter solstice:

TABLE I. ANGLE LIMITS AND RATES

$$\varphi = W_o t \quad (\text{rad}) \quad ; \quad t \ (\text{sec})$$

$$W_o = (GM/R_o^3)^{1/2} \quad (\text{rad/sec})$$

$$A_{mn} = \cos(\alpha_{mn}) \quad , \quad m \text{ and } n = 1, 2, 3$$

$$e = 23.45 \quad (\text{deg})$$

$$0 \le \iota \le 180 \quad (\text{deg})$$

$$\Omega = \Omega_0 + \dot{\Omega} t' \quad (\text{deg})$$

$$0 \le \Omega_0 \le 360 \quad (\text{deg})$$

$$\dot{\Omega} = -9.9728 (R_e/R_o)^{7/2} \cos \iota \quad (\text{deg/day})$$

$$t' = \text{time in days}$$

$$\lambda = \lambda_0 + \dot{\lambda} t' \quad (\text{deg})$$

$$0 \le \lambda_0 \le 360 \quad (\text{deg})$$

$$\dot{\lambda} = 0.98565 \quad (\text{deg/day})$$

$$A_{11} = S\varphi \, C(\iota + e) = S\varphi \, C\psi \quad ,$$

$$A_{12} = C\varphi \, C(\iota + e) = C\varphi \, C\psi \quad ,$$

$$A_{13} = -S(\iota + e) = -S\psi \quad ,$$

$$A_{21} = -C\varphi = -C\varphi \quad ,$$

$$A_{22} = +S\varphi = S\varphi \quad ,$$

$$A_{23} = 0 = 0 \quad ,$$

$$(20)$$

$$A_{31} = S\varphi \, S(\iota + e) = S\varphi \, S\psi \quad ,$$

$$A_{32} = C\varphi \, S(\iota + e) = C\varphi \, S\psi \quad ,$$

<div align="right">

(20)

(cont'd)

</div>

and

$$A_{33} = C(\iota + e) = C\psi \quad .$$

In this simplified form, the directional cosines are functions of only one time varying angle (φ) , one specified angular parameter (ι) and one constant angle (e) , and can easily be evaluated without resorting to elaborate computer routines or facilities. However, the gravity gradient torques and the energy requirements to counteract these torques represent worst case conditions when calculations are based on use of the simplified directional cosines with $\psi = \iota + e = 45$ degrees . Hence, the simplifying conditions can be utilized during preliminary design work to establish maximum fuel reserves and control requirements for an OWS being acted upon by gravitational torques.

At this point, the transformation between local vertical and solar coordinates has been established for both the general case and the simplified fixed time-of-year case. The task remains, however, to relate the OWS body axes to a desired reference frame. As pointed out in the section on coordinate systems, the reference frame is mission dependent. Therefore, for each OWS operational mode or for each configuration, a desired reference frame must be selected, and a transformation derived which relates the body axes to the reference axes. Then the components of the local radius vector, $\overline{R}_o$, must be obtained in body coordinates through use of the derived transformations. These components are substituted into the gravity gradient torque equations and the gravity gradient effects evaluated for each configuration or operational mode. For example, an OWS with rigidly attached ATM must have the reference axes solar oriented during ATM operation to view the sun and to receive the maximum solar energy without gimbals on the solar panels. Under ideal control conditions the body axes are identically aligned with the reference axes and for the example above, the simplified directional cosines can be used to evaluate the gravity gradient torques without additional transformations.

The DWS with end view ATM, as illustrated in Figure 7, has the ATM fixed and viewing in the negative X_b-axis direction. Hence, in an ATM mode of operation the positive longitudinal body axis must be pointing opposite the sun line vector, X_s . This pointing requirement, however, does not place any constraints on either the Y_b - or Z_b - axis. Hence, the solar axes can be related to the body axes by a 180-degree rotation about either the Z_s - or the Y_s-axis . Assuming initial alignment of the body and solar axes, a 180-degree rotation is made about the Z_s-axis to produce the desired solar orientation:

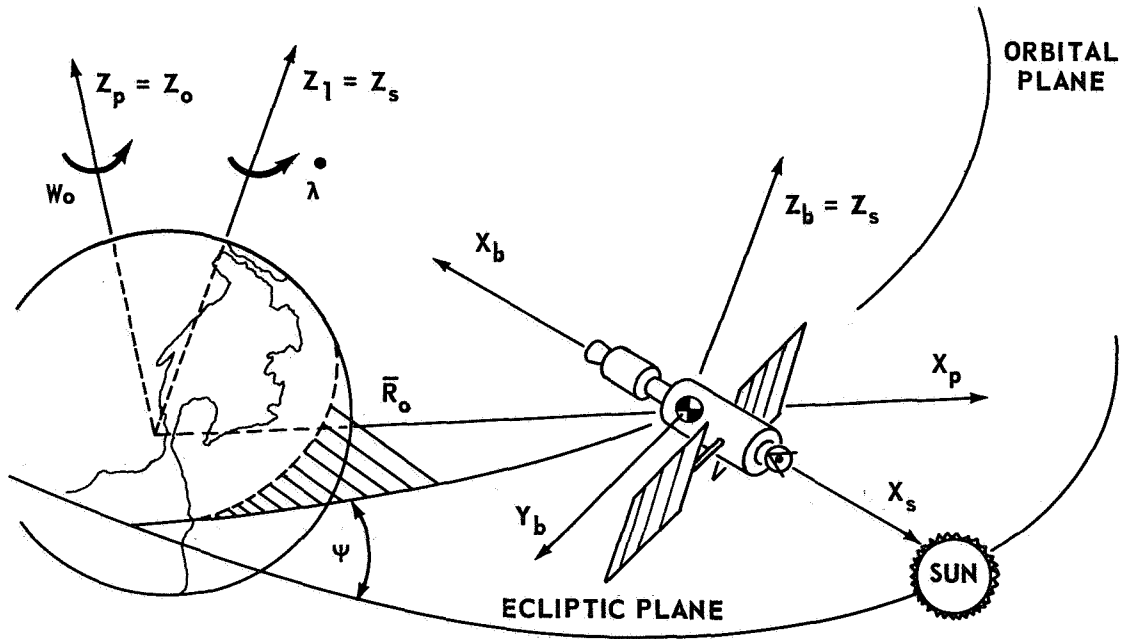$$\tilde{X}_b = A_{bs} \tilde{X}_s \qquad (21)$$

FIGURE 7. END VIEW ATM, SOLAR FIXED ORIENTATION

where

$$A_{bs} = \begin{bmatrix} -1 & 0 & 0 \\ 0 & -1 & 0 \\ 0 & 0 & 1 \end{bmatrix} \ .$$

Combining this transformation with the local vertical to solar transformation, equation (16), gives

$$\tilde{X}_b = A_{bs} A_{sp} \tilde{X}_p \qquad (22)$$

$$\tilde{X}_b = \begin{bmatrix} -A_{11} & -A_{12} & -A_{13} \\ -A_{21} & -A_{22} & -A_{23} \\ A_{31} & A_{32} & A_{33} \end{bmatrix} \tilde{X}_p$$

The above transformation is utilized to obtain the vector components of the radius vector in body coordinates:

$$\bar{R}_o = R_o i_p$$

$$\bar{R}_o = R_o(-A_{11} i_b - A_{21} j_b + A_{31} k_b)$$

and thus

$$R_x = -R_o A_{11} \quad ,$$

$$R_y = -R_o A_{21} \quad , \qquad (23)$$

$$R_z = R_o A_{31}$$

25

Substitution of R_x, R_y, and R_z into the gravity gradient torque equation, (10), with the products of inertia being zero, gives

$$T_x = \frac{-3\mu}{R_o^3}(I_z - I_y)A_{21}A_{31} = -2C_x A_{21}A_{31} \quad ,$$

$$T_y = \frac{-3\mu}{R_o^3}(I_x - I_z)A_{11}A_{31} = -2C_y A_{11}A_{31} \quad , \tag{24}$$

and

$$T_z = \frac{3\mu}{R_o^3}(I_y - I_x)A_{21}A_{11} = 2C_z A_{21}A_{11} \quad ,$$

where the directional cosines (A's) are as defined in the section on transformations, equation (18). For a simplified analysis at the time of winter soltice, the torque equations are evaluated with $\lambda_0 = 270$ degrees and $\Omega_0 = 180$ degrees substituted into the directional cosines, equations (20). The following simplified equations may be utilized to obtain the gravity gradient torque effects on the OWS with end view ATM without resorting to computational facilities:

$$A_{11} = S\varphi\, C\psi$$

$$A_{21} = -C\varphi \tag{25}$$

$$A_{31} = S\varphi\, S\psi$$

and hence,

$$T_x = C_x S2\varphi\, S\psi \quad ,$$

$$T_y = -C_y S^2\varphi\, S2\psi \quad , \tag{26}$$

$$T_z = -C_z S2\varphi\, C\psi \quad .$$

An indication of the energy requirements necessary to counteract the gravitational torques on the OWS with end view ATM in solar orientation is

obtained by integrating the torque equations with φ given as a function of time and with the angle ψ being constant. The resultant momentum vector components are

$$H_x = (-C_x/2W_o) C2\varphi\, S\psi + H_{xo} \quad ,$$

$$H_y = (-C_y/4W_o)(2\varphi - S2\varphi)\, S2\psi + H_{yo} \quad , \tag{27}$$

$$H_z = (C_z/2W_o) C2\varphi\, C\psi + H_{zo} \quad .$$

Two cases of momentum accumulation may be entertained: (1) the constants of integration can be evaluated by assuming the initial values of momentum are zero, and/or (2) the constants of integration can be assumed to be zero, in which case the initial momentum values are not necessarily zero. These cases are evaluated in the section on energy requirements.

Some of the pertinent features of the solar oriented OWS with end view ATM are:

1. The ATM is rigidly attached to the workshop and is not gimbaled. The end of the OWS is always exposed to the sun.

2. Solar panels are perpendicular to the ATM viewing axis and once deployed are not gimbaled. Maximum solar energy is received.

3. The vehicle must continuously pitch, yaw, and roll with respect to the local vertical to maintain its fixed solar orientation. Hence maximum gravity gradient torques are encountered. A secular momentum component occurs about the y-axis where the difference in vehicle inertias is greatest.

4. Torques are maximized at $\psi = 45$ degrees which corresponds to an orbital inclination of 21.55 degrees. The X- and Z-axis torques are cyclic with a period one-half that of the orbit.

5. At $\psi = 90$ degrees the OWS is at an unstable equilibrium point for a symmetric vehicle (the torques are all zero).

SIDE VIEW ATM, XOP MODE

The side view ATM Workshop configuration B-1 (Fig. 8) must have the negative Z_b-axis pointing toward the sun and the Y_b-axis perpendicular to the sun line to preclude articulating the solar panels and to maximize the solar power received. It is also desirable to minimize the momentum required to maintain attitude hold while viewing the sun. One method of minimizing the momentum while satisfying the solar pointing requirements is to align the long-itudinal body axis, X_b, in the orbital plane (XOP mode). Hence, the problem at hand is to relate the body axes to a known coordinate system while satisfying these constraints. It is assumed that the body axes are not misaligned from their desired orientation; therefore, the reference axes are identical to the body axes.

Before the operations defining the body-reference coordinates are carried out, a common vector space must be chosen in which to perform the
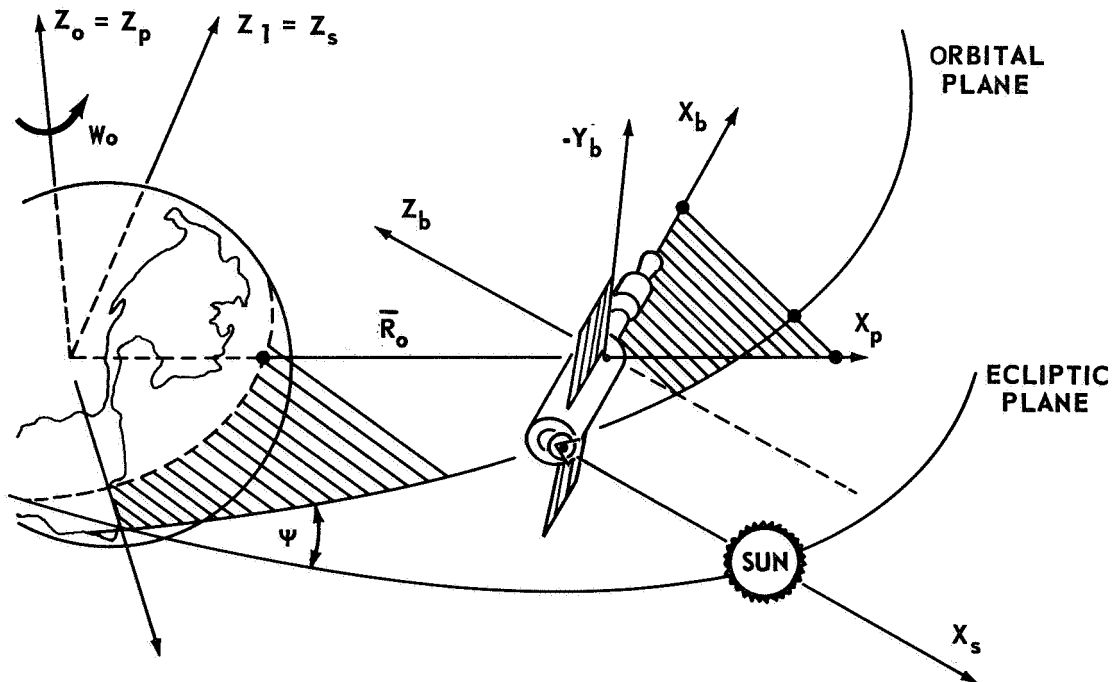

FIGURE 8. SIDE VIEW ATM, SEMISOLAR FIXED ORIENTATION, XOP MODE
(X_b-axis in orbital plane and Z_b-axis opposite sunline)

necessary vector operations. Since one axis is solar oriented, solar coordinates are selected[2]. The vectors in local vertical coordinates are transformed into the solar coordinates by the previously defined directional cosine matrix relating the orbital, equatorial, and ecliptic planes. As previously shown in equations (17) and (18) the unit vectors in local vertical coordinates are

$$i_p = A_{11} i_s + A_{21} j_s + A_{31} k_s \quad ,$$

$$j_p = A_{12} i_s + A_{22} j_s + A_{32} k_s \quad , \tag{28}$$

and

$$k_p = A_{13} i_s + A_{23} j_s + A_{33} k_s \quad ,$$

when expressed as functions of solar coordinates. Now, the body-reference axes may be defined to satisfy the workshop orientation requirements.

Aligning Z_b with the negative sun line vector requires that

$$k_b = - i_s \tag{29}$$

Aligning X_b in the orbital plane requires that X_b be expressed as a linear combination of i_p and j_p which define the orbital plane[3]. Orbital plane alignment requires that X_b be perpendicular to k_p and, by definition, to Z_b. Hence, X_b can be expressed as the cross product between the unit vectors k_p and i_s:

$$X_b = - (i_s) \times (k_p) \tag{30}$$

---

2. Since one axis is to be in the orbital plane either orbital or local vertical coordinates could have been selected as a basis for body axes definition; however, the end result is the same, although the transformation matrices would have been different.

3. Note that the sign of X_b is not uniquely determined. Interchanging the cross product defining X_b would have resulted in a sign change in X_b. Such a sign change could alter the conditions under which control moment gyros would physically saturate.

and

$$i_b = \frac{-(i_s) \times (k_p)}{|(i_s) \times (k_p)|} \qquad .$$

Transforming k_p into solar coordinates and carrying out the indicated operations:

$$\overline{X}_b = -(i_s) \times (k_p) = A_{33} j_s - A_{23} k_s \tag{31}$$

and

$$i_b = \frac{A_{33}}{(A_{33}^2 + A_{23}^2)^{1/2}} j_s - \frac{A_{23}}{(A_{33}^2 + A_{23}^2)^{1/2}} k_s$$

The third reference coordinate Y_b is obtained by taking the cross product between the unit vectors directed along X_b and Z_b to complete a right-hand triad: Letting $D = (A_{33}^2 + A_{23}^2)^{1/2}$,

$$j_b = (k_b) \times (i_b) = (-i_s) \times \left(\frac{A_{33}}{D} j_s - \frac{A_{23}}{D} k_s \right)$$

$$= -\frac{A_{23}}{D} j_s - \frac{A_{33}}{D} k_s \qquad . \tag{32}$$

In vector matrix notation the transformation from solar to body coordinates for the side view ATM [equations (29), (31), and (32)] is

$$\tilde{X}_b = C_{bs} \tilde{X}_s \qquad , \tag{33}$$

where

$$C_{bs} = \begin{vmatrix} 0 & \frac{A_{33}}{D} & -\frac{A_{23}}{D} \\ 0 & -\frac{A_{23}}{D} & -\frac{A_{33}}{D} \\ -1 & 0 & 0 \end{vmatrix}$$

The body system is then related to the local vertical system by

$$\tilde{X}_b = C_{bs} \tilde{X}_s = C_{bs} A_{sp} \tilde{X}_p \equiv B_{bp} \tilde{X}_p \quad , \tag{34}$$

where

$$B_{bp} = \begin{vmatrix} B_{11} & B_{12} & B_{13} \\ B_{21} & B_{22} & B_{23} \\ B_{31} & B_{32} & B_{33} \end{vmatrix} \quad ; \quad A_{sp} \equiv \begin{vmatrix} A_{11} & A_{12} & A_{13} \\ A_{21} & A_{22} & A_{23} \\ A_{31} & A_{32} & A_{33} \end{vmatrix} \quad .$$

Utilizing equation (34), the vector from the earth's center to the spacecraft in body coordinates is

$$\overline{R}_o = R_o B_{11} i_b + R_o B_{21} j_b + R_o B_{31} k_b = R_o i_p \quad .$$

Evaluating the components of $\overline{R}_o$ gives

$$\frac{R_x}{R_o} = B_{11} = \frac{A_{33}}{D} A_{21} - \frac{A_{23}}{D} A_{31} \quad ,$$

$$\frac{R_y}{R_o} = B_{21} = - \frac{A_{23}}{D} A_{21} - \frac{A_{33}}{D} A_{31} \tag{35}$$

$$\frac{R_z}{R_o} = B_{31} = - A_{11}$$

where

$$D^2 = A_{33}^2 + A_{23}^2$$

and the directional cosines are as previously defined in the section on trans-
formations, equations (19).

Substituting the components of $\overline{R}_o$ into the gravity gradient torque
equation (10) with the products of inertia zero gives

$$T_x = \frac{3\mu}{R_o^3}(I_z - I_y) B_{21} B_{31} = 2C_x B_{21} B_{31} \quad ,$$

$$T_y = \frac{3\mu}{R_o^3}(I_x - I_z) B_{11} B_{31} = 2C_y B_{11} B_{31} \quad , \tag{36}$$

and

$$T_z = \frac{3\mu}{R_o^3}(I_y - I_x) B_{11} B_{21} = 2C_z B_{11} B_{21}$$

as the general gravity gradient torque components in the selected body-reference
coordinate system. Notice that the B_{mn}'s are given in terms of five angles,
three of which vary with time. However, valid results can be obtained by
assuming conditions which eliminate two of the time-varying angles.

For a simplified, fixed time-of-year analysis substitute $\lambda = 270$ degrees
for the time of winter solstice and $\Omega = 180$ degrees for the maximum angle
between the ecliptic and orbit planes into the transformation components. The
result is summarized in equation (20) and the elements of B_{bp} become

$$D = (A_{33}^2 + A_{23}^2)^{1/2} = C\psi \quad ,$$

$$B_{11} = -C\varphi \quad ,$$

$$B_{21} = -S\varphi S\psi \quad , \tag{37}$$

and

$$B_{31} = -S\varphi C\psi$$

When these simplified directional cosines, equation (37), are substituted into equation (36),

$$T_x = C_x S^2 \varphi S2\psi \quad ,$$

$$T_y = C_y S2\varphi C\psi \quad ,$$

$$(38)$$

and

$$T_z = C_z S2\varphi S\psi$$

These equations contain only one time varying angle which is known as a function of the orbital angular rate, i.e., $\varphi = W_o t$. Integrating with respect to time gives the following momentum components due to gravity gradient torques:

$$H_x = (C_x/4W_o)(2\varphi - S2\varphi)S2\psi + H_{xo}$$

$$H_y = (-C_y/2W_o)C2\varphi C\psi + H_{yo}$$

$$(39)$$

and

$$H_z = (-C_z/2W_o)C2\varphi S\psi + H_{zo}$$

Meaningful results about the effects of gravity gradient torques on the workshop and the energy requirements to maintain attitude hold can be obtained from the simplified torque and momentum equations. However, long period cyclic effects due to regression of nodes or the earth's rotation about the sun can only be evaluated by using torque equations as a function of three time-varying angles.

Some of the pertinent features of the side view ATM with the long body axis in the orbital plane are illustrated in Figure 8 and the characteristics of such an orientation are:

1. The side view ATM is not gimbaled.

2. The solar panels are not gimbaled, nor are they ever shaded by the ATM. Hence maximum solar energy is received.

3. The vehicle must continuously pitch and/or yaw at the orbital regression rate (about 6 degrees/day) and roll at the solar look angle rate (about 3.5 degrees/day) .

4. With respect to the local vertical, the vehicle pitches and/or yaws continuously at the orbital rate, W_o . Thus, the torques about the Y- and Z-axis are cyclic, peaking at their maximum possible values twice each orbit.

5. The same side of the vehicle is always exposed to the sun, a factor to consider in designing the environmental control system.

6. The X-axis torque is secular, but the moment coefficient is minimum for a near symmetric vehicle.

7. The axes are orientated so that the axis of minimum inertia, X_b , is always in the orbital plane, the axis of maximum inertia, Z_b , is opposite the sun line vector, and the axis of intermediate inertia is perpendicular to the sun line vector. Such a semi-solar fixed orientation minimizes the energy required for solar attitude hold.

PERPENDICULAR TO ORBIT PLANE MODE

The reference coordinates for the OWS in a perpendicular to orbit plane (POP) mode are chosen so that only one degree of freedom is required for sun tracking on the gimbals of either the ATM or solar panels. The gimbal limitation requires an OWS configuration similar to Saturn V Workshop configuration B-1, but with a side view ATM that gimbals in the X_b and Z_b plane. The operational ATM would be aligned in the general negative Z_b direction and point toward the sun. Hence the Z_b-axis must lie in the plane defined by the sun line and the perpendicular to orbit vectors, and the Y_b-axis

34

must be perpendicular to the plane so that maximum solar energy can be received. In a POP mode orientation, the longitudinal body axis, X_b, is by definition perpendicular to the orbit plane and is, therefore, perpendicular to the local radius vector from the earth's center to the OWS, aligned with the orbital momentum vector.

The OWS in POP mode orientation is in an unstable equilibrium position. The gravity gradient torques for a symmetric vehicle would normally be zero without axes misalignment. It has been assumed, however, that the OWS will continuously roll to limit ATM gimbal requirements. The torque about the X-axis will not be zero unless the vehicle is symmetric, so that the products of inertia of the Y- and Z-axis are equal. With axes misalignment, or under the influence of inflight perturbations, the gravity gradient torques tend to destabilize the POP mode oriented OWS. The torque components will be derived in general form and in simplified form using fixed time of year assumptions. The simplified form equations will then be integrated to give an indication of the energy requirements for attitude hold under the influence of gravity.

Figure 9 indicates the pertinent features of an OWS in POP mode orientation. To view the sun, the OWS must continuously roll at the orbital angular rate with respect to the local vertical, and the ATM and solar panels must be slowly gimbaled due to orbital plane regression and seasonal changes in the sun's perpendicular rays upon the earth. The gimbal rate is about 3.5 degrees per day which is the time rate of change in the solar angle β as defined in the section entitled Solar Look Angles. Since the OWS is aligned with the orbital plane and the radius vector from earth to spacecraft, the local vertical coordinates are selected as the system in which to define the reference coordinates.

Since X_b must be perpendicular to the orbital plane and hence the X_p-axis, let

$$X_b = Z_p \quad \text{so that} \quad i_b = k_p \quad . \tag{40}$$

The Y_b-axis must be perpendicular to X_b and also to the sun line vector X_s so that only one degree of freedom is required to maintain the solar panels directed toward the sun. Hence, Y_b is perpendicular to the plane determined by X_b and X_s. A unit vector in the direction[4] of Y_b is defined by the vector cross product,

---

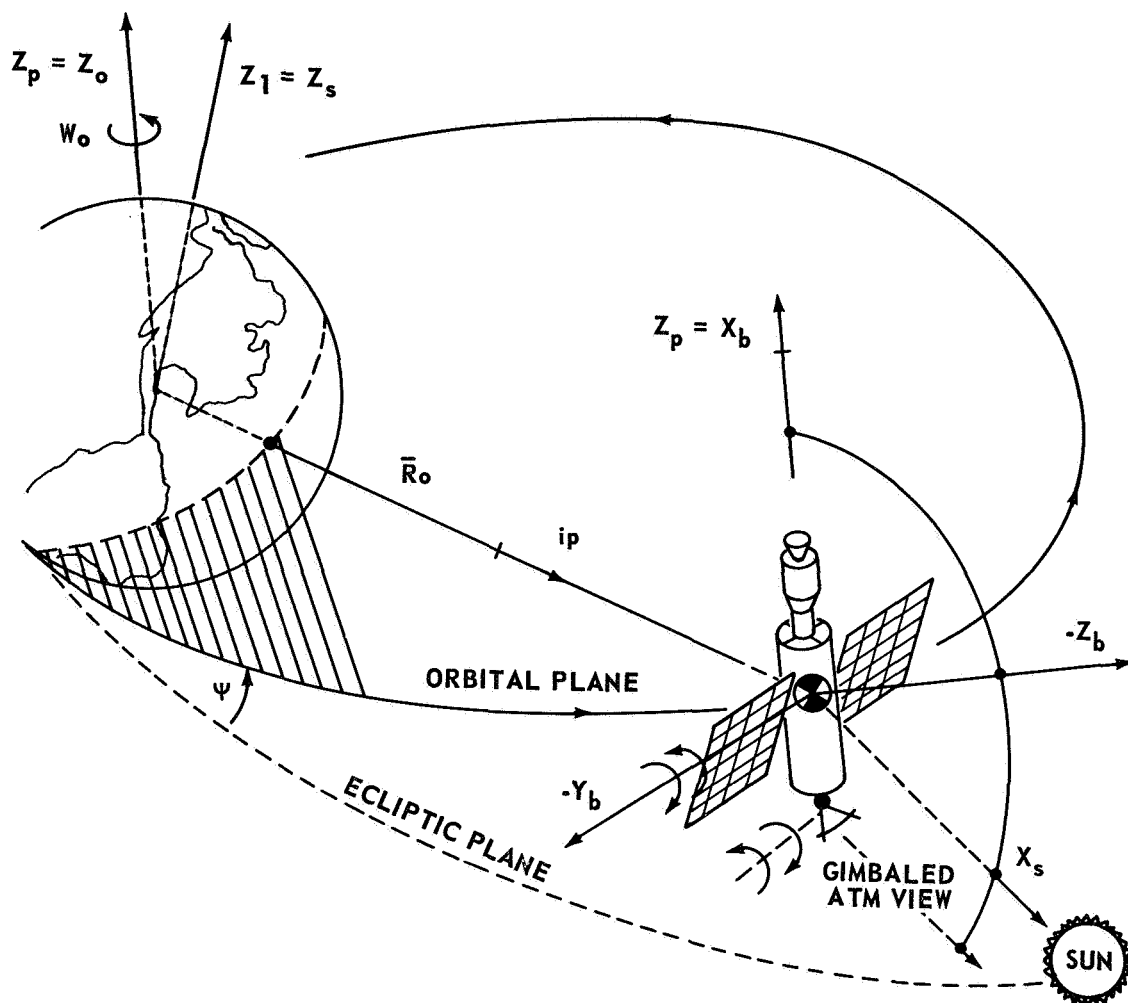4. The sign of j_b is not uniquely determined

FIGURE 9. POP MODE OWS WITH GIMBALED
ATM AND SOLAR PANELS

36

$$j_b = \frac{(k_p) \times (i_s)}{\left|(k_p) \times (i_s)\right|} \tag{41}$$

where i_s in local vertical coordinates is given in terms of previously defined directional cosines, equations (17), as

$$i_s = A_{11} i_p + A_{12} j_p + A_{13} k_p$$

Performing the indicated vector operations and letting $E = \left(A_{11}^2 + A_{12}^2\right)^{1/2}$ gives

$$j_b = -\frac{A_{12}}{E} i_p + \frac{A_{11}}{E} j_p \tag{42}$$

The third reference coordinate, Z_b, is defined by completing a right-hand triad, hence

$$k_b = i_b \times j_b = -\frac{A_{11}}{E} i_p - \frac{A_{12}}{E} j_p \tag{43}$$

Arranging equations (40), (42), and (43) in vector-matrix form, the transformation from reference coordinates (unperturbed body axes) to the local vertical system is given by

$$\tilde{X}_b = \begin{bmatrix} 0 & 0 & 1 \\ -\dfrac{A_{12}}{E} & \dfrac{A_{11}}{E} & 0 \\ -\dfrac{A_{11}}{E} & -\dfrac{A_{12}}{E} & 0 \end{bmatrix} \tilde{X}_p \tag{44}$$

The components of the orbital radius vector are determined by utilizing equation (44),

$$\overline{R}_o = R_o i_p = R_o\left(-\frac{A_{12}}{E} j_b - \frac{A_{11}}{E} k_b\right) \tag{45}$$

Hence,

$$R_x = 0 \quad,$$

$$R_y = -R_o\left(\frac{A_{12}}{E}\right) \quad,$$

and

$$R_z = -R_o\left(\frac{A_{11}}{E}\right) \quad.$$

Substitution of equation (45) into the gravity gradient torque equation (10), where the products of inertia are zero, gives the POP mode torque equations

$$T_x = 2C_x A_{11} A_{12}/\left(A_{11}^2 + A_{12}^2\right)$$

$$T_y = 0 \quad,$$

$$T_z = 0$$

(46)

and

Using the simplified directional cosine values listed in equation (20) gives $A_{11} = S\varphi\, C\psi$ and $A_{12} = C\varphi\, C\psi$, so that equations (46) become

$$T_x = C_x S(2\varphi) \quad,$$

$$T_y = 0$$

(47)

and

$$T_z = 0 \quad.$$

38

Integrating equations (47) with respect to time gives the momentum, i.e., $\varphi = W_o t$, $dt = d\varphi/W_o$, components,

$$H_x = \left(- C_x/2W_o\right)C(2\varphi) + H_{xo}$$

$$H_y = H_{yo} \qquad , \qquad\qquad\qquad (48)$$

and

$$H_z = H_{zo} \qquad .$$

If the OWS is symmetric, the moments of inertia I_z and I_y are identical so that the torque and momentum about the X-axis is also zero. Hence, a symmetric vehicle in the POP mode orientation is at an unstable equilibrium position with the torques about all axes being zero. Any perturbation or axes misalignment tends to force the vehicle from this orientation, which will be further analyzed in the next section, Body Axes Misalignment.

The factors which were pertinent in selecting the POP mode reference coordinates (Fig. 9) and the characteristics of an OWS in such an orientation are listed below:

1. By continuously rolling about the X_b-axis with respect to the local vertical (360 degrees per orbit) only one degree of gimbal freedom is required on both the ATM and solar panels to track the sun.

2. By performing a 180-degree turn about the Z_b-axis each time the orbital and ecliptic planes coincide (about 30-day intervals), the gimbal limits on the ATM and solar panels can be further restricted to 16.5 degrees to 90 degrees on the ATM and 0 degree to 73.5 degrees on the solar panels for an orbital inclination of 50 degrees. Such a manuever would also prevent shadowing of the ATM by the workshop.

3. Since the vehicle is in an unstable equilibrium position, the effects of gravity gradient torques and the energy requirements are minimized.

4. Because the vehicle is broadside to its velocity vector, the aerodynamic torques will be maximized.

5. The vehicle inertial properties will continuously change as the ATM is gimbaled.

6. Body axes misalignment from either the reference coordinates or the principal axes cause a large increase in the energy requirements due to increased gravity gradient torque effects.

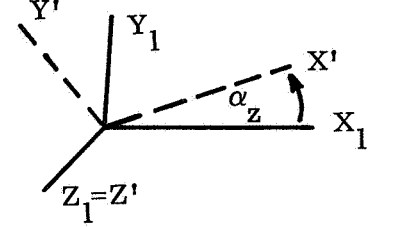7. Gimbal angle control and command for both the ATM and solar panels could come from the same source.
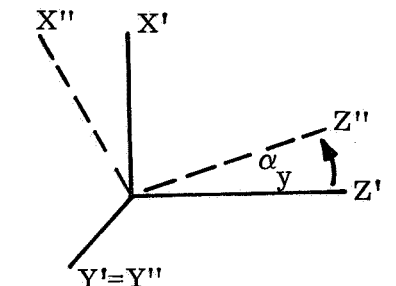
BODY AXES MISALIGNMENT

Two cases of body axes misalignment will be entertained: Case 1, body axes misaligned from the principal axes in which case the products of inertia are not zero by definition of such a misalignment; Case 2, body axes misaligned from the reference axes where to simplify the necessary mathematical manipulations the products of inertia are assumed to be zero. In each case the same coordinate transformation is utilized, but the Euler angle symbols are different to avoid possible confusion between the two cases. Both cases, however, have similar first order effects on torque and momentum. Finally, the gravity gradient torques due to axes misalignment are calculated for a satellite in a gravity gradient stable mode, as well as for the POP mode case.
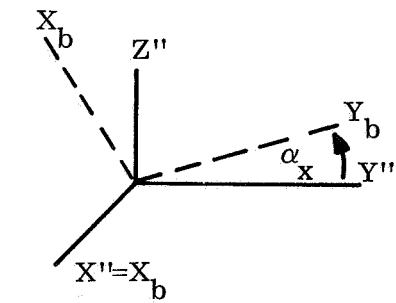
Case 1

Assuming that the body axes are misaligned from the principal axes requires development of an inertia dyadic transformation to relate the moments and products of inertia of the body axes to the moments of inertia of the principal axes in which the products of inertia are zero. This operation will give equations by which the products of inertia can be eliminated from the gravity gradient torque equations and the torque expressed as a function of the misalignment angles and the moments of inertia which are known in the principal axes system. First, the transformation from body to principal axes will be defined; then the tensor transformation will be derived. Finally, the gravity gradient torque equations will be evaluated and the momentum equations obtained by integration of the torque equations. Since the misalignment angles are assumed to be small, small angle approximations and linearization by neglecting second and higher order terms are utilized for simplification.

40

The transformation from principal axis (denoted by the subscript, a) to body axis is obtained through a modified Euler, type 3-2-1, transformation. Initially, the axes are assumed to be aligned. First rotate about Z_1 by the angle α_z , then about the transformed Y'-axis by the angle α_y and finally about the twice-transformed X"-axis by the angle α_x to obtain

$$\tilde{x}' = A_3\tilde{x}_a \quad , \quad A_3 = \begin{bmatrix} 1 & \alpha_z & 0 \\ -\alpha_z & 1 & 0 \\ 0 & 0 & 1 \end{bmatrix} \quad ,$$

$$\tilde{x}'' = A_2\tilde{x}' \quad , \quad A_2 = \begin{bmatrix} 1 & 0 & -\alpha_y \\ 0 & 1 & 0 \\ \alpha_y & 0 & 1 \end{bmatrix} \quad ,$$

$$\tilde{x}_b = A_1\tilde{x}'' \quad , \quad A_1 = \begin{bmatrix} 0 & 0 & 0 \\ 0 & 1 & \alpha_x \\ 0 & -\alpha_x & 1 \end{bmatrix} \quad .$$

Combining the three rotational matrices gives

$$\tilde{x}_b = A_1\tilde{x}'' = A_1A_2A_3\tilde{X}_a = A_{ba}\tilde{X}_a \tag{49}$$

41

where

$$A_{ba} = \begin{bmatrix} 1 & \alpha_z & -\alpha_y \\ -\alpha_z & 1 & \alpha_x \\ \alpha_y & -\alpha_x & 1 \end{bmatrix}$$ (50)

and

$$\tilde{x}_a = A_{ba}^* \tilde{x}_b$$

The inertia dyadic transformation is derived from basic principles by starting with the angular momentum of a body composed of a system of particles about the center of mass,

$$\overline{H} = \sum (\overline{r}_i) \times (m_i \dot{\overline{r}}_i)$$ (51)

where

$$\overline{r}_i = x_i i_b + y_i j_b + z_i k_b$$

is a vector to the ith mass particle expressed in body coordinates. The velocity $\dot{\overline{r}}_i$ can be expressed in the rotating body frame as

$$\dot{\overline{r}}_i = \dot{\overline{r}}_{bi} + \overline{\omega} \times \overline{r}_i$$ (52)

where

$$\overline{\omega} = \omega_x i_b + \omega_y j_b + \omega_z k_b$$

is the angular velocity of the body axes relative to inertial space expressed in body coordinates, and $\dot{\overline{r}}_{bi}$ is the velocity of the mass relative to the body

42

coordinates. Substituting equation (52) into the expression for angular momentum, equation (51), and expanding gives

$$\overline{H} = \sum \left[\left(\overline{r}_i \right) \times m_i \left(\dot{\overline{r}}_{bi} + \overline{\omega} \times \overline{r}_i \right) \right]$$

and (53a)

$$\overline{H} = \sum m_i \left(\overline{r}_i \times \dot{\overline{r}}_{bi} \right) + \sum m_i \left[\overline{r}_i \times \left(\overline{\omega} \times \overline{r}_i \right) \right] \quad .$$

The first term represents the relative angular momentum of the ith mass particle with respect to the body axes. Physically, the first term is due to moving parts such as flywheels or control moment gyros, but for a rigid body r_i is fixed with respect to the body axis; hence, the first term is zero for this derivation. The second term is a vector triple product which can be expanded to produce,

$$\overline{H} = \sum m_i \left[\left(\overline{r}_i \cdot \overline{r}_i \right) \overline{\omega} - \left(\overline{r}_i \cdot \overline{\omega} \right) \overline{r}_i \right] \quad .$$ (53b)

Carrying out the indicated vector operations and substituting the previously defined moment and product of inertia terms, equation (8):

$$\overline{H} = \left(I_{xx} \omega_x - I_{xy} \omega_y - I_{xz} \omega_z \right) i_b + \left(- I_{yx} \omega_x + I_{yy} \omega_y - I_{yz} \omega_z \right) j_b$$

$$+ \left(- I_{zx} \omega_x - I_{zy} \omega_y + I_{zz} \omega_z \right) k_b \quad .$$ (54)

The angular momentum can be written in a more compact form by using vector-matrix notation:

$$\tilde{H} = \tilde{I} \tilde{\omega}$$ (55)

where

$$\tilde{H} = \text{col}(H_x, H_y, H_z) \qquad ,$$

$$\tilde{\omega} = \text{col}(\omega_x, \omega_y, \omega_z) \qquad ,$$

and

$$\tilde{I} = \begin{bmatrix} I_{xx} & -I_{xy} & -I_{xz} \\ -I_{yx} & I_{yy} & -I_{yz} \\ -I_{zx} & -I_{zy} & I_{zz} \end{bmatrix} .$$

The square matrix I is called the inertia matrix of a body. The prop-erties of its elements under a coordinate transformation are such that they qualify as a second order tensor. Hence, the inertia matrix is also called the inertia tensor of a body. As derived, the equation for H is valid for any rigid body with an arbitrary reference point on the body which serves as origin for the body axes. For the case at hand, assume that the body axes are not prin-cipal axes, the elements of I are unknown, and the products of inertia are not necessarily zero. Further assume that the moments of inertia are known in principal coordinates where, by definition, the products are zero for such a reference frame.

As previously derived, the transformation between body and principal axes, equation (49), is given by

$$\tilde{x}_b = A_{ba} \tilde{x}_a \qquad \text{and} \qquad \tilde{x}_a = A_{ba}^* \tilde{x}_b$$

Therefore, the angular momentum can be transformed into the principal coordinated by

$$\tilde{H}_a = A_{ba}^* \tilde{H} = A_{ba}^* \tilde{I} \tilde{\omega} \qquad . \tag{56}$$

44

But in principal coordinates the angular momentum is

$$\tilde{H}_a = \tilde{I}_a \, \tilde{\omega}_a = \tilde{I}_a \, A^*_{ba} \, \tilde{\omega} \qquad (57)$$

By equating coefficients, equations (56) and (57),

$$A^*_{ba} \, \tilde{I} = \tilde{I}_a \, A^*_{ba} \qquad (58)$$

so that

$$\tilde{I} = A_{ba} \, \tilde{I}_a \, A^*_{ba} \qquad (59)$$

is the tensor transformation between the inertia dyadics.

In principal coordinates the elements of I_a are known such that

$$\tilde{I}_a = \begin{bmatrix} I_x & 0 & 0 \\ 0 & I_y & 0 \\ 0 & 0 & I_z \end{bmatrix} \qquad (60)$$

Substituting into the tensor transformation, carrying out the matric multipli-cations and equating elements produces nine equations from which the moments and products of inertia in body axes are determined:

$$\begin{bmatrix} I_{xx} & -I_{xy} & -I_{xz} \\ -I_{yx} & I_{yy} & -I_{yz} \\ -I_{zx} & -I_{zy} & I_{zz} \end{bmatrix} = \begin{bmatrix} 1 & \alpha_z & -\alpha_y \\ -\alpha_z & 1 & \alpha_x \\ \alpha_y & -\alpha_x & 1 \end{bmatrix} \begin{bmatrix} I_x & 0 & 0 \\ 0 & I_y & 0 \\ 0 & 0 & I_z \end{bmatrix} \begin{bmatrix} 1 & -\alpha_z & \alpha_y \\ \alpha_z & 1 & -\alpha_x \\ -\alpha_y & \alpha_x & 1 \end{bmatrix}$$

and

$$
\tilde{I} = \begin{bmatrix} I_x & \alpha_z(I_y - I_x) & \alpha_y(I_x - I_z) \\ \alpha_z(I_y - I_x) & I_y & \alpha_x(I_z - I_y) \\ \alpha_y(I_x - I_z) & \alpha_x(I_z - I_y) & I_z \end{bmatrix} .
$$

Therefore

$$
I_{xx} = I_x \quad , \quad I_{xy} = I_{yx} = -\alpha_z(I_y - I_x)
$$

$$
I_{yy} = I_y \quad , \quad I_{xz} = I_{zx} = -\alpha_y(I_x - I_z) \quad , \tag{61}
$$

and

$$
I_{zz} = I_z \quad , \quad I_{yz} = I_{zy} = -\alpha_x(I_z - I_y)
$$

The equations above are substituted into the gravity gradient torque equation (10) to eliminate the product of inertia terms:

$$
T_x = 3\mu/R_o^5 \left\{ (I_z - I_y)\left[R_y R_z - \alpha_x\left(R_z^2 - R_y^2 \right) \right] - (I_y - I_x)\alpha_z R_z R_x \right.
$$

$$
\left. + (I_x - I_z)\alpha_y R_y R_x \right\} \quad , \tag{62a}
$$

$$
T_y = 3\mu/R_o^5 \left\{ (I_x - I_z)\left[R_z R_x - \alpha_y\left(R_x^2 - R_z^2 \right) \right] - (I_z - I_y)\alpha_x R_x R_y \right.
$$

$$
\left. + (I_y - I_x)\alpha_z R_z R_y \right\} \quad ,
$$

and

46

$$T_z = 3\mu/R_o^5 \left\{ \left(I_y - I_x\right)\left[R_x R_y - \alpha_z\left(R_y^2 - R_x^2\right)\right] - \left(I_x - I_z\right)\alpha_y R_y R_z \\ + \left(I_z - I_y\right)\alpha_x R_x R_z \right\}$$

(62a)

(cont'd)

By utilizing definitions, equations (11), the body-principal axes misalignment torque equations can be written as

$$T_x = 2/R_o^2 \left\{ C_x\left[R_y R_z - \alpha_x\left(R_z^2 - R_y^2\right)\right] - C_z \alpha_z R_z R_x + C_y \alpha_y R_y R_x \right\},$$

$$T_y = 2/R_o^2 \left\{ C_y\left[R_z R_x - \alpha_y\left(R_x^2 - R_z^2\right)\right] - C_x \alpha_x R_x R_y + C_z \alpha_z R_z R_y \right\},$$

and

$$T_z = 2/R_o^2 \left\{ C_z\left[R_x R_y - \alpha_z\left(R_y^2 - R_x^2\right)\right] - C_y \alpha_y R_y R_z + C_x \alpha_x R_x R_z \right\}$$

(62b)

These equations can be utilized to evaluate the effects of body and principal axes misalignment for any vehicle orientation. For each specific vehicle orientation the components of the local radius vector $(R_x, R_y, \text{ and } R_z)$ must be obtained in body coordinates through use of the previously defined directional cosines. The misalignment angles $(\alpha_x, \alpha_y, \text{ and } \alpha_z)$ are free parameters whose values are small (equal or less than 15 degrees); hence, second and higher order misalignment terms have been deleted in deriving equation (62).

The radius vector components for three OWS attitude hold modes are listed in Table II as functions of directional cosines whose values are given in equations (19) on transformations. However, the directional cosines are quasi-cyclic functions of three time varying angles and are not suitable for hand calculations. Valid trends can be obtained for a few orbital periods by using a fixed time-of-year analysis and by neglecting orbital regression. The radius vector components at the time-of-winter solstice (λ= 270 degrees) with maximum angle between the orbit and ecliptic planes (Ω = 180 degrees) are listed in Table III. Using these simplified components the POP mode gravity gradient torque equations with body-principal axes misalignment are

TABLE II. RADIUS VECTOR COMPONENTS FOR THREE OWS MODES
AS FUNCTIONS OF DIRECTIONAL COSINES

	R_x	R_y	R_z
SIDE	$\dfrac{R_o(-A_{33}A_{21} + A_{23}A_{31})}{(A_{33}^2 + A_{23}^2)^{1/2}}$	$\dfrac{R_o(A_{23}A_{21} + A_{33}A_{31})}{(A_{33}^2 + A_{23}^2)^{1/2}}$	$-R_o A_{11}$
END	$-R_o A_{11}$	$-R_o A_{21}$	$R_o A_{31}$
POP	0	$\dfrac{-R_o A_{12}}{(A_{11}^2 + A_{12}^2)^{1/2}}$	$\dfrac{-R_o A_{11}}{(A_{11}^2 + A_{12}^2)^{1/2}}$

TABLE III. SIMPLIFIED RADIUS VECTOR COMPONENTS
WITH $\lambda = 270$ DEGREES AND $\Omega = 180$ DEGREES

	R_x	R_y	R_z
SIDE	$-R_o C\varphi$	$R_o S\varphi S\psi$	$R_o S\varphi C\psi$
END	$R_o S\varphi C\psi$	$R_o C\varphi$	$R_o S\varphi S\psi$
POP	0	$-R_o C\varphi$	$-R_o S\varphi$

$$T_x = C_x(S2\varphi + 2\alpha_x C2\varphi) \quad ,$$

$$T_y = C_y 2\alpha_y S^2\varphi + C_z \alpha_z S2\varphi \quad ,$$

(63)

48

and

$$T_z = -C_z 2\alpha_z C^2\varphi - C_y \alpha_y S2\varphi \qquad (63)$$

<div align="right">(cont'd)</div>

The POP mode torque, equations (63), can be integrated to give

$$H_x = (C_x/2W_o)(-C2\varphi + 2\alpha_x S2\varphi) + H_{xo} \quad,$$

$$H_y = (\alpha_y C_y/2W_o)(2\varphi - S2\varphi) - (\alpha_z C_z/2W_o)C2\varphi + H_{yo} \quad, \qquad (64)$$

and

$$H_z = -(\alpha_z C_z/2W_o)(2\varphi + S2\varphi) + (\alpha_y C_y/2W_o)C2\varphi + H_{zo}$$

where H_o are the constants of integration.

The simplified gravity gradient torque and momentum equations for the side and end view configurations under body-principal axes misalignment can be obtained by substitution of the simplified radius vector components for each configuration. However, the equations are more complex and difficult to integrate than those for the POP mode case.

Case 2

Assuming that the body axes are misaligned from the reference axes also requires use of the modified Euler transformation developed for Case 1 where the angle symbols have been changed. The body axes are carried into the reference axes by first rolling about the X_b-axis by the angle δ_x, then by pitching about the transformed Y_b-axis by the angle δ_y, and finally by yawing about the twice transformed Z_b-axis by the angle δ_z. The resultant transformation using small angle approximations and linearization is resummarized by

$$\widetilde{X}_b = A_{br}\widetilde{X}_r \qquad (65)$$

where

$$A_{br} = \begin{bmatrix} 1 & -\delta_z & \delta_y \\ \delta_z & 1 & -\delta_x \\ -\delta_y & \delta_x & 1 \end{bmatrix} \; .$$

In the previous sections where specific vehicle orientations were evaluated, the body axes were assumed to be ideally aligned with the reference axes. In the present case the body-reference axes are assumed to be misaligned and the transformation is utilized as an operator on the R_x, R_y, and R_z components which are assumed to be obtainable in the reference frame. Let X_b, Y_b, and Z_b be the local radius vector components as used in the gravity gradient torque equations:

$$X_b = R_x - \delta_z R_y + \delta_y R_z \qquad ,$$

$$Y_b = \delta_z R_x + R_y - \delta_x R_z \qquad \qquad (66)$$

and

$$Z_b = - \delta_y R_x + \delta_x R_y + R_z$$

Assuming that the products of inertia are zero, the gravity gradient torque equation (10) , for body — reference axes misalignment using equations (66) are

$$T_x = \left(2/R_o^2\right)C_x\left[R_y R_z - \delta_x\left(R_z^2 - R_y^2\right) + \delta_z R_z R_x - \delta_y R_y R_x\right] \qquad ,$$

$$\qquad\qquad\qquad\qquad\qquad\qquad\qquad\qquad\qquad\qquad (67)$$

$$T_y = \left(2/R_o^2\right)C_y\left[R_z R_x - \delta_y\left(R_x^2 - R_z^2\right) + \delta_x R_x R_y - \delta_z R_z R_y\right] \qquad ,$$

and

$$T_z = (2/R_o^2)C_z\left[R_xR_y - \delta_z(R_y^2 - R_x^2) + \delta_yR_yR_z - \delta_xR_xR_z\right] \quad (67) \atop (cont'd)$$

where second order misalignment terms are dropped.

These body-reference equations are very similar to the body-principal axes misalignment equations. With the aid of $C_x + C_y + C_z = 0$, equations (62) can be rewritten so that the components of equations (67) appear as terms. However, two additional terms are also produced that represent cross coupling between each axis for the body-principal misalignment case. For a vehicle that is near symmetric about one axis, the cross coupling terms are zero for several selected orientations. In particular the gravity gradient stable mode in which case the body-reference and body-principal axes misalignment equations are identical, as will be shown, and the POP mode for a symmetric vehicle.

For a nonsymmetric vehicle the POP mode radius vector components from Table III are substituted into equations (67) to produce

$$T_x = C_x(S2\varphi + 2\delta_xC2\varphi)$$

$$T_y = C_y(2\delta_yS^2\varphi - \delta_zS2\varphi) \quad ,$$

and

$$T_z = C_z(-2\delta_zC^2\varphi + \delta_yS2\varphi)$$

$$(68)$$

The similarity between equations (68) and (63) can readily be seen. For a symmetric vehicle $C_x = 0$ and $C_y = -C_z$ in which case equations (68) and (63) are identical. Hence for a symmetric vehicle in POP mode orientation the effect of body-principal and body-reference axes misalignment is identical.

The momentum equations for body-reference axes misalignment are obtained by integrating equations (68) with respect to $\varphi = W_o t$:

$$H_x = (C_x/2W_o)(-C2\varphi + 2\delta_x S2\varphi) + H_{xo}$$

$$H_y = (C_y/2W_o)[\delta_y(2\varphi - S2\varphi) + \delta_z C2\varphi] + H_{yo} \quad ,$$

and

<div align="right">(69)</div>

$$H_z = (C_z/2W_o)[- \delta_z(2\varphi + S2\varphi) - \delta_y C2\varphi] + H_{zo}$$

These equations are evaluated using the side view ATM configuration parameters and a comparison made between the body-principal and body-reference misalignment effects in the section on energy requirements.

To further illustrate the similarity of axes misalignment effects due to body-reference misalignment, consider an OWS in a gravity gradient stable mode. Let the X_b-axis of minimum inertia be aligned with the local vertical and the Z_b-axis be aligned with the orbital spin vector. A right-hand triad is completed by the Y_b-axis which is aligned with the velocity vector. In this case the body axes are identically aligned with the local vertical coordinate system (X_p, Y_p, Z_p), and the components of the local vertical vector are $R_x = R_o$, $R_y = 0$, and $R_z = 0$. These values are substituted into the general gravity gradient torque equation (10) to get

$$T_x = 0$$

$$T_y = \frac{3\mu}{R_o^3} I_{xz} \quad ,$$

<div align="right">(70)</div>

and

$$T_z = \frac{-3\mu}{R_o^3} I_{yx} \quad .$$

These torques are due only to product of inertia terms and are zero if the body axes are also principal axes. During Case 1, equations (61), it was shown that the product of inertia terms could be replaced by principal moments of inertia

and angular misalignments, that is

$$I_{yz} = - \alpha_x (I_z - I_y) \quad ,$$

$$I_{xz} = - \alpha_y (I_x - I_z) \quad , \tag{71}$$

and

$$I_{yx} = - \alpha_z (I_y - I_x)$$

Utilizing these relations, the gravity gradient torque components, equations (70), become

$$T_x = 0$$

$$T_y = \frac{-3\mu}{R_o^3} (I_x - I_z) \alpha_y = - 2C_y \alpha_y \tag{72}$$

and

$$T_z = \frac{3\mu}{R_o^3} (I_y - I_x) \alpha_z = 2C_z \alpha_z$$

The results are verified by assuming that the body axes are misaligned from the principal axes by an infinitesimal rotation. The local radius vector components are substituted into equations (62) derived for Case 1, producing the same torque components as given above.

Finally, let the body axes be misaligned from the reference axes. Utilizing the torque equations (67) developed for body-reference misalignment (Case 2) and substituting for the components of the local radius vector produces

$$T_x = 0 \quad , \tag{73}$$

$$T_y = \frac{-3\mu}{R_o^3}(I_x - I_z)\delta_y = -2C_y\delta_y \quad ,$$

and

$$T_z = \frac{3\mu}{R_o^3}(I_y - I_x)\delta_z = 2C_z\delta_z$$

These components are the same as those of the previous case, equations (72), if the δ-angles are set equal to the α-angles. Hence, in a gravity gradient stable mode the effects of body-reference and body-principal misalignments are identical for small angle displacements. The torques due to selecting body axes that are not principal axes are also identical to those produced by axes misalignments. The equivalent misalignment angles can be determined by using equations (61).

SOLAR LOOK ANGLES

Often it is desirable to examine the variation in angles which describe an object's position with respect to a given coordinate system or the OWS's body axes. For example if the OWS is in POP mode orientation it is necessary to examine the angle between the longitudinal body axis and the sun line vector to determine the angular limits and rates required on the ATM gimbal for sun tracking. Or, if an onboard experiment can be gimbaled with respect to the OWS, it is desirable to establish the gimbal angles and angular rates between the OWS body and experiment reference axes. Such angles are commonly referred to as "look" angles, which usually represent directional cosine angles and can be derived by taking the scalar (dot) product between the vectors involved. In most cases, the scalar product will be between vectors that are known in different reference frames, hence the previously defined transformations can be utilized to obtain the vector components in a common vector space before performing the necessary vector operations.

The angle, ψ , between the ecliptic and orbital planes can be obtained by first defining vector perpendiculars to both the planes, and then taking the dot product between the defined vectors. Let $\bar{c}$ and $\bar{o}$ be vectors perpendicular to the ecliptic and orbital planes, respectively. From the previously defined coordinate systems, $\bar{c} = k_s$ and $\bar{o} = k_o = k_p$. Using the directional

54

cosine matrix in equations (17) to obtain the components of $\bar{o}$ in solar coordinates,

$$\bar{o} = k_p = A_{13} i_s + A_{23} j_s + {}'A_{33} k_s \tag{74}$$

Taking the dot product defines

$$\cos\psi = \bar{c} \cdot \bar{o} = A_{33} = C\Omega S\iota Se + C\iota Ce \tag{75}$$

when using the simplified directional cosines of equations (20) with $\Omega = 180$ degrees, $\psi = \iota + e$, its maximum possible value which is depicted in Figure 5. The variation of ψ as a function of orbital time is shown in Figure 10. Its
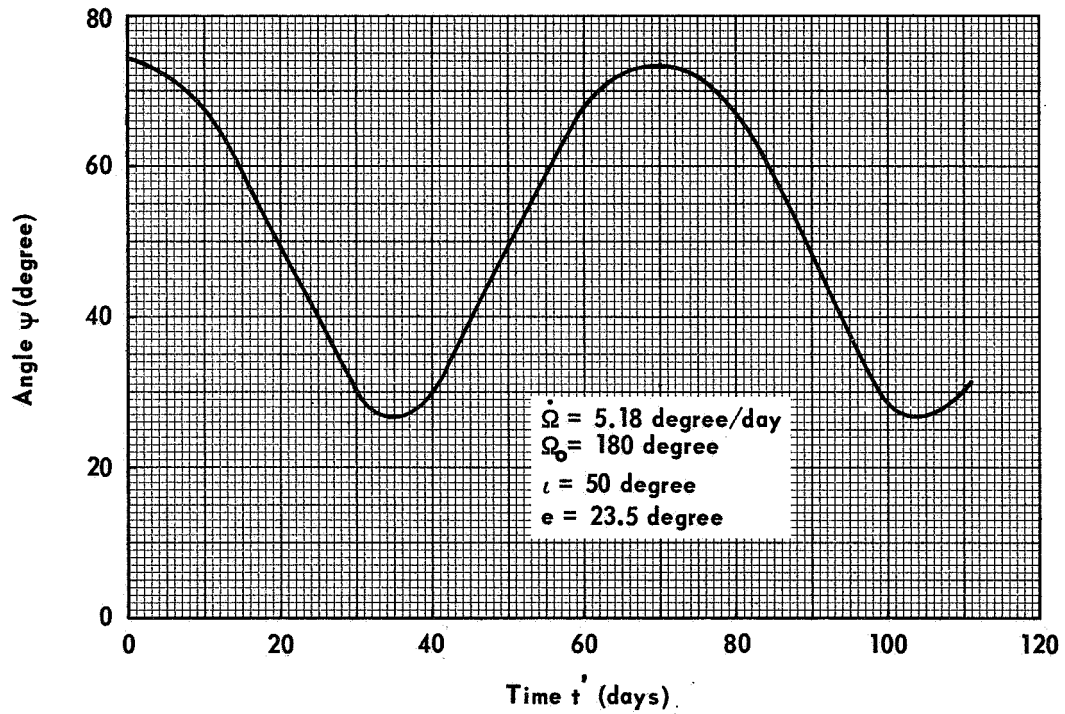
FIGURE 10. ECLIPTIC-ORBITAL PLANE ANGLE VERSUS TIME

55

period is about 70 days for an inclination of 50 degrees. This period is the same as the orbital regression period which rate is shown in Figure 11 as a function of orbital inclination.
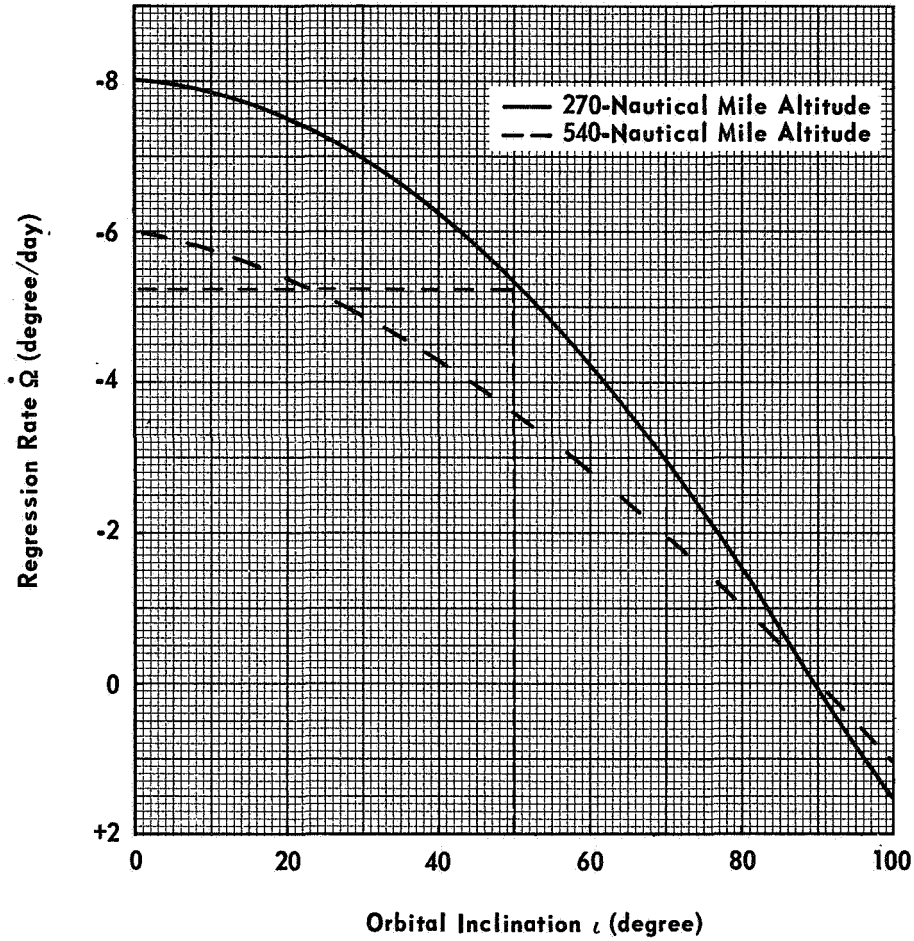

FIGURE 11. ORBITAL REGRESSION RATE VERSUS INCLINATION

The angle (γ) between the longitudinal body axis (the orbital spin vector) of the OWS in POP mode orientation and the sun line can be obtained by first defining the sun line vector $\bar{s}$ and then dotting $\bar{s}$ with the X_b-axis for the POP mode configuration. Using the coordinate systems defined in equations (28), and directional cosines, $\bar{s} = i_s$, and

$$\bar{x}_b = i_b = k_p = k_o = A_{13} i_s + A_{23} j_s + A_{33} k_s$$

Taking the dot product yields

56

$$\cos\gamma = \bar{s} \cdot \bar{x}_b = A_{13} = -S\iota(-C\lambda S\Omega + S\lambda C\Omega Ce) + C\iota S\lambda Se \quad . \quad (76)$$

The projection of the sun line vector upon the orbital plane defines an angle β which is often referred to as the solar look angle. Since any vector in the orbital plane is always 90 degrees from the perpendicular to the orbital plane the solar look angle can be expressed as a function of γ from the relation $\gamma = \beta + 90$ degrees . Substituting this relation for γ gives

$$\cos\gamma = \cos(\beta + 90 \text{ degrees}) = -\sin\beta \qquad (77)$$

Therefore,

$$\beta = \sin^{-1}(A_{13})$$

and

$$\beta = \sin^{-1}\left[S\iota(-C\lambda S\Omega + S\lambda C\Omega Ce) - C\iota S\lambda Se\right] \qquad (78)$$

The solar look angle is plotted in Figure 12 for a 270-n.mi. orbit at an inclination of 28 degrees. Over a one-year interval β is repetitive with a period of about 45 days and an angular rate of about 2.6 degrees per day. The zero values of β indicate times when the sun is on the line of nodes between the orbit and ecliptic planes. The intersection of the β and E curves represent times when the sun is on the line of nodes between the orbit and equatorial planes. The magnitude of β is within an envelope determined by the angle $E \pm \iota$, where E is defined by the projection of the sun line vector upon the equatorial plane and is indicative of the seasonal time of year.

The angle $E + 90$ degrees is defined by the dot product between the sun line vector $\bar{s}$ and a vector $\bar{e}$ perpendicular to the equatorial plane. Using the previously defined transformations, the vectors are obtained in solar coordinates as

$$\bar{s} = i_s$$

and

$$\bar{e} = k_e = S\lambda Se\, i_s + C\lambda Se\, j_s + Ce\, k_s \qquad (79)$$
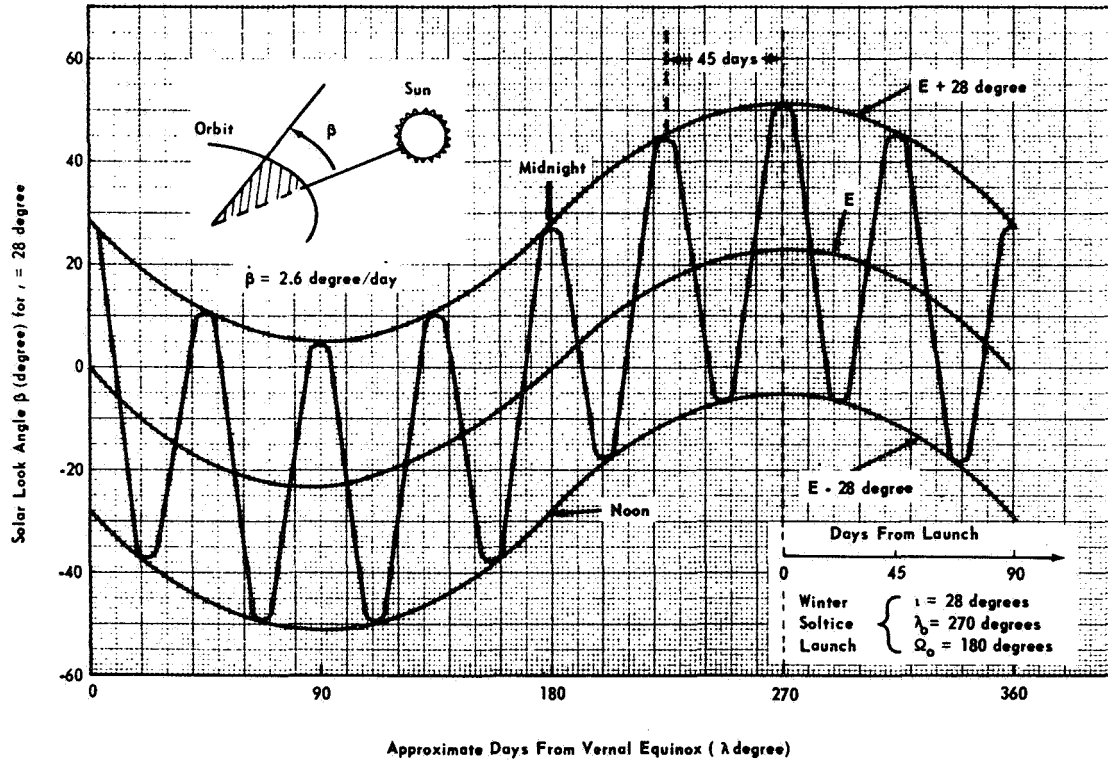
FIGURE 12. SOLAR LOOK ANGLE AS A FUNCTION OF
THE EARTH'S INERTIAL POSITION

Taking the scalar product yields

$$\cos(E + 90 \text{ degrees}) = -\sin E = S\lambda Se$$

and   (80)

$$E = \sin^{-1}(-S\lambda Se)$$

The angle E as well as $E \pm \iota$ is superimposed on Figure 12 along
with β . For the special equatorial orbit case with $\iota = 0$ the solar look angle
is identical to E . It is convenient to show plots of β and E with time start-
ing at the vernal equinox. However, the actual initial value of β is deter-
mined by both the time of year, specified by λ_0 , and the time of day of orbital
injection, specified by Ω_0 . For β to attain its maximum value at the time of

58

winter solstice ($\lambda_0 =$ 270 degrees) requires that $\Omega_0 =$ 180 degrees. In this case $\beta(\max) =$ 73.5 degrees for $\iota =$ 50 degrees as shown in Figure 13.
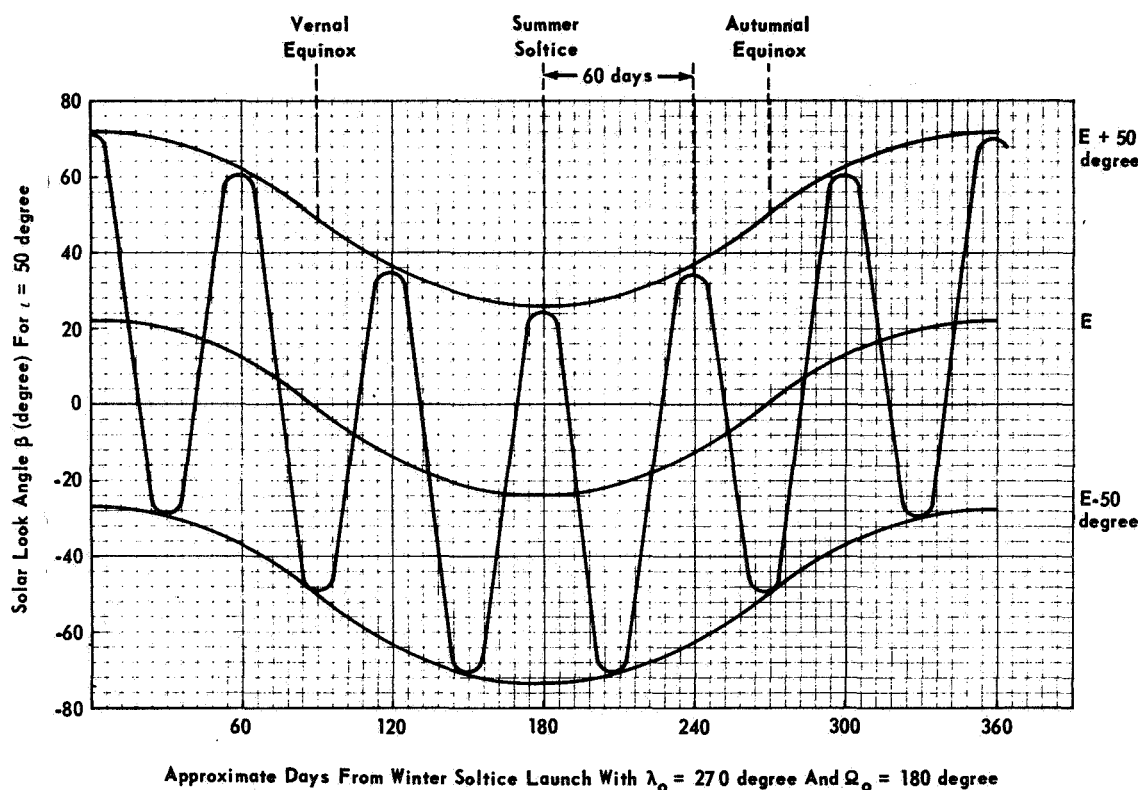

FIGURE 13. SOLAR LOOK ANGLE AS A FUNCTION OF
TIME AFTER LAUNCH

The solar angle has a period of 60 days and a rate of about 3.3 degrees per day. Figure 14 represents β for a polar orbit case with $\iota =$ 90 degrees . As pointed out in the section on coordinate systems, many authorities specify the earth's position on the celestial sphere by $\lambda +$ 180 degrees, in which case a sign change is introduced in both β and E .

A rather interesting orbit with respect to the sun line results by selecting the orbital inclination such that the orbital regression rate is equal to the earth's rotational rate about the sun. Such a near polar orbit is called a sun synchronous orbit. The orbit precesses such that the orbital plane is relatively constant when referenced to the ecliptic plane; hence, excursions in the solar look angle are small over an extended period of time. A spacecraft in sun
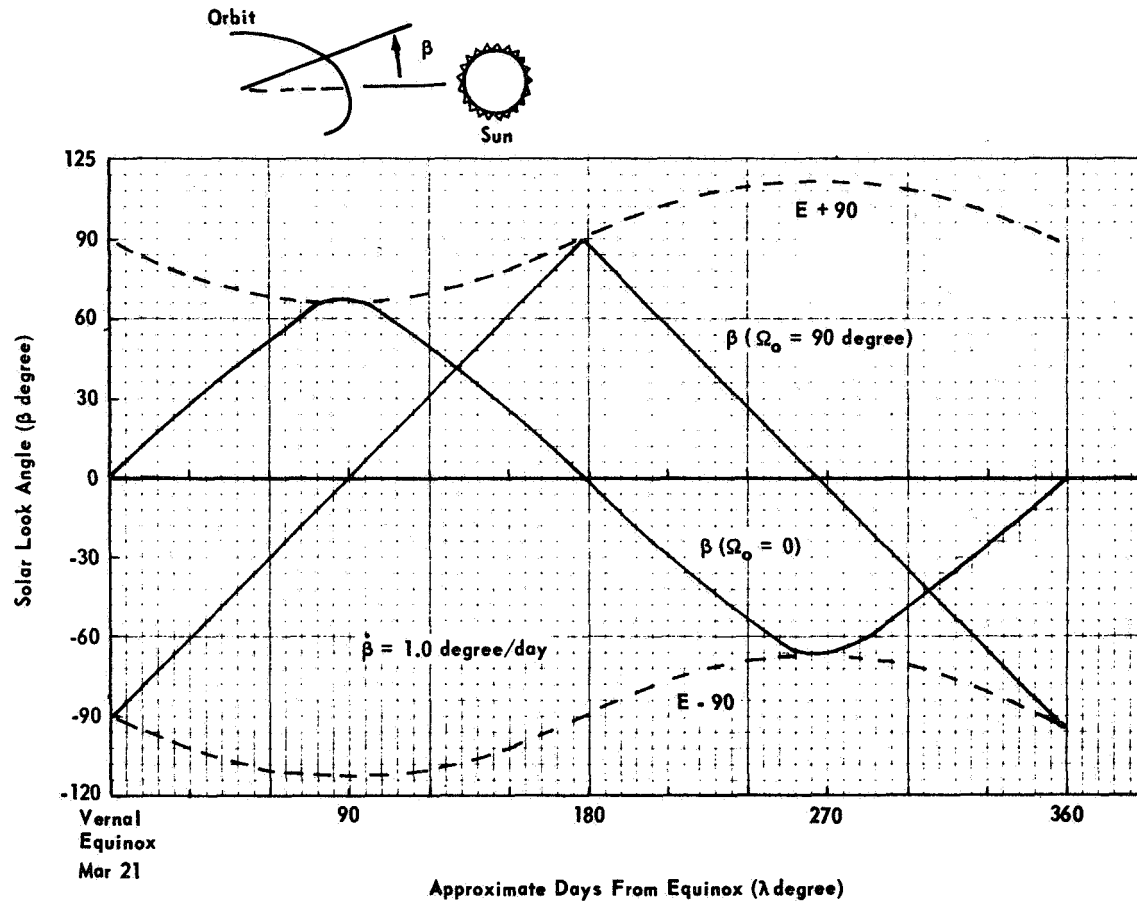
FIGURE 14. SOLAR LOOK ANGLE, ι = 90 DEGREES

synchronous orbit would have several apparent advantages as minimization of the energy required to maintain a specified attitude orientation and the hardware required to point various experimental modules as the ATM or an earth resource module. The earth's rotation of about 15 degrees per hour would allow total ground coverage from a sun synchronous satellite in about two weeks.

The nodal regression rate plotted in Figure 11 is given by

$$\dot{\Omega} = -9.9728(R_e/R_o)^{7/2} \cos \iota \qquad \text{(degrees per day)} \qquad (81)$$

Solving for the orbital inclination and setting $\dot{\Omega} = \dot{\lambda} = 0.98565$ degree per day gives

60

$$\iota \;=\; \cos^{-1}\left[\; -\;\frac{0.98565}{9.9728\,(R_e/R_o)^{7/2}}\;\right] \qquad (82)$$

For an orbital altitude of 270 n.mi., $R_o = (R_e + 270)$ n.mi. where

$R_e = 3444$ n.mi. is the earth's radius, the orbital inclination for a sun synchronous orbit is calculated to be 97.2 degrees. At this inclination the orbit precesses in phase with the earth's movement about the sun. Launch conditions are selected to produce the initial values of Ω_0 and λ_0, and hence the orbit and some relatively constant magnitude for the solar look angle.

The solar look angle for three initial values of Ω_0 is shown in Figure 15 as a function of the earth's position about the sun. Launch at the vernal
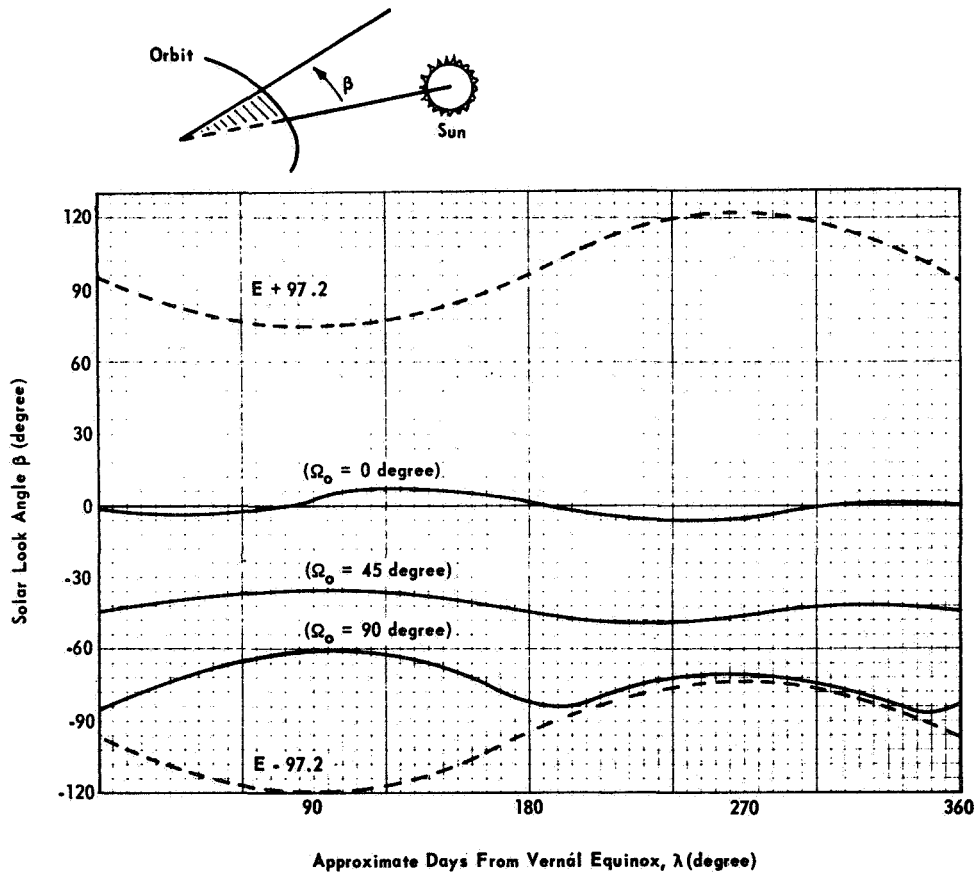

FIGURE 15. SOLAR LOOK ANGLE FOR SUN SYNCHRONOUS ORBIT,
$\iota = 97.2$ DEGREES

equinox with $\Omega_0 = 0$ produces on orbit with dark/light cycles, the orbital plane contains the sun vector. Utilizing this orbit the OWS with side view ATM could operate in POP mode and view the sun without requiring gimbals on either the ATM or on the solar panels, hence minimizing both energy and hardware requirements. On the other extreme, launch at the vernal equinox with $\Omega_0 = 90$ degrees produces an all-light orbit, the orbit plane is almost perpendicular to the sun vector. An OWS with side view ATM could operate in a gravity gradient stable mode, an earth resources module could view the earth obtaining total ground coverage over a few-day period, maximum solar power could be received and the sun could be observed continuously, all without requiring large angular degrees of freedom or module gimbals.

Additional angles of interest can be derived. However, most look angles are either mission dependent or dependent upon the mounting of an experiment with respect to the OWS body axes, in which cases additional transformations may be necessary to relate the coordinates.

ENERGY REQUIREMENTS

In this section, the energy requirements necessary for attitude hold against gravity gradient torques are calculated for the previously selected orientations. The torque and momentum vector components are plotted over a one-orbit time interval as a function of the orbital angular position. Then the total momentum, the square root of the sum of the components squared, is plotted and related to fuel weight and the number of control moment gyros as defined for use on the ATM. For quick fuel weight estimations graphical methods are suggested for relating angular misalignments from the local vertical to momentum and momentum to fuel weight. Since much of the analysis contained in this report was done to support the "Early Saturn V Workshop" study conducted by MSFC May 15, 1968, the spacecraft vehicle data are taken to reflect the OWS-B physical parameters and orbital data. A representative picture of OWS-B is shown in Figure 16 with the side view ATM. The end view ATM configuration is obtained by rotating the ATM 90 degrees about the Y-axis such that the ATM points in negative X-axis direction instead of along the negative Z-axis.

The vehicle data shown in Table IV were obtained from a memo dated January 9, 1968, R-P&VE-AAD, "Saturn V Workshop — Configuration B-1." The numerical values shown are for a dry launch workshop with light

TABLE IV. VEHICLE PARAMETERS, OWS CONF. B

Parameter	Side ATM	End ATM	Units
I_x	0.6514×10^6	0.5396×10^6	$kg\text{-}m^2$
I_y	6.1729×10^6	6.2194×10^6	$kg\text{-}m^2$
I_z	6.3400×10^6	6.3418×10^6	$kg\text{-}m^2$
$I_z - I_y$	0.1671×10^6	0.1224×10^6	$kg\text{-}m^2$
$I_x - I_z$	-5.6886×10^6	-5.8022×10^6	$kg\text{-}m^2$
$I_y - I_x$	5.5215×10^6	5.6798	$kg\text{-}m^2$
m	53 513	53 513	kg
$3/2\ W_o^2$	1.8382×10^{-6}	1.8382×10^{-6}	sec^{-2}
C_x	0.3072	0.2250	N-m
C_y	-10.4568	-10.6656	N-m
C_z	10.1496	10.4406	N-m
$C_x/2W_o$	138.8	101.6	N-m-s
$C_y/2W_o$	-4723.0	-4817.3	N-m-s
$C_z/2W_o$	4584.3	4715.7	N-m-s
W_o	1.107×10^{-3}	1.107×10^{-3}	s
R_e	6.3768×10^6	6.3768×10^6	m
Altitude	0.5005×10^6	(270 n.mi.)	m
R_o	6.8773×10^6	6.8773×10^6	m
T(orbit)	5673	5673	s
$GM_e = \mu$	3.986×10^{14}	3.986×10^{14}	m^3/s^2
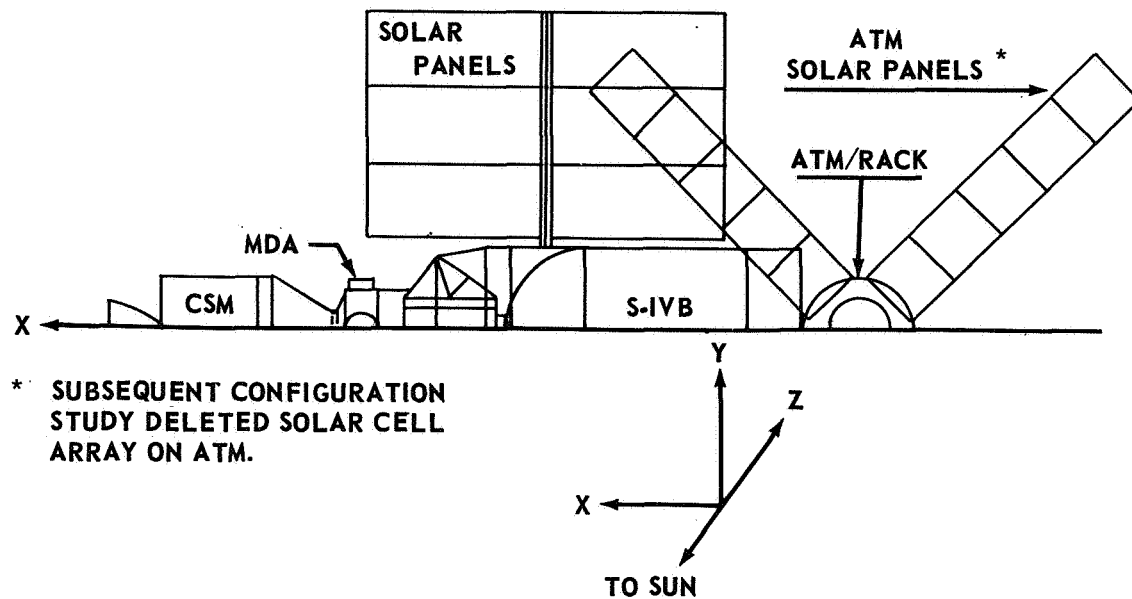
FIGURE 16. WORKSHOP CONFIGURATION B, SIDE VIEW ATM

CSM (Command Service Module). Two of the basic orientations for the two configurations are the side viewing ATM shown in Figure 8 with the -Z-axis pointing toward the sun, and the end viewing ATM shown in Figure 7 with the X-axis pointing toward the sun. As used in this study the X-, Y-, and Z-axes are denoted as the roll, pitch, and yaw axes, respectively. In addition, both the light and heavy CSM cases were analyzed. The vehicle parameters and numerical results are shown only for the light CSM case which required more energy to maintain a specified attitude, because of the greater differences in the moments of inertia. The desired orbit is circular at 270 n.mi. altitude with a preferred inclination of 50 degrees, which corresponds to an angle, ψ, of 73.5 degrees between the orbit and ecliptic plane at winter solstice.

Various environmental forces act on the orbiting spacecraft, with gravity gradient producing the major disturbance. Unless the OWS is in a gravity gradient stable mode some form of energy must be continuously applied to counteract the gravity gradient torques and maintain the desired orientation. This energy may be in the form of fuel which is expelled through a reaction jet control system (RCS), a spinning gyroscopic device such as a control moment gyro (CMG), reaction wheel or fluid flywheel. In the first case, the RCS motor produces a force, F, which acts through a lever arm, L, to produce a torque, T. By definition the time rate of change in momentum is equal to torque, hence

64

$$T = dH/dt \tag{83}$$

Integrating both sides with respect to time gives the angular impulse which is identical to the momentum accumulated over the time interval of integration, Δt_b :

$$H = \int T \, dt = \int L F \, dt = L F \Delta t_b \tag{84}$$

The time interval Δt_b represents the time that the RCS motors were thrusting. The fuel weight, W, is given by

$$W = \dot{m} \Delta t_b \tag{85}$$

where $\dot{m}$ is the rate at which fuel is burned in pounds per second. For chemical propellants, the performance of a fuel is rated by the fuel's specific impulse (I_{sp}) which is defined as the thrust of a pound of propellant multiplied by the number of seconds required to burn it :

$$I_{sp} = F \Delta t / \Delta m = F/\dot{m} \tag{86}$$

The time of burn from equation (84) and the fuel burn rate from equation (86) are substituted in equation (85) to obtain

$$W = H/I_{sp} L \tag{87}$$

Since I_{sp} is in units of "seconds" and H as used in this report is in "N-m-s" then if L is given in "feet" a conversion factor must be used to obtain W in "pounds." That factor is 0.7375 ft-lb/N-m, which gives

$$W(lb) = 0.7375 H(N\text{-}m\text{-}s)/I_{sp}(s) L(ft) \tag{88}$$

65

Equation (88) is plotted in Figure 17 for I_{sp} = 220(s) , a typical value; and L = 10 ft , the approximate radius of the S-IVB stage. Once the momentum due to gravity gradient is obtained, either Figure 17 or equation (88) is utilized to obtain the fuel requirements for attitude hold against gravity gradient torques. The fuel weight, however, becomes excessive for long lifetime missions. For such missions, it is desirable to utilize in some manner the natural environmental forces in conjunction with a momentum interchange device for space-craft attitude control.

Reaction wheels, CMG's and fluid flywheels are gyroscopic devices which convert electrical power into control torque. Both the reaction wheel and fluid flywheel control are based on the principle of reaction torque. By accelerating the wheel or fluid a reaction torque is generated on the vehicle. In addition, a secondary torque is generated by the angular momentum of the device. In either case the device is hard mounted to the vehicle; hence, momentum cannot be interchanged with the environmental forces.
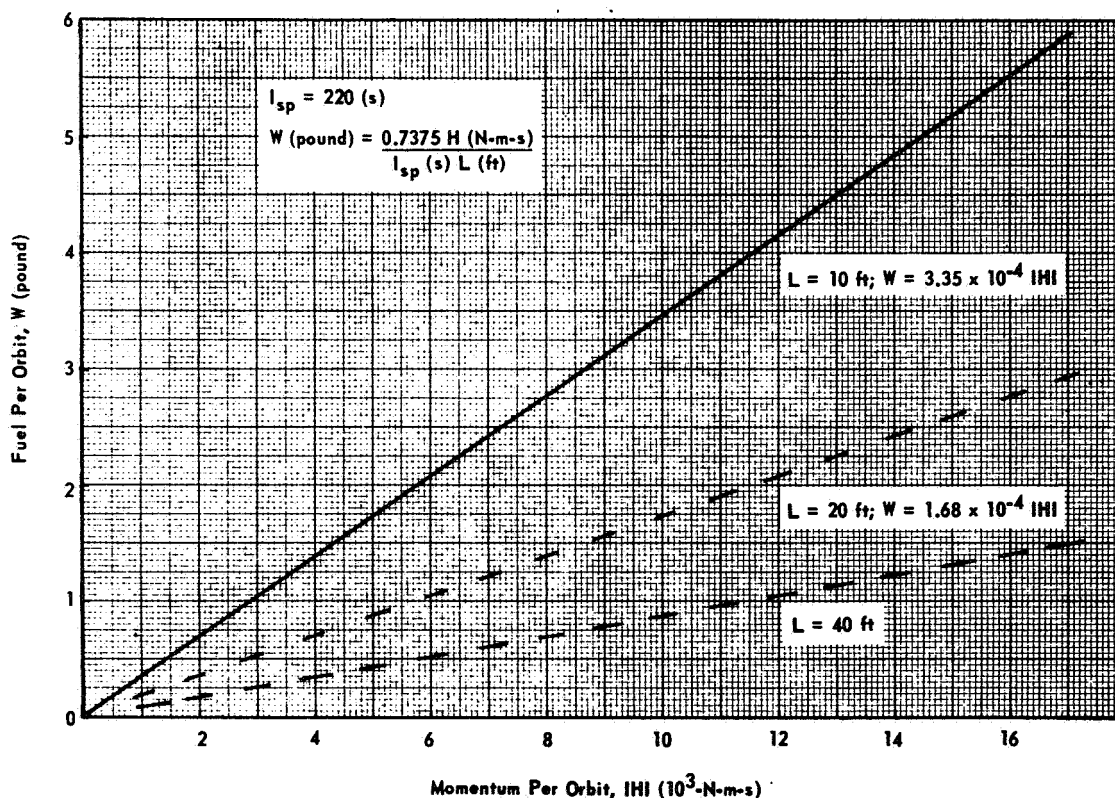
FIGURE 17. FUEL WEIGHT VERSUS MOMENTUM

66

CMG's are mounted on gimbals and have momentum interchange capability. The CMG rotor runs at a constant spin rate, providing a constant angular momentum vector parallel to the vehicle angular momentum vector under zero torque conditions. Control torques are obtained when the gimbals are deflected to some angle, causing the CMG rotor to precess and change the CMG's momentum vector. The time rate of change in the momentum vector produces a control torque. Once the gimbals reach their physical limits the CMG can no longer produce control torques and must be desaturated, which means that the momentum added to the system by the CMG's must be removed. One method of CMG desaturation is to use RCS in which case fuel weight may pose a problem for long lifetime missions. A more practical method of CMG desaturation is to interchange momentum with the spacecraft's natural environmental forces. Such an interchange requires that the attitude pointing requirements be relaxed during the desaturation period; however, the total energy requirements for long lifetime missions can be minimized. For example, if the solar pointing requirements for an OWS in an ATM mode of operation can be relaxed during the dark one-half orbit, then gravity gradient torques can be utilized for desaturation. CMG's with gravity gradient desaturation are planned for use on the first OWS with an operational ATM. A system of three CMG's each with double gimbals will provide attitude control. The control logic for CMG gimbal control and desaturation is rather complex and is outside the scope of this report, but the characteristics of a single CMG are given in Table V. Under ideal control without physical gimbal limitations a system of three such CMG's could produce a maximum of about 480 ft-lb (645 N-m) torque and 6000 ft-lb-s (8100 N-m-s) momentum. As a reference value for accumulated momentum, the saturation value of 8100 N-m-s has been superimposed on the total momentum-versus-orbital position graphs contained in this report. In practice, the CMG's would be desaturated long before they approached their saturation value.

For preliminary design purposes it is desirable to obtain a quick evaluation of the magnitude of the gravity torques acting on the orbiting vehicle so that the control system can be "sized." Once the environmental torques and momentum are calculated, the necessary fuel weight and/or number of CMG's for attitude pointing control can be estimated. The equations developed in this report can be readily utilized for "quick-look" analysis and preliminary design purposes.

The torque and momentum component equations for the attitude hold modes considered in this report are summarized below for a winter solstice launch holding the orbital regression angle and the earth's position about the

TABLE V. SINGLE CMG CHARACTERISTICS[a]

Characteristic	Value
Rotor Diameter (0.56 m)	22 in.
Rotor Weight (67 kg)	148 lb
Rotor Speed	7850 rpm
Rotor Spin Up Time	7 hr
Rotor Stop Time	2.25 hr
Start Power	170 W
Run Power	54 W
Volume (0.47 m^3)	16.7 ft^3
Weight (190 kg)	418 lb
Threshold Torque (0.08 N-m)	0.059 ft-lb
Maximum Torque (215 N-m)	160 ft-lb
Threshold Gimbal Rate	0.0034 deg/s
Maximum Gimbal Rate	4.54 deg/s
Angular Momentum (2700 N-m-s)	2000 ft-lb-s

a. Taken from "Apollo Telescope Mount Subsystem — Black Box Preliminary Design Review," October 30, 1967, MSFC, R-ASTR-BA-251-67.

sun constant ($\lambda = 270$ degrees and $\Omega = 180$ degrees). The constants of integration in the momentum components have been selected such that the momentum is zero at time zero. The definition of equations (11) and some of the angle relations are reiterated in equations (89) for completeness;

$$\psi = i + e \quad ,$$

$$W_o = \left(GM/R_o^3\right)^{1/2} \quad , \tag{89}$$

$$\varphi = W_o t \quad ,$$

$$C_x = (3W_o^2/2)(I_z - I_y) \quad ,$$

$$C_y = (3W_o^2/2)(I_x - I_z) \quad ,$$

and

$$C_z = (3W_o^2/2)(I_y - I_x) \quad .$$

(89)
(cont'd)

Equations for the following attitude hold cases have been derived:

1. End View ATM, Solar Fixed, equations (26) and (27)

$$T_x = C_x \, S\psi \, S2\varphi \quad ,$$

$$T_y = - C_y \, S2\psi \, S^2\varphi$$

$$T_z = - C_z \, C\psi \, S2\varphi$$

$$H_x = (C_x/2W_o) \, S\psi(1 - C2\varphi) \quad ,$$

$$H_y = (- C_y/2W_o) \, S2\psi(2\varphi - S2\varphi)/2 \quad ,$$

and

$$H_z = (- C_z/2W_o) \, C\psi(1 - C2\varphi) \quad .$$

(90)

2. Side View ATM, Solar Fixed-XOP Mode, equations (38) and (39)

$$T_x = C_x \, S2\psi \, S^2\varphi \quad ,$$

$$T_y = C_y \, C\psi \, S2\varphi$$

(91)

$$T_z = C_z \, S\psi \, S2\varphi \quad ,$$

$$H_x = (C_x/2W_o) \, S2\psi(\, 2\varphi \, - S2\varphi)/2 \quad ,$$

$$H_y = (\dot{C}_y/2W_o) \, C\psi(1 - C2\varphi) \quad ,$$

<div align="right">(91)
(cont'd)</div>

and

$$H_z = (C_z/2W_o) \, S\psi(1 - C2\varphi)$$

3. POP Mode, Gimbaled ATM, equations (47) and (48)

$$T_x = C_x \, S2\varphi \quad ,$$

$$T_y = 0 \quad ,$$

$$T_z = 0$$

<div align="right">(92)</div>

$$H_x = (C_x/2W_o)(1 - C2\varphi) \quad ,$$

$$H_y = 0$$

and

$$H_z = 0 \quad .$$

4. POP Mode, Body-Principal Axes Misalignment, equations (63) and (64)

$$T_x = C_x(2\alpha_x \, C2\varphi + S2\varphi) \qquad ,$$

$$T_y = C_y(2\alpha_y \, S^2\varphi) + C_z(\alpha_z \, S2\varphi) \qquad ,$$

$$T_z = -C_z(2\alpha_z \, C^2\varphi) - C_y(\alpha_y \, S2\varphi) \qquad ,$$

$$H_x = (C_x \, 2W_o)(2\alpha_x \, S2\varphi + 1 - C2\varphi) \qquad , \qquad\qquad (93)$$

$$H_y = (\alpha_y \, C_y/2W_o)(2\varphi - S2\varphi) + (\alpha_z \, C_z/2W_o)(1 - C2\varphi) \qquad ,$$

and

$$H_z = (\alpha_z \, C_z/2W_o)(2\varphi + S2\varphi) - (\alpha_y \, C_y/2W_o)(1 - C2\varphi)$$

5. POP Mode, Body-Reference Axes Misalignment, equations (68) and (69)

$$T_x = C_x(2\delta_x \, C2\varphi + S2\varphi)$$

$$T_y = C_y(2\delta_y \, S^2\varphi - \delta_z \, S2\varphi)$$

$$T_z = C_z(-2\delta_z \, C^2\varphi + \delta_y \, S2\varphi)$$

$$H_x = (C_x/2W_o)(2\delta_x \, S2\varphi + 1 - C2\varphi) \qquad\qquad (94)$$

$$H_y = (C_y/2W_o)[\delta_y(2\varphi - S2\varphi) - \delta_z(1 - C2\varphi)]$$

and

$$H_z = (C_z/2W_o)[-\delta_z(2\varphi + S2\varphi) + \delta_y(1 - C2\varphi)]$$

6. Gravity Gradient Mode, Axes Misalignment, equations (72)

$$T_x = 0 \quad ,$$

$$T_y = -2C_y \alpha_y \quad ,$$

$$T_z = 2C_z \alpha_z \quad ,$$

$$H_x = 0 \quad , \tag{95}$$

$$H_y = T_y \Delta t_o \quad ,$$

and

$$H_z = T_z \Delta t_o$$

(Δt_o is the time interval over which momentum is evaluated.)

For one orbit at 270 n.mi., $\Delta t_o = 5673$ seconds.

All the torque and momentum equations are functions of three multiplicative terms. The first term, C_x, C_y, or C_z, contains vehicle and orbital parameters that produce a multiplicative constant. The momentum equations contain the orbital angular rate and the last three sets of equations (93), (94), and (95) contain misalignment angles all of which can be grouped into the multiplicative constant. The second term, sine or cosine functions of ψ, is a function of the orbital inclination and the angle between the ecliptic and equatorial planes. Once the inclination is specified, ψ becomes constant; hence the second term $g(\psi)$ is also constant. It is interesting to note that the first and second term when multiplied serve only as a scaling factor in either the torque or momentum equations. The third term, $f(\varphi)$, a function of the orbital angle $\varphi = W_o t$, determines the shape of both the torque and momentum when graphed as a function of orbital time. Since torque is, by definition, the time rate of change of momentum, those values of φ which make the torque zero produce maximum or minimum values for corresponding momentum components.

Only the end and side view ATM configurations in a solar fixed orientation have torque or momentum components, equations (90) and (91), that are a function of ψ — all the other equations are independent of orbital inclination. The $g(\psi)$ coefficients are plotted in Figure 18 as a function of both orbital inclination and the angle ψ. The gravity gradient effects are maximized by letting $\psi = 45$ degrees, which corresponds to an orbital inclination of 21.5 degrees. The biased torque components, those containing $S^2\varphi$ terms, produce momentum components that are secular. Since the biased and secular components are multiplied by $S(2\psi)$, they are maximized by $\psi = 45$ degrees. The secular momentum occurs about the Y-axis for the end view case where the difference in moments of inertia is greatest and about the X-axis for the side view case where the difference in moments of inertia is least. Hence the end view case will require more energy to maintain its orientation over a one-orbit or longer time interval than the side view case.

On examination of equations (90) and (91) with the aid of Figure 18, it is apparent that the biased torques and secular momentum can be zeroed out by letting $\psi = 0$ or 90 degrees. These values correspond to an orbital inclination of -23.5 degrees or 66.5 degrees, respectively. However, orbital injection conditions other than $\lambda = 270$ degrees and $\psi = 180$ degrees would produce different ψ values for which the gravity gradient effects would be maximized or minimized, although, as pointed out in Figure 5, the maximum or minimum values of ψ are obtained at either a summer or winter solstice launch. It is further noted that the end view case, equations (90), reduces to the POP mode case, equations (92), for $\psi = 90$ degrees, and that the two axes misalignment POP mode cases, equations (93) and (94), also reduce to the POP mode case when the misalignment angles are zero. Next, the torque and momentum components will be evaluated for a selected vehicle configuration.

The end and side view torque and momentum equations are evaluated using the vehicle data listed in Table IV. Several selected values for the ecliptic-orbital plane angle are substituted into equations (90) and (91). The results are summarized in Tables VI and VII for $\psi = 0$, 45, 73.5, and 90 degrees. The last column is the $f(\varphi)$ multiplicative factor which completes the equations, that is, each equation is of the form

$$T_k(\psi, \varphi) \quad \text{or} \quad H_k(\psi, \varphi) = \left[C_k \, g_k(\psi) \right] f_k(\varphi) \tag{96}$$

where C is the first multiplicative term containing vehicle parameters, $g(\psi)$ is the second multiplicative term, a function of orbital inclination, and $f(\varphi)$
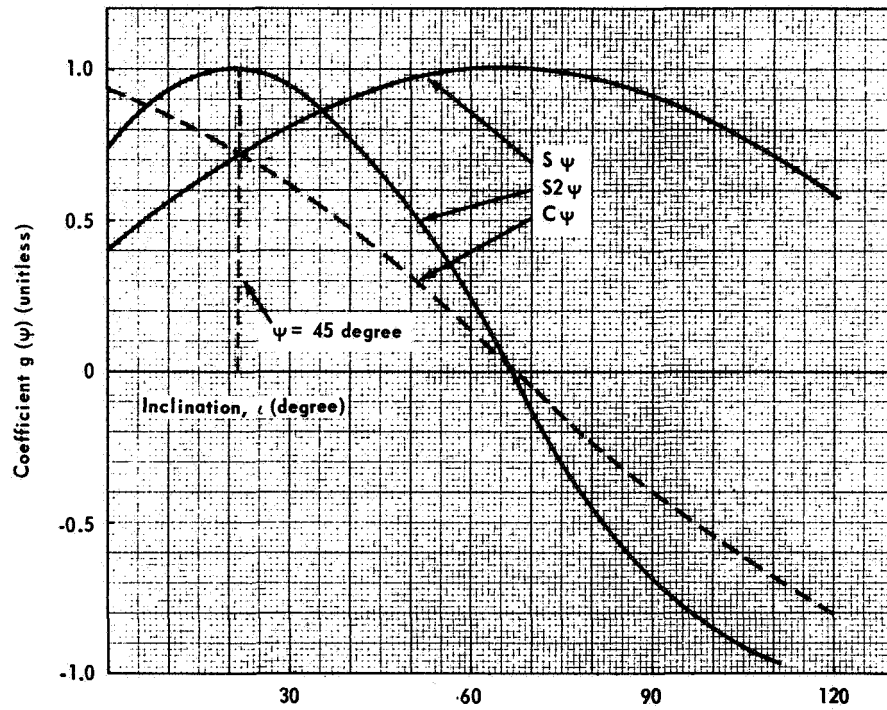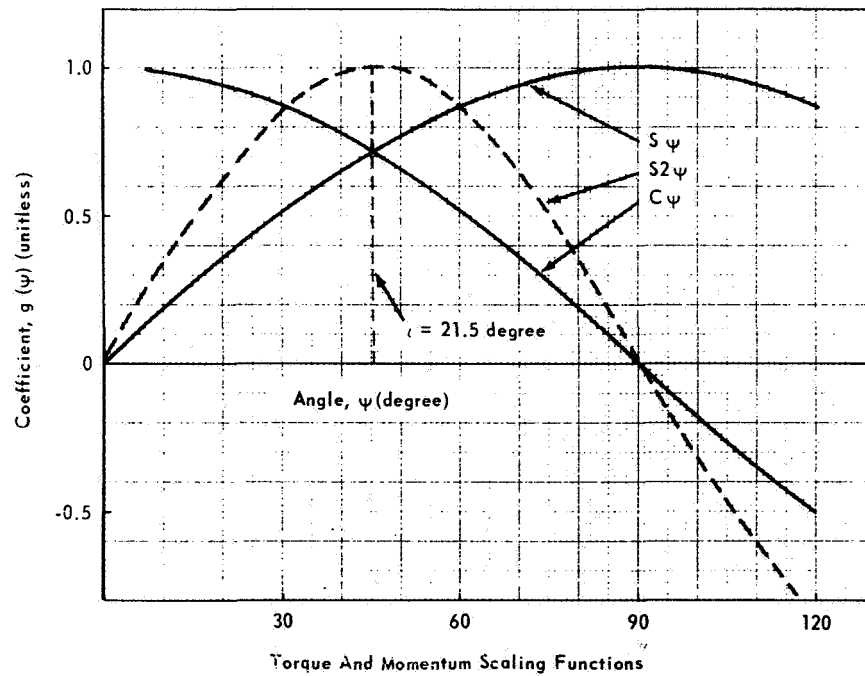
FIGURE 18. TORQUE AND MOMENTUM SCALING FUNCTIONS

TABLE VI. END VIEW ATM TORQUE AND MOMENTUM

	C g(ψ)	$\psi = 0$	$\psi = 45$	$\psi = 73.5$	$\psi = 90$	X f(φ)
T_x	0.225 Sψ	0	0.159	0.216	0.225	S2φ
T_y	10.67 S(2ψ)	0	10.67	5.82	0	S$^2\varphi$
T_z	-10.44 Cψ	-10.44	-7.38	-2.96	0	S2φ
H_x	102 Sψ	0	72.1	97.8	102	1 - C2φ
H_y	4817 S2ψ	0	4817	2625	0	(2φ - S2φ)/2
H_z	-4716 Cψ	-4716	-3334	-1339	0	1 - C2φ

TABLE VII. SIDE VIEW ATM TORQUE AND MOMENTUM

	C g(ψ)	$\psi = 0$	$\psi = 45$	$\psi = 73.5$	$\psi = 90$	X f(φ)
T_x	0.307 S2ψ	0	0.307	0.167	0	S$^2\varphi$
T_y	-10.46 Cψ	-10.46	-7.40	-2.97	0	S2φ
T_z	10.15 Sψ	0	7.18	9.73	10.15	S2φ
H_x	138.8 S2ψ	0	138.8	75.65	0	(2φ - S2φ)/2
H_y	4723 Cψ	4723	3392	1341	0	1 - C2φ
H_z	-4584 Sψ	0	-3241	-4396	-4584	1 - C2φ

is the third multiplicative term which determines the shape of the torque or momentum. The first and second terms are grouped together to produce a scaling factor for each ψ value. The $f(\varphi)$ functions are plotted in Figure 19. Multiplying $f(\varphi)$ by the appropriate scaling factor produces the torque and momentum components.

The total angular momentum, a measure of energy required for attitude hold, is obtained by taking the square root of the sum of the components squared, that is

$$|H| = \left(H_x^2 + H_y^2 + H_z^2\right)^{1/2} \tag{97}$$

It is convenient to plot the torque and momentum components as well as the total angular momentum as a function of the orbital angle $\varphi = W_o t$. To establish a reference point for momentum, the saturation value of a three-CMG system, as used on the ATM, is superimposed on the graphs of total momentum.

The torque and momentum for the end view ATM configuration in a solar inertially fixed orientation (Table VI) are shown in Figures 20 through 24. Two cases for momentum have been plotted, one with the constants of integration evaluated to make the momentum zero at $\varphi = 0$ and the other with the constants of integration set equal to zero in which case the momentum at $\varphi = 0$ is not necessarily zero. As noted from Figure 20 the biased torque occurs about the Y-axis to produce a secular momentum component on the same axis as shown in both Figures 21 and 22. The biased torque is a maximum value since the differences in moments of inertia are greatest in the gravity gradient torque equation for the Y-axis. The secular momentum components exceed the 3-CMG saturation level after one-fourth orbit for either momentum case with $\psi = 45$ degrees . The total momentum for each case is shown in Figures 23 and 24. Note that about six CMG's would be required for attitude hold over one-half orbit.

The torque and momentum for the side view ATM configuration (Table VII) in a semi-solar fixed orientation (XOP Mode) are shown in Figures 25 and 29. The biased torque component is about the X-axis, Figure 25, where the differences in inertias are least. Again two momentum cases are shown, Figures 26 and 27. Although the vehicle parameters are similar, the accumulated momentum for the XOP mode is much less than the end view ATM, solar fixed mode. This difference is due to constraining the axis of minimum principal
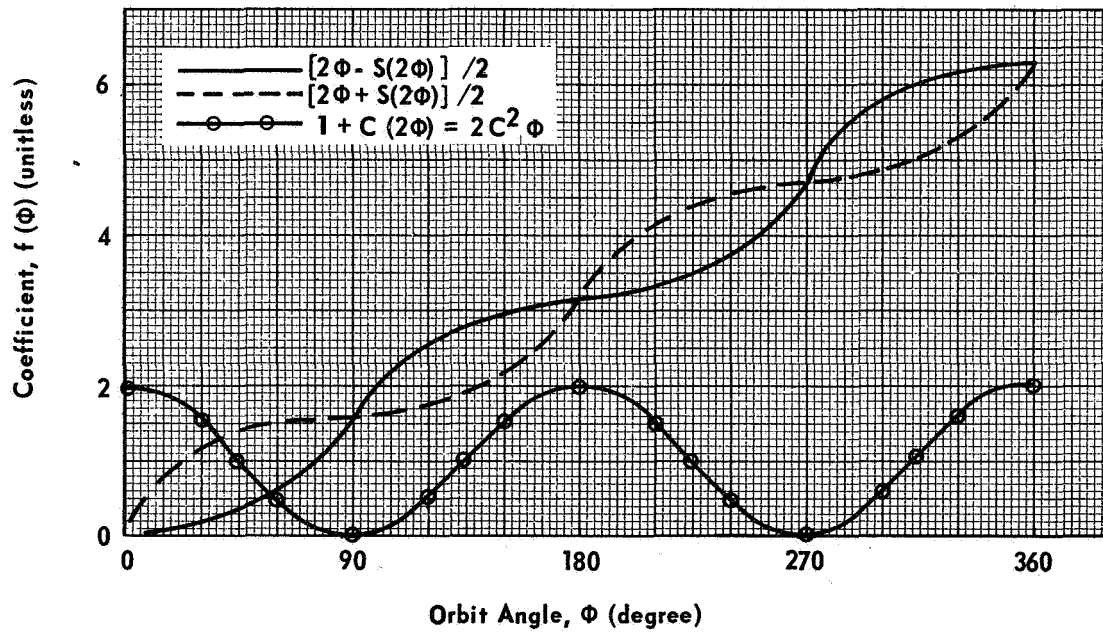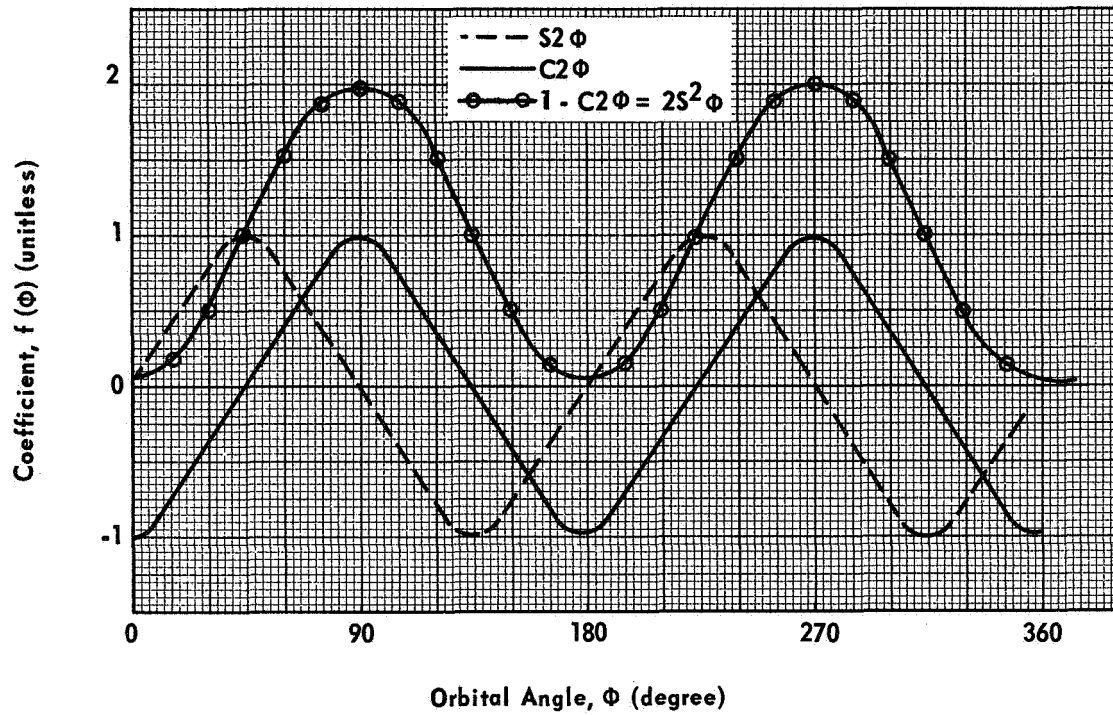
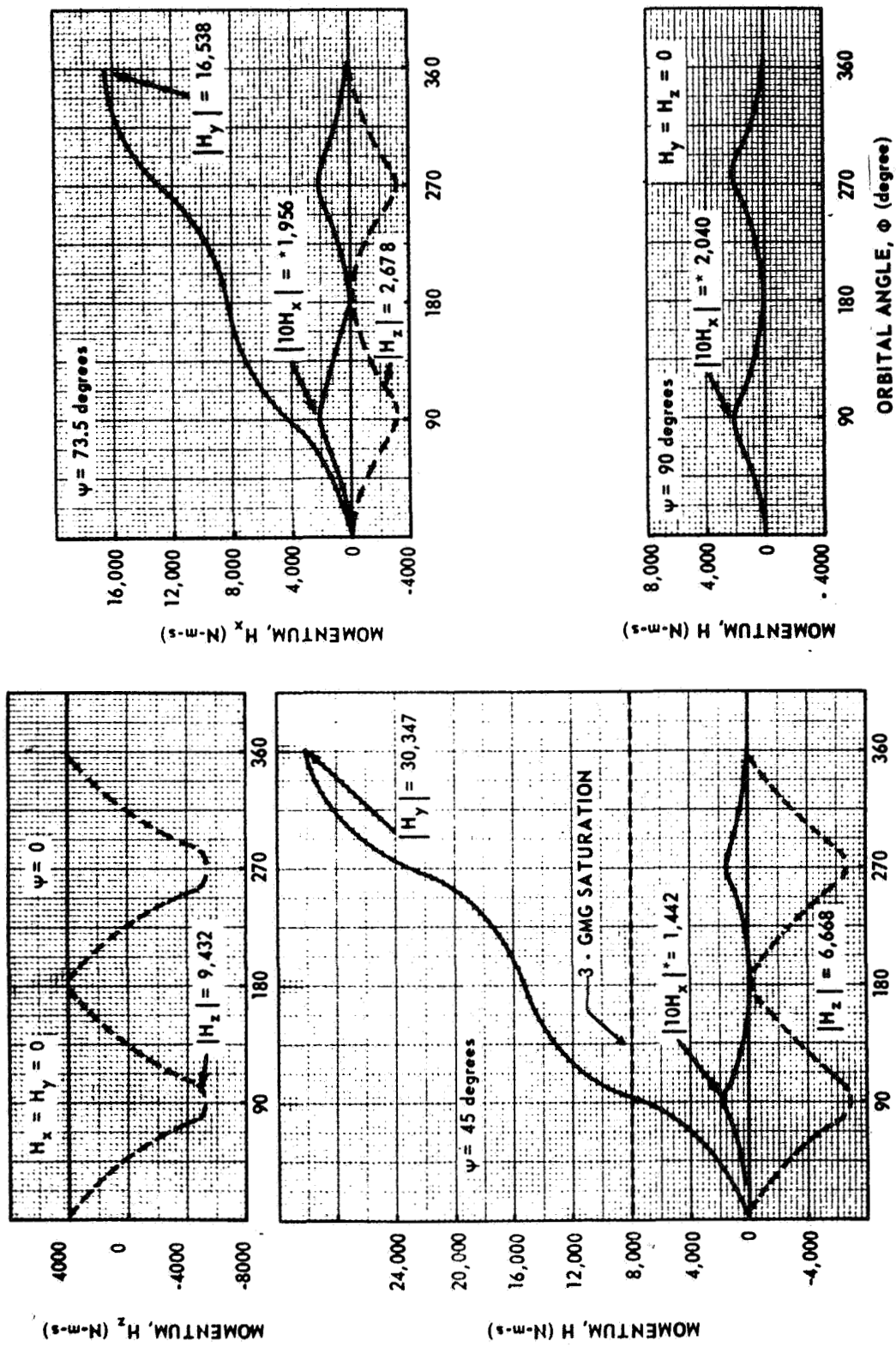FIGURE 19. TORQUE AND MOMENTUM SHAPING FUNCTIONS
VERSUS ORBITAL POSITION

77
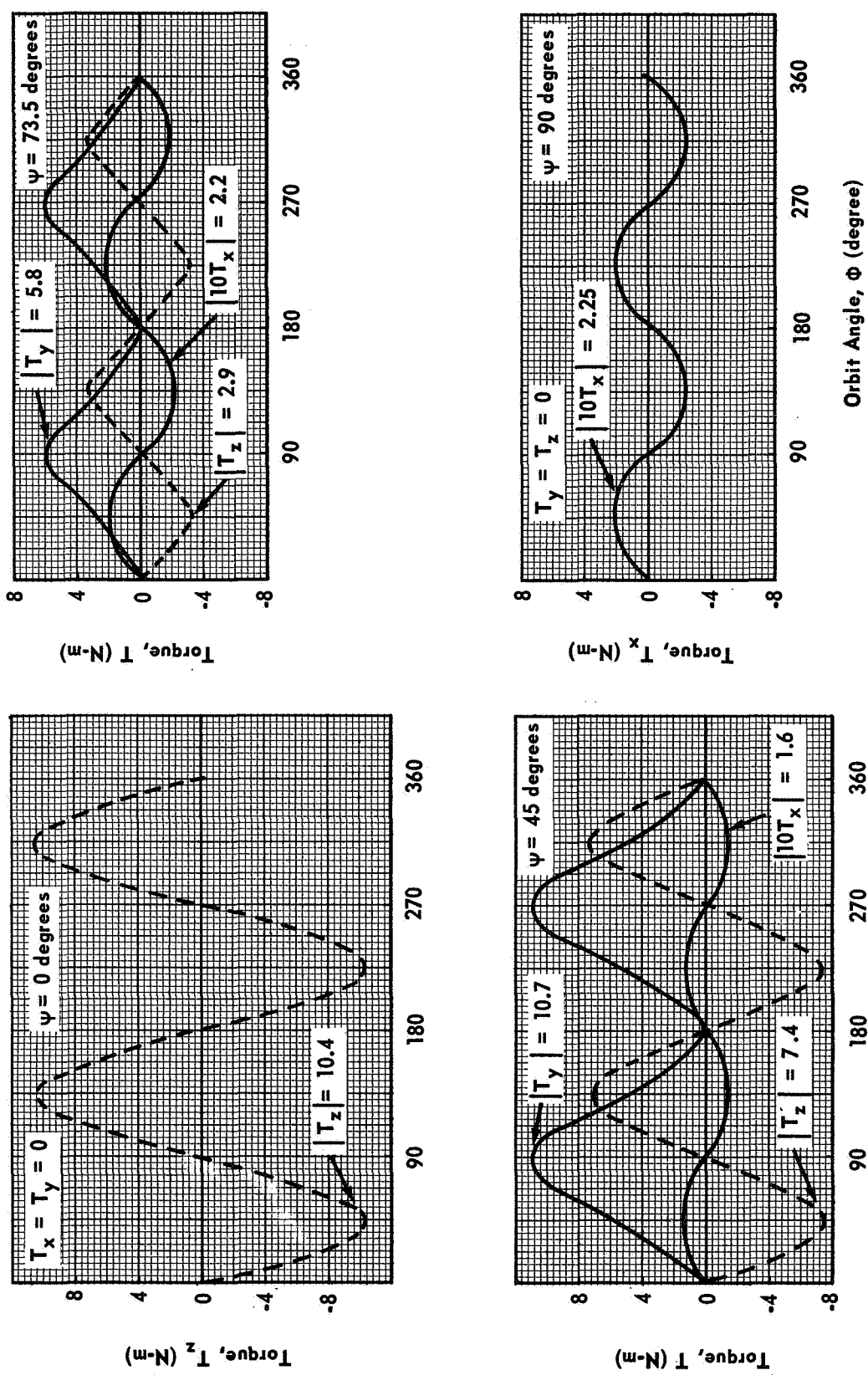
FIGURE 20. END VIEW ATM, TORQUE VERSUS ORBITAL POSITION

78

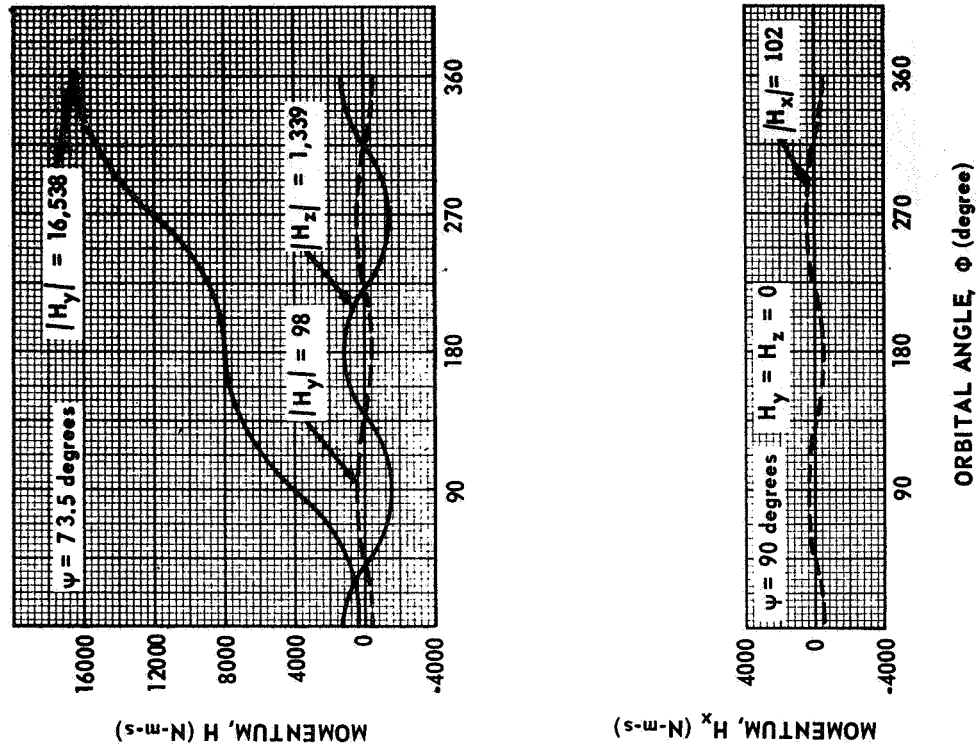FIGURE 21. END VIEW ATM, MOMENTUM VERSUS ORBITAL POSITION [H(0) = 0]

79

FIGURE 22. END VIEW ATM, MOMENTUM VERSUS ORBITAL POSITION
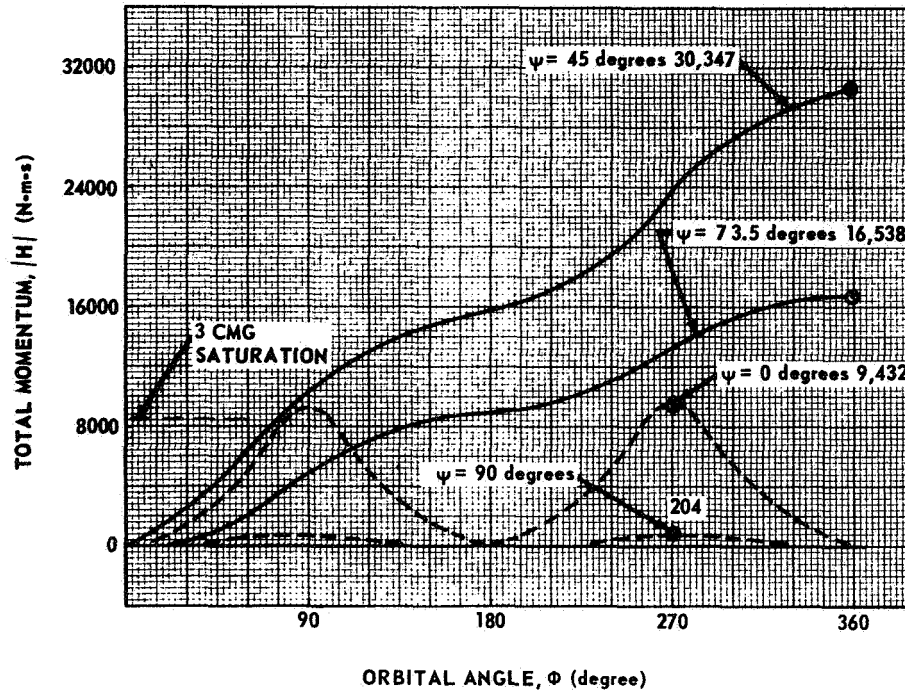WITH ZERO CONSTANTS OF INTEGRATION, $[H(0) \neq 0]$

80

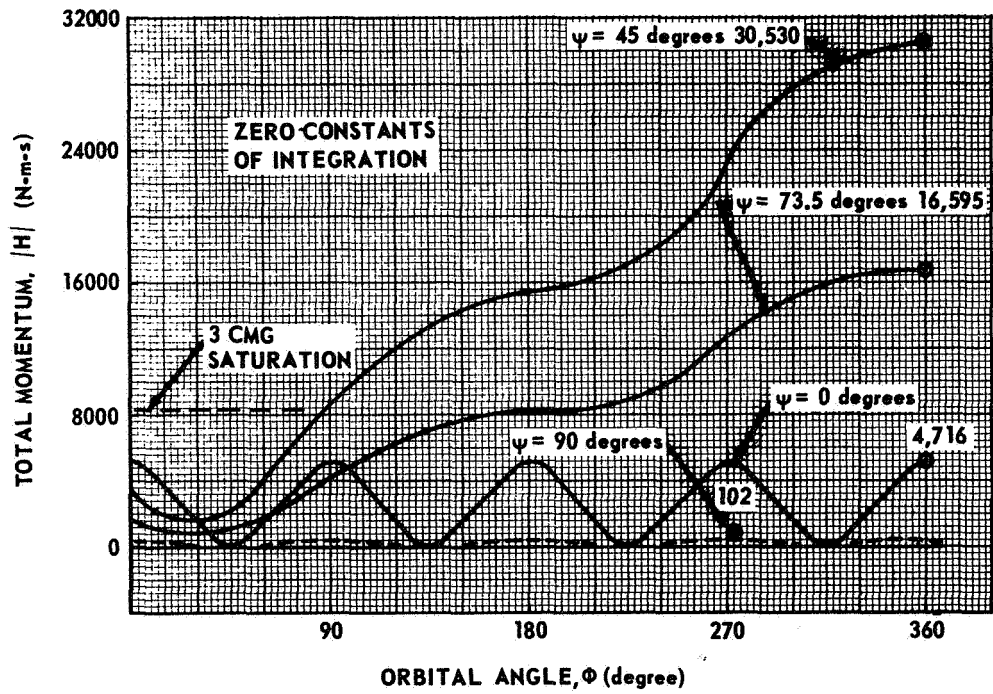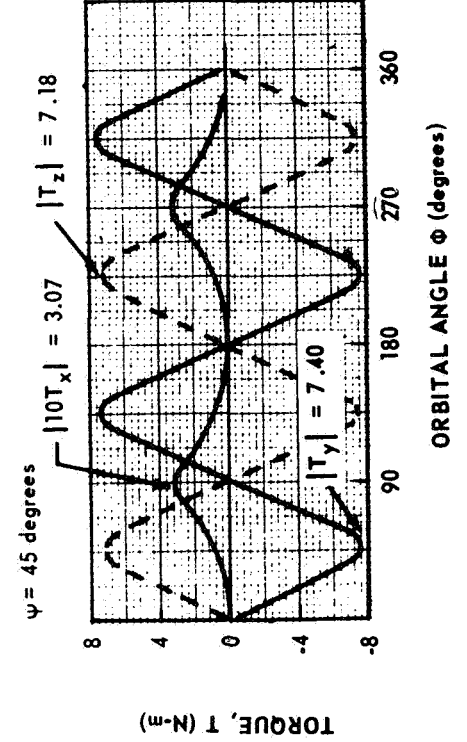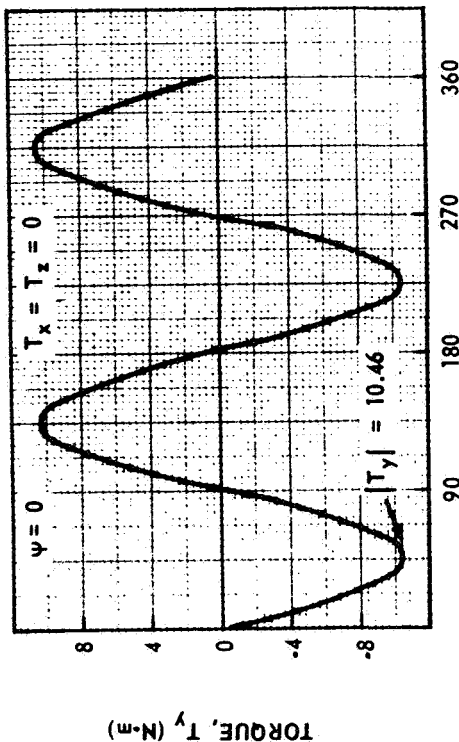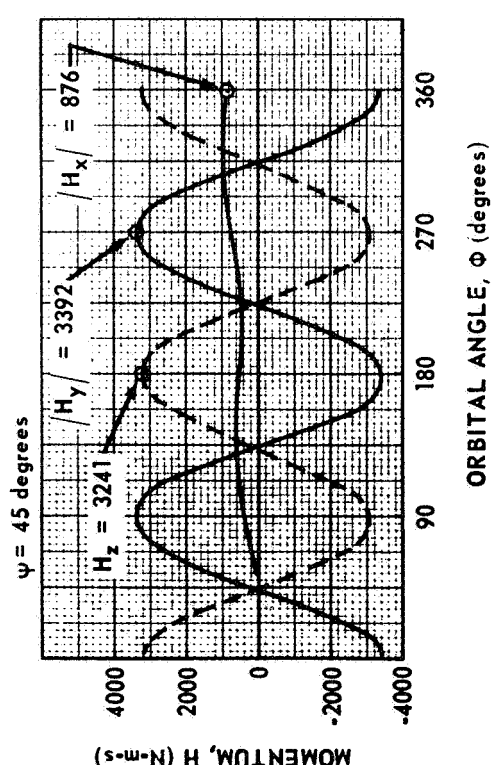FIGURE 23. END VIEW ATM, TOTAL MOMENTUM [H(0) = 0]

FIGURE 24. END VIEW, TOTAL MOMENTUM [H(0) ≠ 0]

FIGURE 25. SIDE VIEW ATM, TORQUE VERSUS ORBITAL POSITION
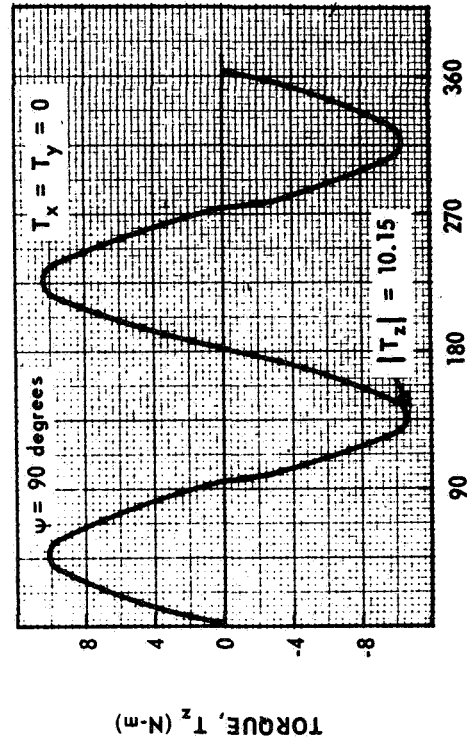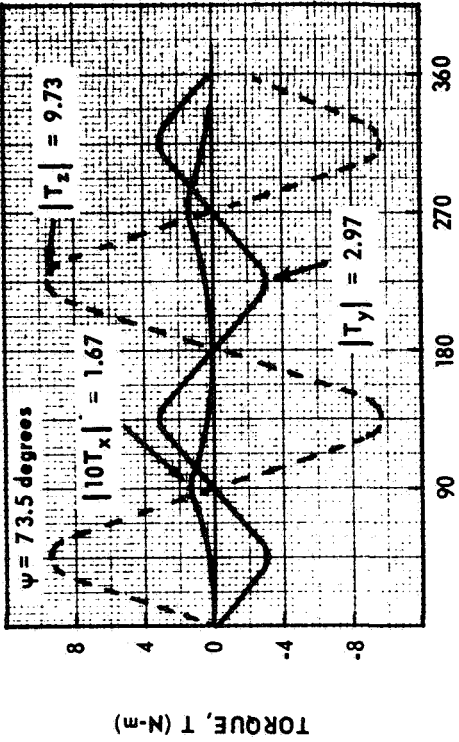
(NOTE: The plotted value of T_x is 10 times the actual value)

82
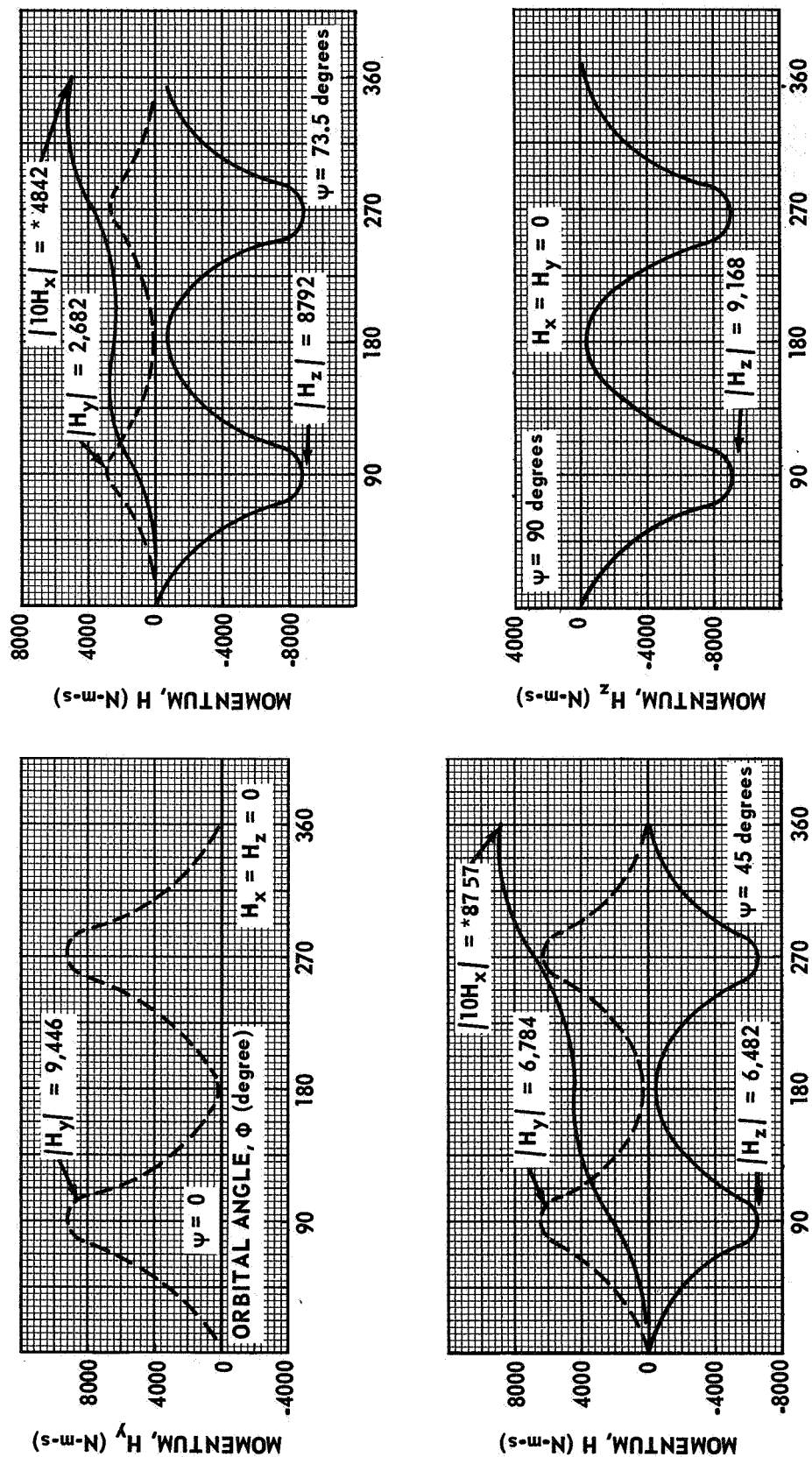
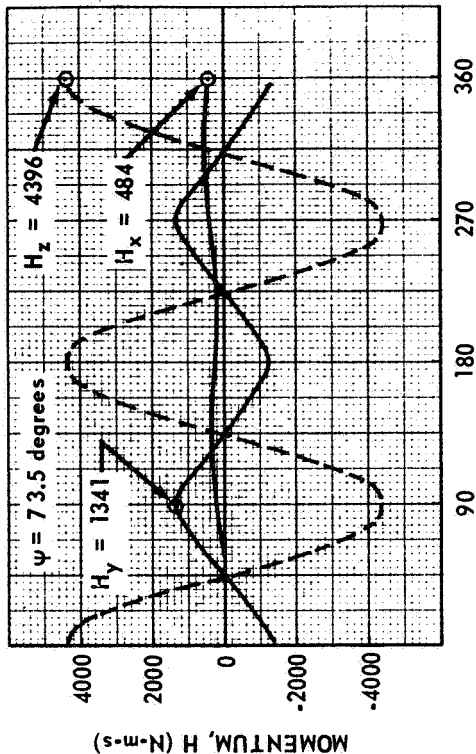FIGURE 26. SIDE VIEW ATM, MOMENTUM VERSUS ORBITAL POSITION [H(0) = 0]

83
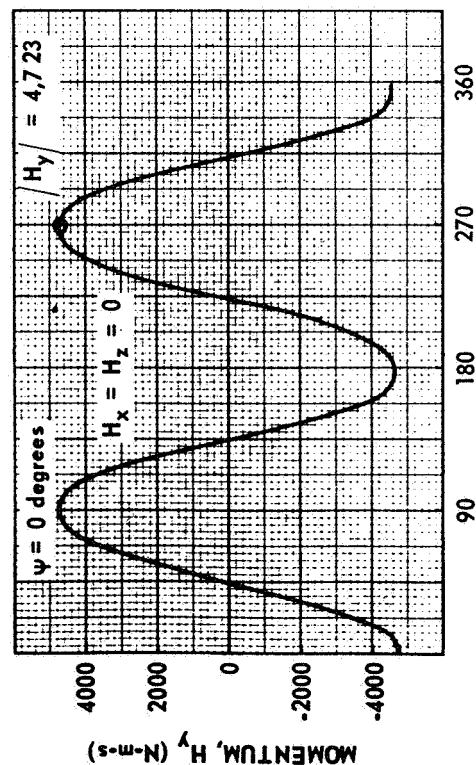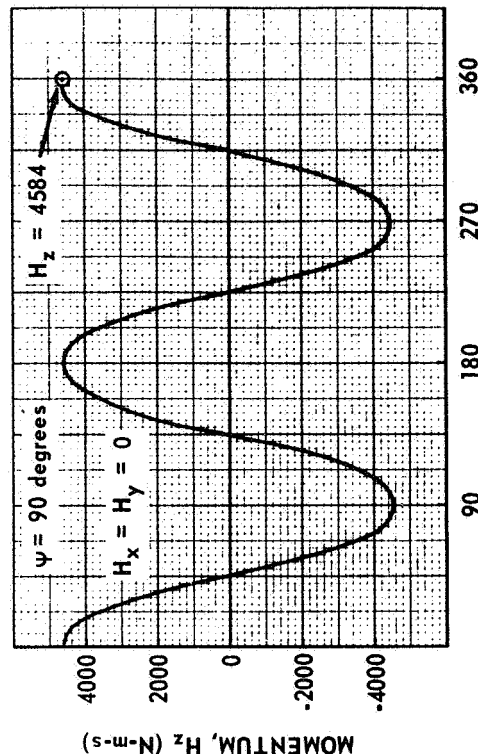
FIGURE 27. SIDE VIEW ATM, MOMENTUM VERSUS ORBITAL POSITION
WITH ZERO CONSTANTS OF INTEGRATION [H(0) ≠ 0]

inertia to lie in the orbital plane. The momentum components for the two side view cases are different. Figure 26 indicates that the Y and Z momentum components are biased; whereas, Figure 27 indicates that they are cyclic. This difference is dramatically portrayed in Figures 28 and 29. With H(0) = 0 , the 3-CMG saturation limit occurs before one-fourth orbit; whereas, for H(0) ≠ 0 , the limit is not reached in one orbit. Plotting the values shown in Figure 29 over a much longer time interval shows that the limit is reached after 7 orbits for ψ = 45 degrees and after 15 orbits for ψ = 73.5 degrees , corresponding to an inclination of 50 degrees (Fig. 30). Hence, a comparison of the two momentum cases illustrates the value of initialization. However, the conclusion should not be assumed that letting the constants of integration be zero [H(0) ≠ 0] always procedures the least severe momentum requirements. Once the number of CMG's necessary for control has been determined, it is the secular momentum build-up that determines the time at which the CMG's must be desaturated. The number of CMG's is determined by the magnitude of momentum accumulated over the time interval during which pointing control must be maintained. Initialization is equivalent to mounting the CMG's so that the center of their linear operating range corresponds to that of the gravity gradient disturbance momentum.
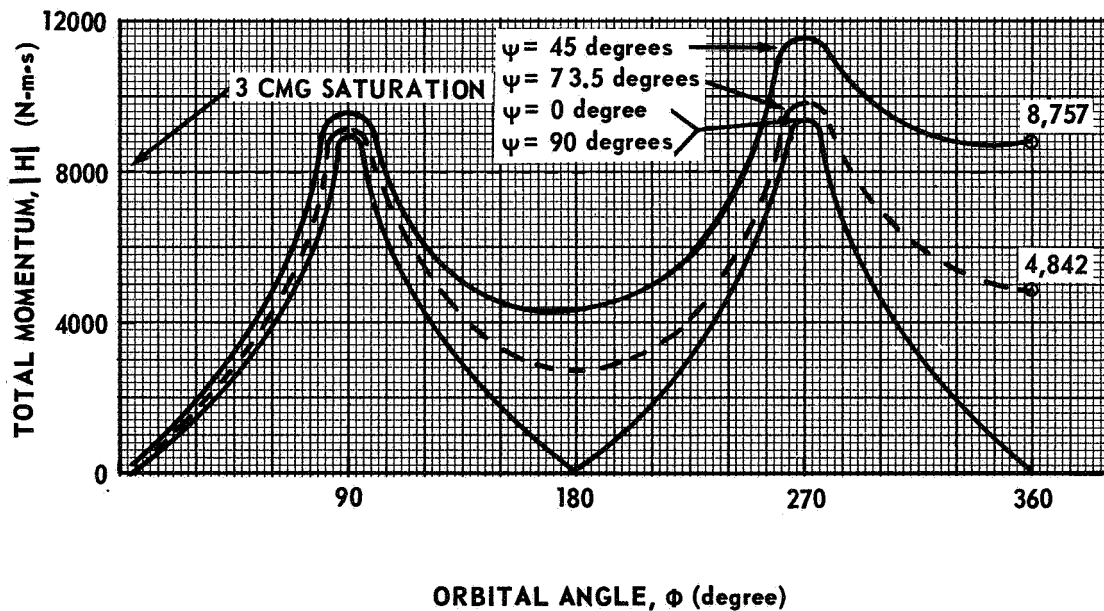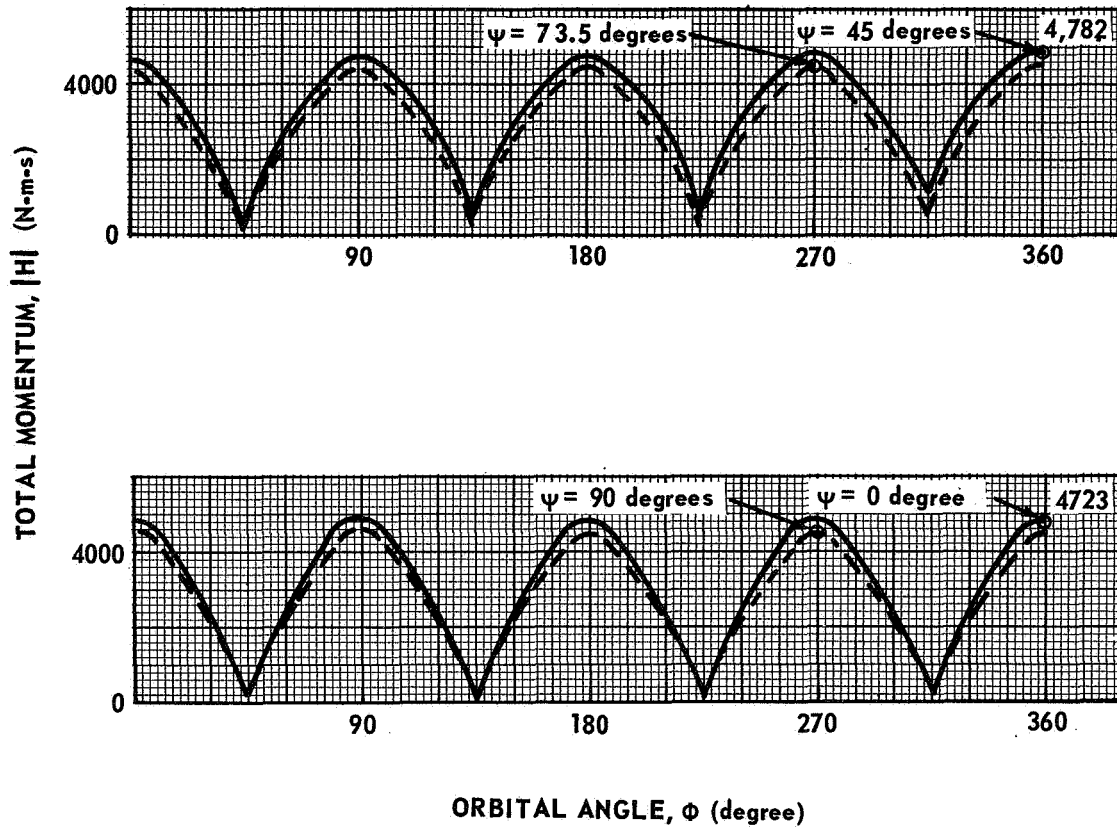

FIGURE 28. SIDE VIEW ATM, TOTAL MOMENTUM [H(0) = 0]

85

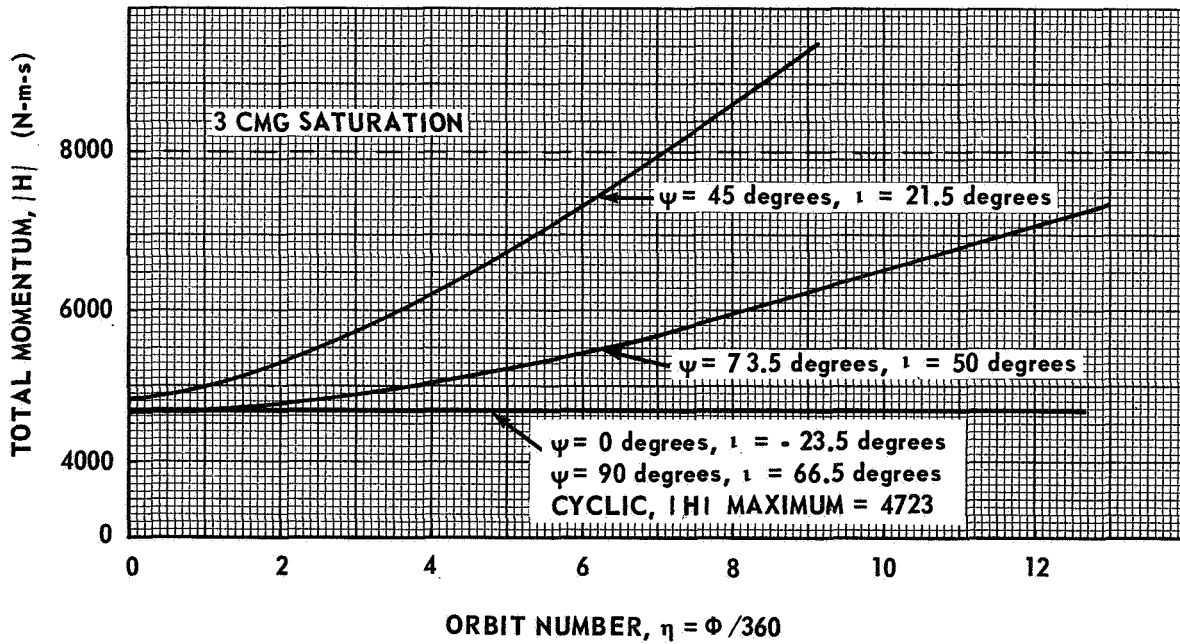FIGURE 29: SIDE VIEW ATM, TOTAL MOMENTUM, [H(0)≠0]

FIGURE 30: SIDE VIEW ATM, MOMENTUM VERSUS ORBIT NUMBER

86

The side view ATM configuration parameters are used in equations (92) to generate the torque and momentum components for the POP Mode case shown in Figure 31. A vehicle in the POP Mode orientation is in an unstable equilibrium position. For a symmetric vehicle, both the torque and momentum would be zero without axes misalignment; but since the side view configuration is not quite symmetric, a cyclic torque appears about the X-axis. Both the torque and momentum are in the noise level as compared to either the end or side view cases. However when axes misalignment cases are considered the torque and momentum requirements go up drastically. Figure 32 shows the torque and Figure 33 the momentum components for the principal axes being misaligned from the body axes by an angle of 6 degrees on each axis, equations (93). Biased torque and secular momentum components appear about both the Y- and Z-axis. A similar result occurs for reference axes misalignment, equations (94), which is shown in Figures 34 and 35. The total momentum, plotted in Figures 36 and 37, indicates that either principal-body or reference-body axes misalignment produces the same magnitude of momentum requirements for attitude hold . against gravity torques. The torque and momentum components were evaluated for three misalignment angles, 0.6, 3.0, and 6.0 degrees, about each axis. Although the components are not shown for the first two angles, the total momentum is shown for each angle. The results indicate a linear increase in accumulated momentum as the angles are increased. A three-degree angle produces 4150 N-m-s momentum after a one-orbit time period, which is about the same as the end view case with initialization so that a 3-CMG system could provide control. As illustrated, the POP mode without misalignments produces virtually no control requirements, but as misalignment angles are introduced the requirements become rather severe. This trend would be expected to occur for the other modes or orientation, which poses the unanswered question: with what accuracy are the principal axes known for a large clustered space station ?

Equation (95) represents a spacecraft in a gravity gradient stable mode; that is, the axis of minimum inertia is aligned with the local vertical and the axis of maximum inertia is aligned with the orbital spin vector. Without axes misalignments, both the torque and momentum requirements are zero. As small misalignment errors are introduced about each principal body axis, torque and momentum build up linearly about the Y- and Z-axes. For a given angle both the torque and momentum are constant, hence graphs versus orbital position are not shown. But the total momentum as a function of angle errors about the Y- and Z-axes is depicted in Figure 38. The 3-CMG saturation value is reached after one orbit by assuming a 3-degree misalignment angle about the principal axes. A 3-degree error is equivalent to an angle of 4.24 degrees measured from the local vertical to the vehicle axis of minimum inertia (the
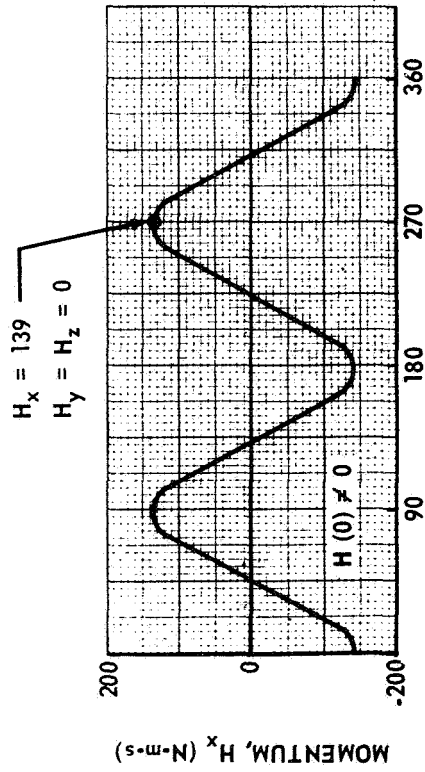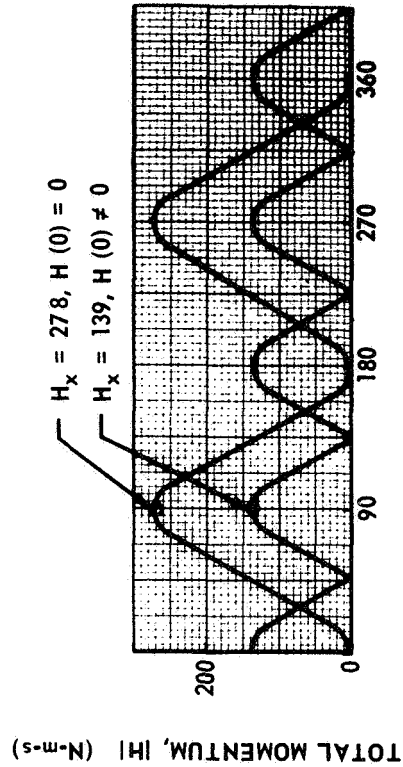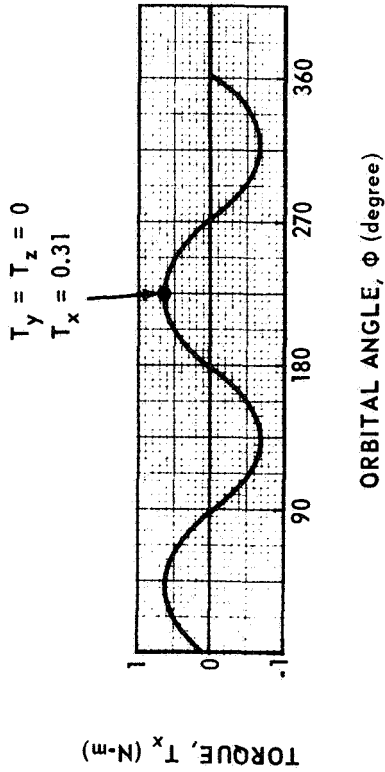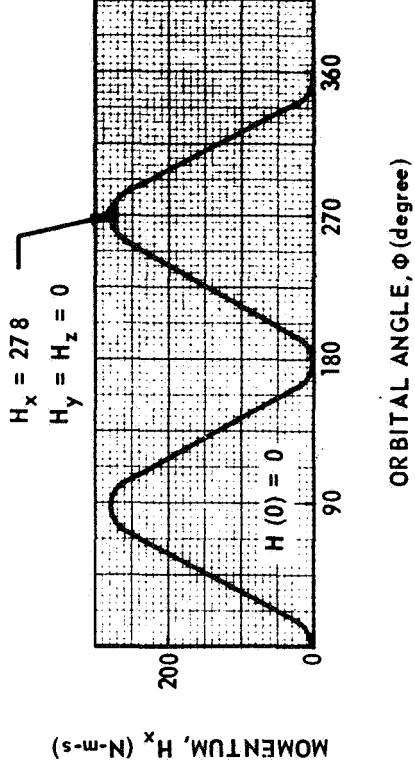
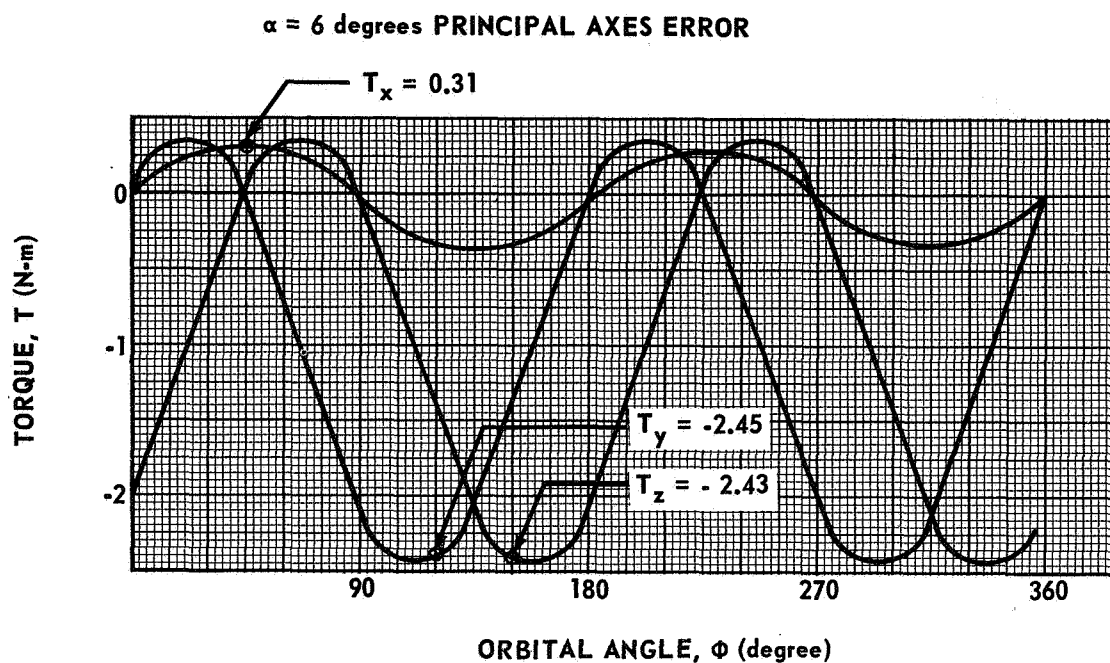FIGURE 31. POP MODE, GIMBALED ATM CONFIGURATION, TORQUE AND MOMENTUM VERSUS ORBITAL POSITION

88

α = 6 degrees PRINCIPAL AXES ERROR

$T_x = 0.31$

$T_y = -2.45$

$T_z = -2.43$

TORQUE, T (N-m)

0

-1

-2

90   180   270   360

ORBITAL ANGLE, Φ (degree)

FIGURE 32. POP MODE TORQUE VERSUS ORBITAL ANGLE
FOR PRINCIPAL AXES MISALIGNMENT

$H_x = 278$

α = 6 degrees

$H_z = -5776$

$H_y = -5950$

MOMENTUM, H (N-m·s)

1000

0

-2000

-4000

-6000

90   180   270   360
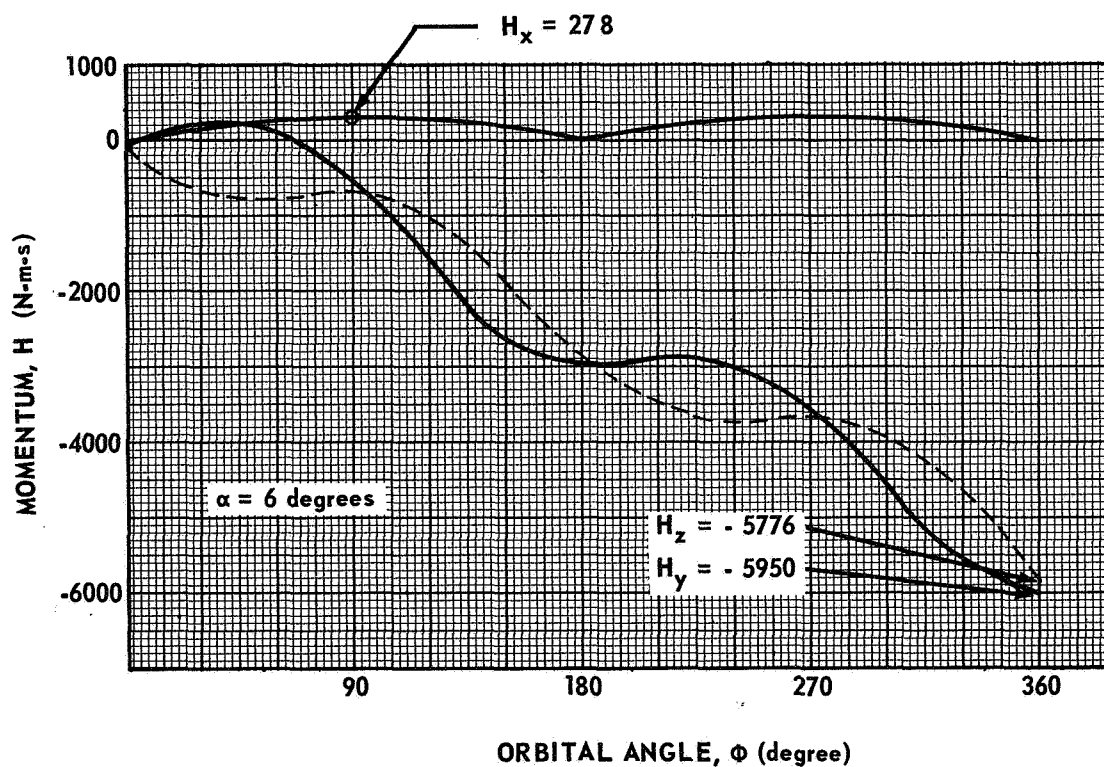
ORBITAL ANGLE, Φ (degree)

FIGURE 33. POP MODE MOMENTUM VERSUS ORBITAL ANGLE
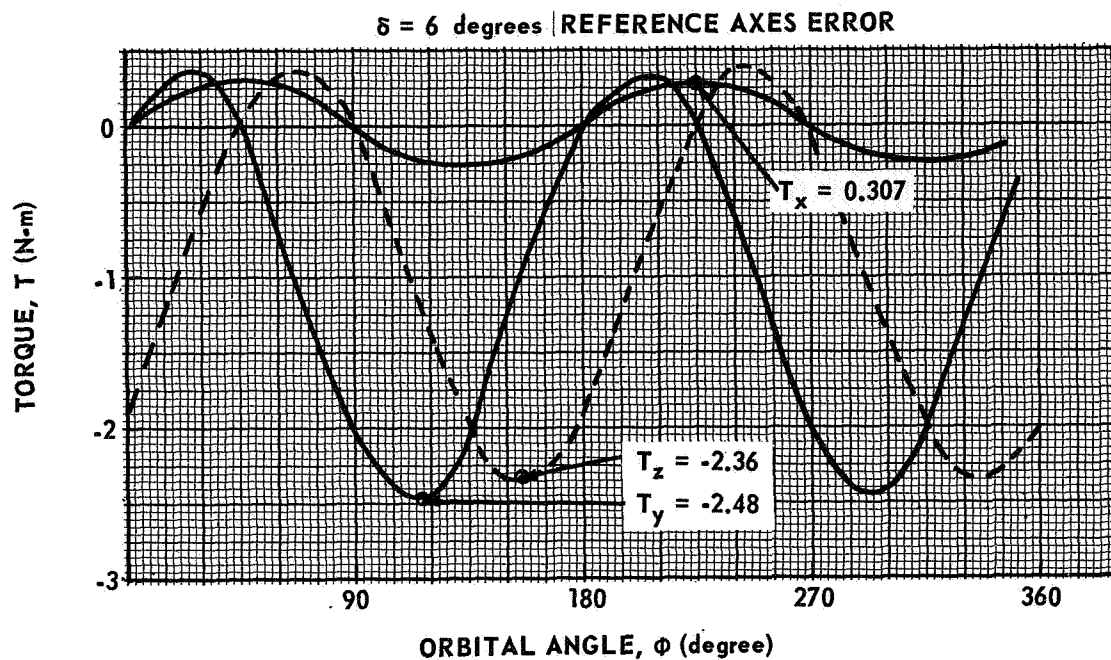FOR 6-DEGREE PRINCIPAL AXES MISALIGNMENT

89

FIGURE 34. POP MODE TORQUES VERSUS ORBITAL ANGLE
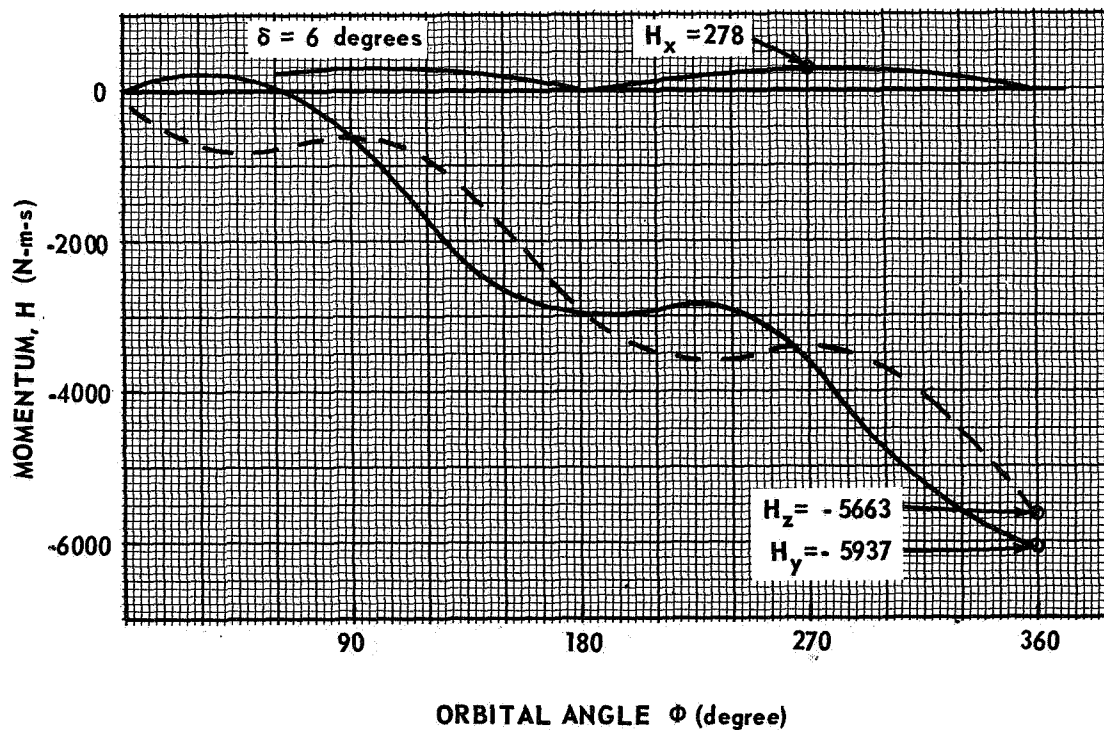FOR REFERENCE AXES MISALI:NMENT

FIGURE 35. POP MODE MOMENTUM VERSUS ORBITAL
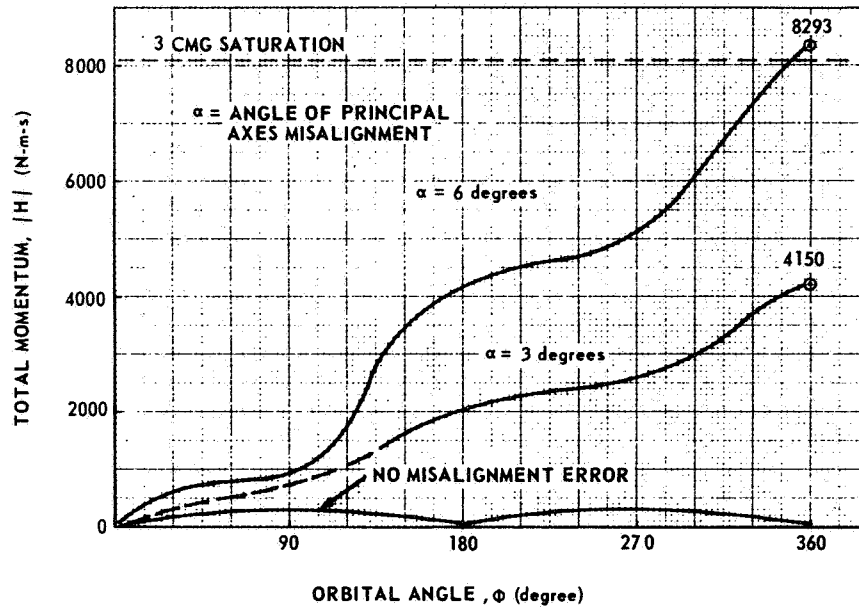POSITION FOR REFERENCE AXES MISALIGNMENT

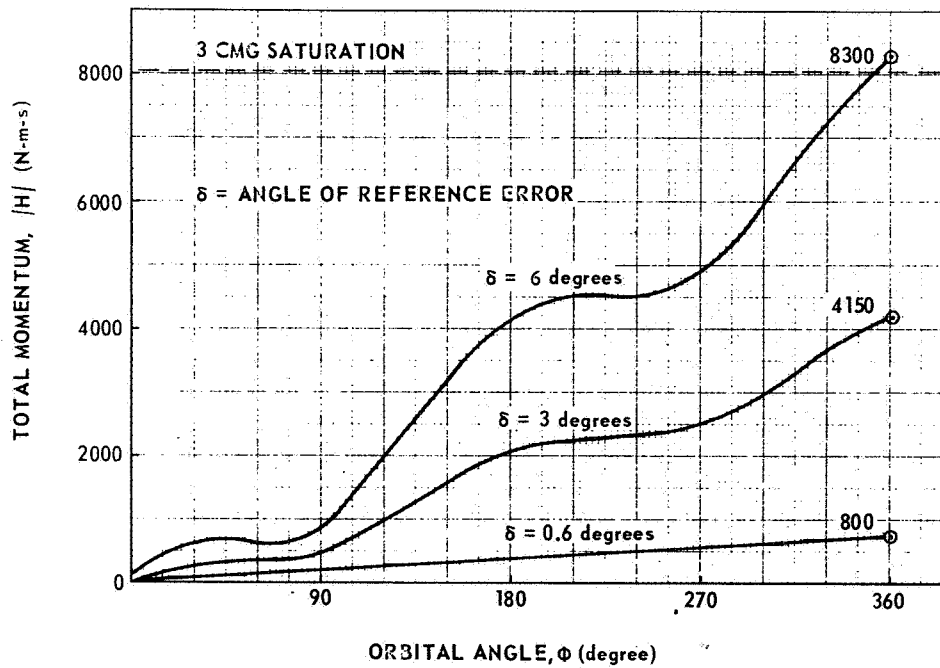FIGURE 36. POP MODE, TOTAL MOMENTUM FOR
PRINCIPAL AXES MISALIGNMENT

FIGURE 37. POP MODE, TOTAL MOMENTUM FOR
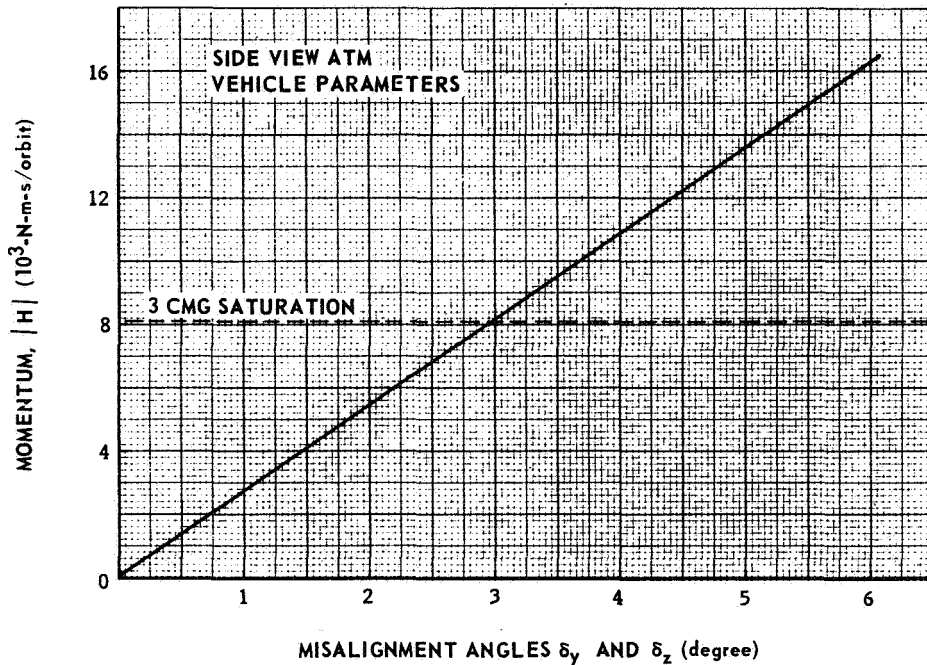REFERENCE AXES MISALIGNMENT

91

FIGURE 38. GRAVITY GRADIENT MODE MOMENTUM
DUE TO AXES MISALIGNMENT

X-axis) . Since small angle approximations have been used, Θ is defined by
the square root of the sum of the misalignment angles squared.

Using Θ as a parameter and assuming that two principal axes of inertia
are identical $(I_y = I_z)$, normalized momentum as a function of Θ is shown in
Figure 39. This chart can readily be used for preliminary design, along with
Figure 17, to determine fuel weight requirements. First the attitude error,
Θ , from local vertical is either assumed or calculated using equation (61)
and the products of inertia. Then the normalized momentum value is obtained
from Figure 39 and using specific vehicle parameters for $(I_y - I_x)$ the total
momentum is calculated. Last, the equivalent fuel weight is determined
using Figure 17. Using vehicle parameters for the side view ATM configura-
tion, the fuel weight per orbit as a function of misalignment angles and attitude
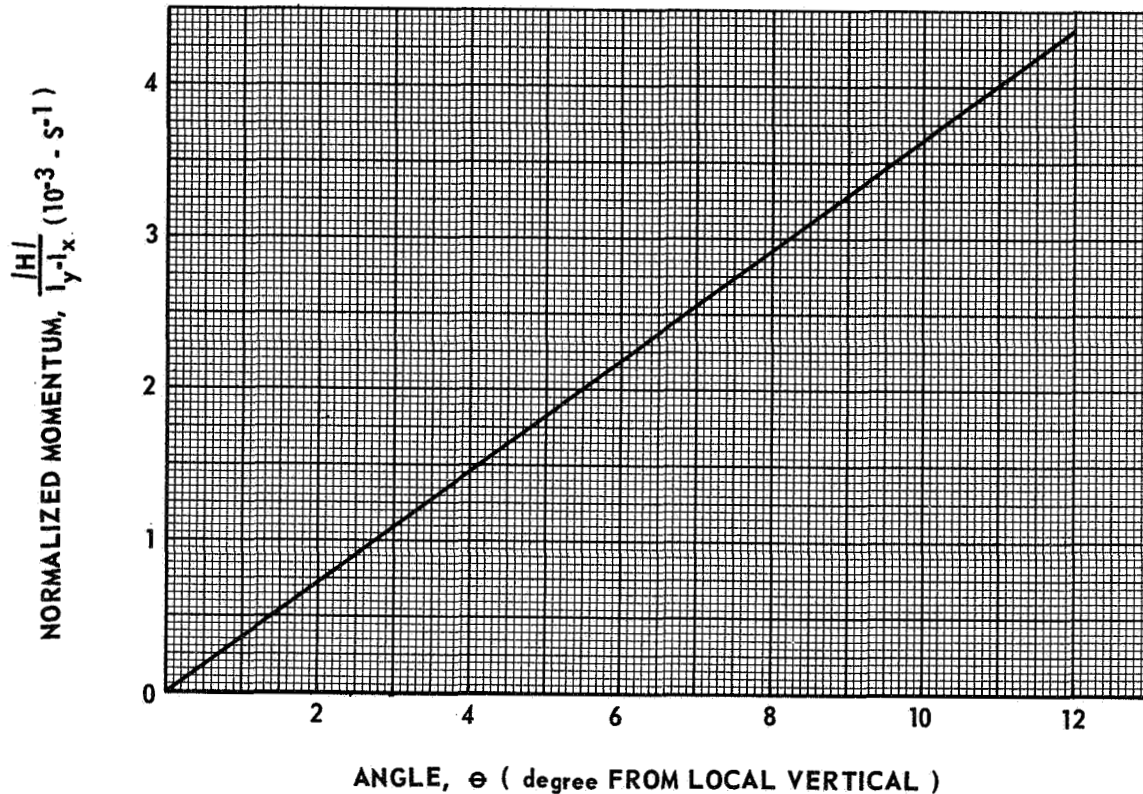error from the local vertical is shown in Figure 40.

92

FIGURE 39. GRAVITY GRADIENT MODE NORMALIZED MOMENTUM
DUE TO AXIS MISALIGNMENT

The energy requirements for attitude hold are summarized for various orientations in Table VIII for $\psi = 45$ degrees , a maximizing value. The type torque and the maximum accumulated momentum about each axis over a one-orbit time period is given for each mode. The number of control moment gyros is determined to counteract both the cyclic and secular gravity gradient momentum components over one-half orbit. Since the cyclic torques have a period one-half that of the orbit, the number of CMG's listed can counteract the cyclic components over an extended time period. Therefore, the pounds of fuel listed under each mode is the amount required to counteract only the secular momentum components that result from biased torques. In calculating the fuel weight per orbit, a specific impulse of 220 seconds for the fuel and a RCS lever arm of 10 feet are assumed. If a 20-foot lever arm is assumed, the fuel weights listed would be halved.

The maximum momentum values are obtained from the momentum component versus orbital position plots. The values listed with biased torques
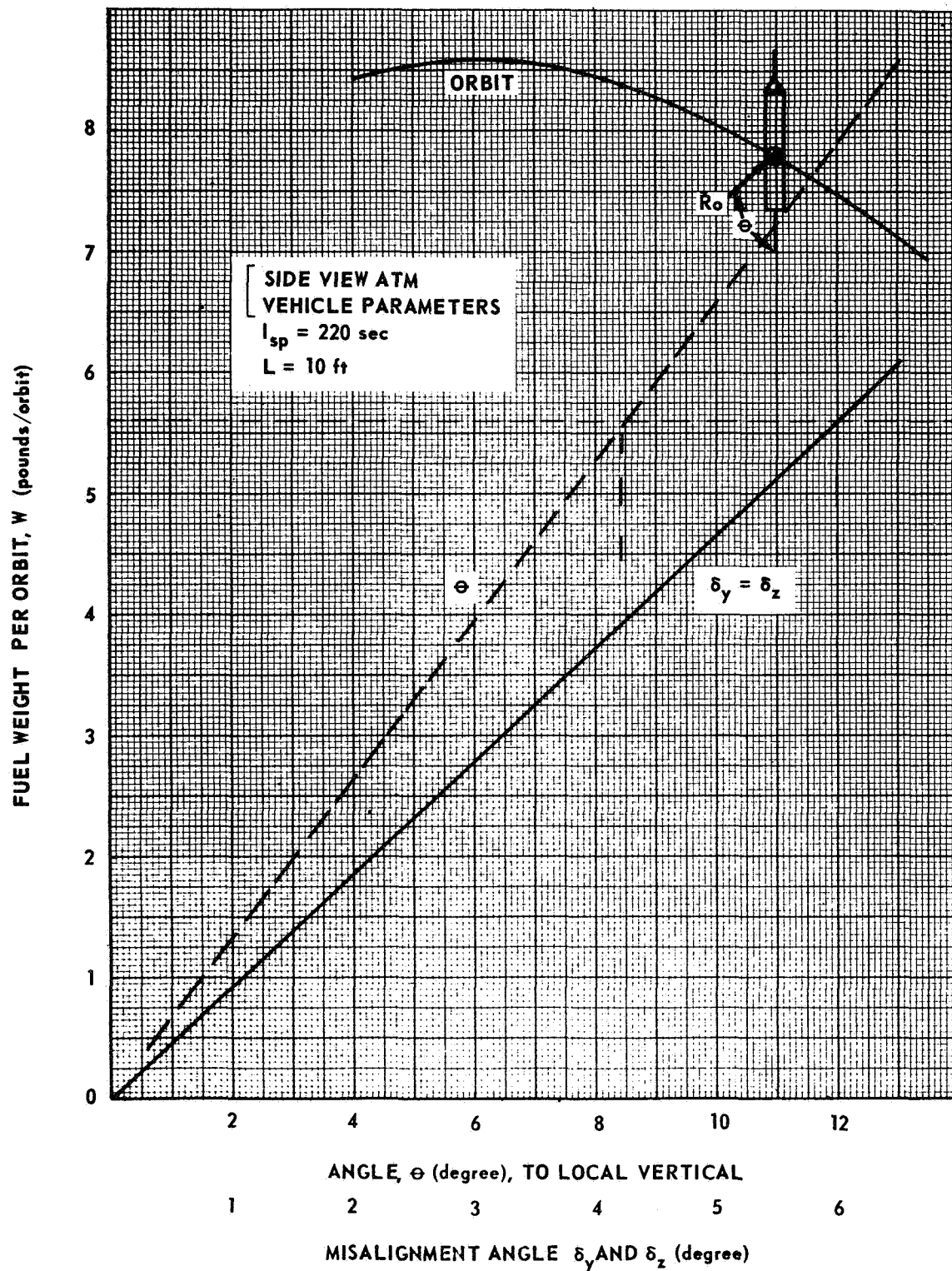
FIGURE 40. FUEL WEIGHT REQUIRED FOR ATTITUDE HOLD
IN G. G. MODE WITH AXES MISALIGNMENT

TABLE VIII. TYPE TORQUE, FUEL AND CMG REQUIREMENTS
FOR SELECTED ATTITUDE HOLD MODES (ψ = 45 degrees)

Mode	Type Torque (Momentum)			Pounds Fuel[a]			Number of CMG's
	X	Y	Z	Orbit	Day	Year	
1. Solar	cyclic (144)	biased (30 347)	cyclic (6668)	10.2	153	55 845	6
2. XOP	biased (876)	cyclic (3392)	cyclic (3241)	1.6	24	8760	3
3. POP	cyclic (278)	0	0	0.4	6	2190	0
4. POP (6 deg)	cyclic (278)	biased (5950)	biased (5776)	2.8	42	15 330	3
5. G.G. (6 deg)	0	constant (11 879)	constant (11 516)	5.6	84	30 660	3

a. Assuming an I_{sp} of 220 seconds and lever arm of 10 feet, the fuel is that required to counteract only the secular momentum components over one orbit.

1. Solar inertially fixed, end view ATM, H(0) = 0 .
2. Solar inertially fixed with the X-axis in the orbital plane, side view ATM, H(0) ≠ 0.
3. X-axis perpendicular to the orbital plane, gimbaled ATM, H(0) = 0 .
4. Same as 3, but with 6-degree principal axes misalignments.
5. Gravity gradient with 6-degree principal axes misalignments.

NOTE: CMG's are sized to counteract cyclic and biased components over one-half orbit.

are taken at the end of one orbit and represent secular momentum components. If there is more than one secular component per mode, as in Mode 4 POP (6 degrees), then the total value, the square root of the sum of secular components squared, is used for fuel weight calculations. Once the momentum is determined, the fuel weight per orbit is obtained by using Figure 17. Since a spacecraft makes about fifteen orbits per day in a 270 n.mi. orbit , daily fuel consumption is obtained by multiplying the fuel per orbit by fifteen.

In comparing the solar fixed modes the advantage of the side view ATM configuration with the axes of minimum inertia in the orbital plane (XOP Mode) over the end view ATM configuration (Solar Mode) is apparent. The solar mode requires 6-CMG's and 55 845 pounds of fuel per year, whereas the XOP mode only requires 3-CMG's and 8760 pounds of fuel per year. The solar mode, with $\psi = 45$ degrees, represents the worst possible case; because axes misalignments would, in this case, reduce energy requirements, whereas axes misalignments on the optimized XOP mode would increase energy requirements.

There are no biased torques in the POP mode case and the cyclic components are small in magnitude. For comparative purposes an all RCS control system is assumed, and the fuel weights listed are those required to counteract the cyclic torque. After one-fourth orbit the maximum accumulated momentum is 278 N-m-s [in Figure 31, $H(0) = 0$], after which the momentum decreases to zero at one-half orbit. During the period from $\varphi = 90$ degrees to 180 degrees, momentum equal to 278 N-m-s is taken from the system. Hence the total momentum for one orbit is 4×278 N-m-s = 1112 N-m-s which is equivalent to 0.4 pound of fuel per orbit (taken from Figure 17 and listed in Table VIII). However, when axes misalignments are introduced, Mode 4 POP (6 degrees) in Table VIII, secular momentum components appear about both the Y- and Z-axes resulting in a factor of seven increase in fuel requirements for 6 degrees misalignment as compared to the no misalignment case.

A vehicle in a gravity gradient hold mode with 6-degree misalignments about each principal axis experiences constant magnitude torques. The case represented by Mode 5 G.G. (6 degrees) of Table VIII is equivalent to attitude hold with the axis of minimum inertia at an angle of 8.4 degrees to the local vertical. Constant magnitude torques produce momentum which increases linearly with orbital time. After one orbit at 270 n.mi. the total accumulated momentum is 16 500 N-m-s (Fig. 38) which required a fuel weight of 5.6 pounds (Fig. 17). However, the same results can be directly obtained from Figure 40 which gives the fuel weight as a function of the misalignment angles for the side view ATM configuration. When compared with the POP mode misalignment case, the gravity gradient mode with misalignments requires twice as much fuel for

attitude hold, an unexpected result. However, the POP mode has one axis oriented in the plane defined by a vector perpendicular to the orbital plane and the sun line vector; hence the vehicle continuously rolls with respect to the local vertical. In the G.G. mode, the vehicle is stationary with respect to the local vertical. The vehicle can be made stationary in the POP mode with respect to the local vertical by setting $\varphi = 0$ in either equations (93) or (94), in which case constant torques appear about the X- and Z-axes and the Y-axis component is zero. Since the vehicle is near symmetric about X-axis, the X-axis torque and momentum is near zero, and the Z-axis contributes most of the momentum requirements which are one-half that of the G.G. mode. But if the POP mode is rotated 90 degrees so that the X-axis is aligned with the velocity vector then the momentum is identical with the G.G. case with constant torques on the Y- and Z-axes. The conclusion is that axes misalignment effects are twice as severe for a G.G. mode as for a POP mode.

CONCLUSIONS AND RECOMMENDATIONS

In the previous sections the basic gravity gradient torque and momentum equations have been derived for a spacecraft in an earth orbit. Various coordinate systems were then defined in order to specify the spacecraft's position at any time relative to an inertial reference frame and to resolve the local radius vector into body fixed components. Transformations relating the defined coordinate systems were derived in the form of a matrix composed of directional cosines. Next, several specific vehicle attitude hold orientations, as solar inertial, XOP and POP modes, were selected and the gravity gradient torque equations were derived for each case, utilizing the transformational matrix to resolve the local vertical vector into body axes components. Then, the effects of body axes misalignments on gravity torque were considered and expressions for several "look angles" of interest were derived. Finally, the energy requirements for attitude hold against gravity gradient were calculated for the previously selected orientations and a comparison between attitude hold modes was made.

Based on the energy requirements, the POP mode with the axis of minimum inertia aligned perpendicular to the orbital plane optimizes fuel and CMG requirements, especially when principal axes misalignments are considered. If a solar inertially fixed mode is desired, then constraining the axis of minimum inertia to lie in the orbital plane (XOP mode) results in minimum energy requirements. Furthermore, momentum storage initialization can be

effectively utilized to reduce either the number of CMG's or the size required for control of cyclic perturbations, especially for the POP mode orientation. The equations developed for the various attitude hold modes can easily be adapted for use on configurations other than the side and end view ATM workshops.

The coordinate systems and transformations can be utilized to evaluate the effect of time of year and time of launch on gravity gradient torques, providing a means of relating the orbital, equatorial and ecliptic planes through physically meaningful parameters. The resulting directional cosines can be quickly evaluated for fixed time of year and orbital plane analysis which produces simplified transformations that can be used to evaluate the gravity torque and momentum components without resorting to elaborate machine computations. It has been shown that these simplified components are always scaled sine or cosine functions, $f(\varphi)$, of the orbital angle (Fig. 19). For preliminary design purposes, the scaling factor is determined using specified vehicle and orbital parameters, then the torque or momentum component is obtained by multiplying the scaling factor by the appropriate $f(\varphi)$ function. Energy requirements to counteract gravity gradient is the dominant consideration in recommending a preferred attitude hold orientation.

The equations derived for various look angles enable the engineer to determine gimbal angle limits and rates required for experiment pointing control. Also, the solar look angles help establish both solar panel and ATM gimbal requirements, especially if the OWS is in an orbital fixed mode, such as POP. Closed form solutions are given for several angles of interest; others can be readily derived using the defined coordinate systems and transformations.

Addtional work should be done to relate momentum components to fuel weight and CMG requirements for various attitude hold orientations. Nomographs could be prepared in normalized nondimensional form for each specific orientation, and utilized for "quick look" analysis needed to size the control system and establish fuel storage requirements. Basic stability characteristics and sensor locations should be related to vehicle orientation and the various attitude hold modes.

APPENDIX

EULER EQUATIONS

For completeness, a derivation of the Euler equations is outlined below, along with a systematic procedure for obtaining the Euler kinematic relations. The Euler equations express the rotational dynamics of an orbiting spacecraft in response to the applied torques as functions of the vehicle inertial properties and body angular rates. The Euler kinematic relations are three equations which express the body angular rates as functions of the transformational angles and rates used in the directional cosine matrix relating the body and inertial reference coordinate systems.

The torque required to change the angular momentum of a system is equal to the time rate of change in angular momentum, from equation (55) the angular momentum is given by

$$\widetilde{H} = \widetilde{I} \, \widetilde{\omega} \tag{A1}$$

Hence, the applied torque T is equal to

$$\widetilde{T} = \dot{\widetilde{H}} + \widetilde{\omega} \times \widetilde{H} \tag{A2}$$

Carrying out the vector-matrix operations and regrouping terms, the components of torque are

$$T_x = \dot{h}_x + h_z \omega_y - h_y \omega_z$$

$$T_y = \dot{h}_y + h_x \omega_z - h_z \omega_x \quad , \tag{A3}$$

and

$$T_z = \dot{h}_z + h_y \omega_x - h_x \omega_y$$

Equations (A3) are known as Euler's moment equations. The components of H are defined by equation (54) as

$$h_x = I_x \omega_x - I_{xy} \omega_y - I_{xz} \omega_z \quad ,$$

$$h_y = -I_{yx} \omega_x + I_y \omega_y - I_{yz} \omega_z \quad , \tag{A4}$$

and

$$h_z = I_{zx} \omega_x - I_{zy} \omega_y + I_z \omega_z \quad .$$

Assuming that principal axes are selected as control axes, the products of inertia are zero. By setting the applied torques $(T_x, T_y, \text{ and } T_z)$ equal to the gravity gradient torques of equation (10), the Euler equations (A3) for principal control axes become

$$T_x = I_x \dot{\omega}_x + (I_z - I_y) \omega_z \omega_y = C_x R_z R_y$$

$$T_y = I_y \dot{\omega}_y + (I_x - I_z) \omega_x \omega_z = C_y R_x R_z \tag{A5}$$

and

$$T_z = I_z \dot{\omega}_z + (I_y - I_x) \omega_y \omega_x = C_z R_y R_x$$

The applied gravity torques contain components of the local radius vector which are known functions of the directional cosines in the transformational matrix that relates the inertial and moving body reference frames. The Euler equations contain components of angular velocity which are known only in general body axis components. However, if the directional cosine matrix is known the components of angular velocity can be obtained as functions of the rotational angular rates, which are then substituted into Euler's moment equations.

Consider the rows of the transformational matrix as vectors,

$$A = \begin{bmatrix} e_1 \\ \overline{e_2} \\ \overline{e_3} \end{bmatrix} = \begin{bmatrix} A_{11} & A_{12} & A_{13} \\ A_{21} & A_{22} & A_{23} \\ A_{31} & A_{32} & A_{33} \end{bmatrix} \tag{A6}$$

It can be shown that

$$\omega_x = \dot{\bar{e}}_2 \cdot \bar{e}_3 \quad ,$$

$$\omega_y = \dot{\bar{e}}_3 \cdot \bar{e}_1 \quad , \tag{A7}$$

and

$$\omega_z = \dot{\bar{e}}_1 \cdot \bar{e}_2$$

Equations (A7) relate the body axes angular rates to rotational rates and angles used in the transformation matrix and are known as Euler's kinematical relations. These relations are commonly derived by transforming each angular rate into body coordinates and then summing the components to produce the body angular rates $(\omega_x, \omega_y, \omega_z)$. The Euler kinematic relations, however, can be obtained by a systematic procedure using equations (A7), after which the body angular rates are substituted into the Euler equations (A5) to obtain the dynamic rotational equations for an earth orbiting spacecraft under the influence of gravity.

BIBLIOGRAPHY

Besonis, et al.: Launch and Space Vehicle Control Studies, Vol. 11, LMSC/HREC A784590-11, 1967.

Bhuta, P. G.: Gravity Gradient Stabilization Principles, 9990-6890-KU000, TRW Space Technology Laboratories, March 16, 1965.

Blue, J., and Glahn, T.: Attitude Control and Pointing, Appendix C to ED-2002-136, Martin Marietta Corp., July 7, 1967.

Cagle, et al.: Apollo Telescope Mount Sub-Systems — Black Box Preliminary Design Review, MSFC, R-ASTR-DIR, October 30, 1967.

Ellsworth, et al.: Early Saturn V Workshop, MSFC, Advanced Studies Office, May 15, 1968.

Goldstein, H.: Classical Mechanics, Addison-Wesley Publishing Co., 1959.

Hubbard, C. R.: A Technique for Stabilizing The ATM Vehicle ---, Space Support Division of Sperry Rand Corp., Huntsville, Ala., 1968.

Nelson and Loff: Space Mechanics, Prentice-Hall, Inc., 1962.

Phillips, Samual C., et al.: Project Apollo Coordinate System Standards, NASA SE008-001-1, June 1965.

Thompson, W. T.: Introductive To Space Dynamics, John Wiley and Sons, Inc., 1961.

A DISCUSSION OF ORBITAL WORKSHOP ORIENTATION AND GRAVITATIONAL EFFECTS

By Billy G. Davis

The information in this report has been reviewed for security classification. Review of any information concerning Department of Defense or Atomic Energy Commission programs has been made by the MSFC Security Classification Officer. This report, in its entirety, has been determined to be unclassified.

This document has also been reviewed and approved for technical accuracy.

FRED E. DIGESU
Chief, Electronics and Controls Division

ERICH E. GOERNER
Director, Preliminary Design Office

W. R. LUCAS
Director, Program Development

INTERNAL

DIR
   Dr. von Braun

DEP-T
   Dr. Rees

AD-S
   Dr. Stuhlinger

PD-DIR
   Dr. Lucas

PD-MS-DIR
   Mr. Flynn

PD-AP-DIR
   Mr. Becker (2)

PD-MP-DIR
   Mr. Downey (2)

PD-PP-DIR
   Mr. Sneed (2)

PD-PS-DIR
   Mr. Goodrum (2)

PD-SA-DIR
   Mr. Huber (5)

PD-DO-DIR
   Mr. Goerner
   Dr. Thomason
   Mr. Heyer
   Mrs. Andrews

PD-DO-S
   Mr. Marshall (5)

PD-DO-M
   Mr. Barker (5)

PD-DO-P
   Dr. Thomae (5)

PD-DO-E
   Mr. Digesu (15)

PD-DO-ES
   Mr. Davis (50)

S&E-AERO-DIR
   Dr. Geissler (10)

S&E-AERO-D
   Mr. Rheinfurth (5)

S&E-ASTN-DIR
   Mr. Heimburg (5)

S&E-ASTR-DIR
   Mr. Moore (10)

S&E-ASTR-N
   Mr. Hosenthien (5)

S&E-COMP-DIR
   Dr. Hoelzer (5)

S&E-CSE-DIR
   Dr. Haeussermann (5)

DISTRIBUTION (Concluded)

S&E-CSE-A
  Dr. McDonough (2)

S&E-CSE-S
  Mr. Wiesenmaier (5)

S&E-ME-DIR
  Dr. Siebel (2)

S&E-P-DIR
  Mr. Vreuls (2)

S&E-SSL-DIR
  Mr. Heller (2)

PM-PR-M
  Mr. Goldston

A&TS-PAT

A&TS-MS-H

A&TS-MS-IP

A&TS-MS-IL (8)

A&TS-MS-TU (6)

EXTERNAL

Dr. Walter Green (2)
Dept. of Electrical Engineering
University of Tennessee
Knoxville, Tennessee 37616

Dr. Larry Jacowitz (2)
IBM Space Systems Center
Huntsville, Alabama 35805

Mr. J. Kranton (2)
Bellcomm, Inc.
1100 Seventeenth Street, NW
Washington, D. C. 20036

Dr. W. Trautwein (2)
Lockheed Missiles & Space Co.
Research Park
Huntsville, Alabama 35805

Scientific and Technical Information
    Facility (25)
Attn: NASA Representative (S-AK/RKT)
P. O. Box 33
College Park, Maryland 20740

Mr. Carey F. Lively, Jr. (5)
G&C Systems Analysis, EG23
NASA
Manned Spacecraft Center
Houston, Texas 77058